Influence of Saturation and Geometry on Surface Electrical Resistivity Measurements

Jose Miguel Sanchez Marquez

A Thesis
in
The Department
of
Building, Civil and Environmental Engineering

Presented in Partial Fulfillment of the Requirements
for the Degree of Master of Applied Science Building Engineering at
Concordia University
Montreal, Quebec, Canada

June 2015

CONCORDIA UNIVERSITY
School of Graduate Studies

This is to certify that the thesis prepared

By: Jose Miguel Sanchez Marquez

Entitled: Influence of Saturation and Geometry on Surface Electrical Resistivity Measurements

and submitted in partial fulfillment of the requirements for the degree of.

Master of Applied Science (Building Engineering)

complies with the regulations of the University and meets the accepted standards with respect to originality and quality.

Signed by the final Examining Committee:

Dr. Christopher W. Trueman	Chair
Dr. Fuzhan Nasiri	Examiner
Dr. Luis Amador	Examiner
Dr. Michelle R. Nokken	Supervisor

Approved by

Chair of Department or Graduate Program Director

June 2015

Dean of Faculty

Abstract

Influence of Saturation and Geometry on Surface Electrical Resistivity Measurements

Jose Miguel Sanchez Marquez
Concordia University, 2015

Non-destructive tests are the future for early concrete deterioration detection. The interest in surface electrical resistivity as for the quality control of concrete structures has increased in the last several years. A standardized laboratory method has recently been adopted as AASHTO TP 95-11 and an ASTM method is under consideration. Both these methods measure surface resistance by a Wenner four-electrode probe device, in which the electrodes are equally spaced on the surface of saturated concrete elements. Currently, the standardized method is restricted to laboratory specimens. For this method to be applicable to field measurements requires first to identify how much time a concrete element needs to reach saturation and how reliable resistivity values are under different saturation stages. Phase one of this research investigated the duration of saturation required to achieve stable resistivity for 20 mixture designs at a range of ages. It was generally determined that resistivity varies until 24 hours. Past that duration, some increases in surface resistivity were observed and attributed to further hydration. In the field, concrete elements are generally large and the assumptions of infinite geometry hold. Lab specimens, on the other hand, have a constricted flow of electrical current. In Phase two, the influences of geometry and saturation fluid were examined. It was found that using published geometrical conversion factors did not result in equivalent surface resistivity between cylinders and small slabs or for cylinders of different sizes, suggesting more work required in this area.

The use of tap water was investigated as it would be more available on site; it was found that at 28 days, there were minimal differences between tap water and limewater. At later ages, limewater generally resulted in higher resistivity. Phase Three investigated published temperature corrections to adjust site measured resistivity to standard temperature. Regardless of the correction, significant difference was observed between the site and laboratory measurements. Lastly in Phase four, two alternate techniques were tested for potential on site use. It was found that neither resulted in any significant changes in resistivity.

Acknowledgement

It is with sincere and with enormous gratitude that I thank my advisor Dr. Michelle R. Nokken for choosing me and believe in me. This experience was a dream come true. She never doubted my abilities and always motivated me with her knowledge, kindness and patience. Thanks again Professor for your supervision, consideration and your strong commitment in this work

Dedication

To the greatest of my life, mom, dad and Andres;

Thanks for the company, patience, positive energy and trust through the distance, without your support this work never could have been done. You are always in my mind, los amo.

Table of Contents

Table of Figures

Table of Tables

1 Introduction

Concrete is one of the most commonly used products today in the construction industry. This product needs to be mixed, transported, placed, finished and cured to exhibit the desired performance. Once placed, finished and cured, two main properties that take special attention are compressive strength and durability. The first is the ability of concrete to resist mechanical stresses and the second one can be defined as, the concrete's ability to keep quality, form and serviceability under different environmental conditions over a period of time without requiring excessive effort for maintenance. Durability is mainly influenced by: (a) hardened concrete properties, (b) environmental exposure conditions and (c) construction practices.

Hardened concrete properties are a function of the water to cementitious material ratio and mixture design. Particularly important for durability are the cement paste's pore size and distribution. For the case of high performance concrete (HPC), the pore structure should be as impervious as possible (Swamy 1996). This will prevent the degradation process due to environmental conditions that involves the penetration and subsequent movement of air, water or other fluids transporting aggressive agents into the concrete pore system. These conditions can generate deterioration due to freezing and thawing, sulfate attack, alkali-silica and alkali-carbonate reactions (Bryant et al. 2009) or corrosion of reinforcing steel. Reinforcement corrosion is one of the most prevalent forms of deterioration, and

once corrosion has initiated, cracks in concrete can propagate (Presuel-Moreno et al. 2010).

Construction practices also greatly influence concrete's durability due to the human factor involved. The correct placement, consolidation, finishing and curing processes are steps that can lead to the achievement of the required pore network and maximum density. One of the most common construction practices issues is failure in proper consolidating and placing concrete, which can result in honeycombing. Also, it can be found as a result of excessive vibration, segregation and air-void system alteration which can lead to reducing the concrete's resistance of freezing and thawing (Taylor et al., 2013). In other words, a good durable concrete will be attained if the concrete has a low water to cement ratio, has achieved adequate thermal and moisture curing, and has achieved a discontinuous capillary pore structure free of significant micro or macro defects.

Consequently, the penetration properties, such as resistance to absorption and permeation, should be used as the principal criteria for determining concrete's durability. Since the permeability of the outer zone of concrete can be very different from that of the bulk concrete due to compaction, bleeding, finishing and curing, as well as the choice of constituent materials used, the solution to the problem of durability in structures is most likely to come about from understanding of its outer layer or covercrete. (DeSouza 1996).

Currently there is no standardized, non-destructive technique or method to measure in-place concrete durability. Several methods exist for laboratory investigations, but many are time consuming. Electrically based methods have been identified as having the potential to be rapid tests for durability (Polder, 2005). One potential method is AASHTO TP 95-11. Presently, it is only standardized as a laboratory method, but the fact is that it is portable and is therefore relevant for in-situ investigation. This method utilizes a Wenner probe with four equally spaced electrodes. In the Wenner four electrode technique, an alternating current is applied between the outer two electrodes and the voltage is measured between the middle two electrodes indicating the electrical surface resistivity of the element. A lower electrical resistivity value is obtained when the applied electrical current can easily pass through the pore structure, which in terms of permeability corresponds to a highly permeable concrete (Shahroodi 2010).

Since only the surface is being tested, this procedure has the advantage of measuring concrete's quality and the influence of alternative curing methods on the exposed surface. It should be mentioned that several factors can influence concrete's surface resistivity such as inclusion of supplementary cementitious materials, saturation degree, temperature, water to cement ratio (w/c) and age. These factors will be further detailed in the Literature review chapter.

1.1 Research Objectives

The primary focus of this study is to analyze the use of the electrical resistivity device as a suitable, non-destructive method to evaluate the potential durability of the surface layer or covercrete in field situations. Since moisture content of concrete in the field will vary, a large part of the research was devoted to quantify the influence of surface saturation on the test, comparing results obtained from full immersion, humid air, pressurized water and static surface ponding with a Wenner four probe with four equally spaced electrodes was used from the commercial brand Proceq that works with frequency of 40Hz. The specific objectives are to:

- Determine the immersion time required for concrete to achieve a stable resistivity in the laboratory. Determine the influence of water cement ratio (w/c), supplementary cementitious materials and concrete age on the saturation required for stable surface electrical resistivity test.
- Examine how the specimen's geometry (cylinders, circular slabs, field placed concrete) influences the surface electrical resistivity after periods of saturation.
- Determine if the use of tap water may be feasible for saturation purposes.
- Investigate alternate methods to saturate concrete elements to obtain reliable surface electrical measurements but in less time, similar to the ones obtained in the laboratory after long periods of saturation.

1.2 Chapter Outline

The thesis begins with a literature review about the importance of electrical resistivity methods and how they are related to the concrete's physical properties such as, porosity and permeability. In addition, the background of different types of electrical methods developed through the years bearing on concrete's quality assurance is considered with special emphasis on the Wenner four-electrode technique. Outlined are some of the common mistakes that can be made assessing concrete resistivity plus some steps that can be taken to minimize errors. In-depth descriptions of the principal factors that influence surface electrical resistivity such as pore structure, temperature, saturation degree and use of supplementary cementitious materials are presented.

Chapter 3 details the experimental methodology used to achieve the research objectives described previously. Several different phases comprise this effort. A commercial device, based on the Wenner probe device, was primarily used during this research.

Chapter 4 analyses the results from each phase of the experimental program. A detailed description of how resistivity is influenced by different durations of saturation at different ages (28, 56 and 91 days) on a total of five binder combinations on cylinders (Ø10x20 cm) cast under laboratory conditions, establishing the time required for concrete to achieve a stable resistivity under these conditions as well as analyzing the effect of supplementary

cementitious materials – blast furnace slag and fly ash on concrete. A second round of samples were cast using different specimen geometries, circular slabs Ø30x12cm and standard cylinders Ø10x20cm and Ø15x30cm to analyze the influence of geometry and surface layer on electrical resistivity. Additionally, both geometry samples were stored under two solutions to determine if exist different between the surface resistivity measured values. An analysis is presented further of correlations established to normalize the temperature effect on site and the influence of curved and plane surfaces are also analyzed. Lastly, the influence of two different saturation practices on surface electrical resistivity are presented.

Chapter 5 discusses three main topics; (a) the minimum duration to obtain reliable surface resistivity values on laboratory samples; (b) Geometry effect and type of solution to storage; (c) misreading surface electrical resistivity results due to poor saturation based on results achieved in chapter 4.

Finally, a number of conclusions over this work are presented with recommendations for future work and suggestions to continue improving a methodology able to achieve reliable measurements on site situations.

1.3 List of Abbreviations

ASTM	American Society for Testing Materials.
AASHTO	American Association of State Highway and Transportation Officials.
W/C	Water cement ratio.
ASR	Alkali-silica reaction.
HPC	High performance concrete.
SCMs	Supplementary cementitious materials.
(ϕ)	Porosity.
(k)	Permeability.
AC	Alternating current.
DC	Direct current.
(ρ)	Resistivity.
(a)	Probe spacing.
RCP	Rapid Chloride Permeability.
SD	Saturation degree.
LW	Limewater solution.
TW	Tap water.
PC	Portland cement type I/II.
TI	Mixture with Portland cement type I/II.
FA	Fly ash.
S	Slag cement.
L	Limestone cement.

2 Literature Review

Concrete mixture design must be carefully considered in regards to its eventual exposure conditions. Freezing and thawing, alkali silica reaction and corrosion are the most commonly encountered deterioration mechanisms. Each of these can be directly related to the concrete's pore structure.

Water can enter the pore system and subsequently freeze upon exposure to cold conditions. The effect of freezing-and-thawing is widely known, in most of the cases it generates deep and widespread deterioration, especially in permeable concretes (high w/c) more susceptible to absorb and retain moisture through time. Once, water freezes, it produces hydraulic pressures in the capillaries and pores of the cement paste and aggregates. If these pressures exceed the tensile strength of the surrounding paste or aggregate, cracks will form. Initially, this deterioration will not affect the structural capacity of the element but will affect the concrete's durability. Its extent cannot be determined through visual inspections alone and once it has spread in a large area, it can lead to cracking, scaling, delamination or spalling (Montgomery et al., 2013). However, in order to improve the long-term performance, the concrete must have a good air-void system especially in places with marine environments or with possibility of exposure to deicing salts during winter seasons in northern countries (Taylor et al., 2013).

To minimize the likelihood of alkali-silica reaction (ASR), the use of non-reactive aggregate, low alkali cement or the use of supplementary cementitious materials is recommended. These material choices coupled with a discontinuous pore network minimize the likelihood of deterioration. For reinforced concrete to avoid excessive carbonation and consequent danger of steel corrosion, the steel should have an adequate cover of concrete with low permeability. In order resist the effects of sulfate attack, corrosion and chloride permeability, low permeability for high performance concretes is highly required.

A durable concrete must have a complex pore network structure, with narrower void spaces avoiding connectedness between them. Ideally, high performance concretes (HPC) must have low porosity (ϕ) and low permeability (k) characteristics that are going to be presented in this section.

2.1 Terminology

Durability of cementitious materials highly depends on their ability to prevent the ingress of water and deleterious materials (such as chloride ions from de-icing salts) into the material body. In this section, terms such as, porosity, permeability, and sorptivity will be described, with special emphasis in the difference between porosity and permeability.

2.1.1 Porosity

Porosity is defined as the percentage of void spaces as compared to the total material volume, in this case, concrete. However, void spaces or pore sizes can easily change over time due to the continuous hydration and sometimes the deterioration process during the lifetime of concrete. These pores influence concrete properties as durability, creep, permeability and shrinkage.

2.1.2 Permeability

Permeability is a property that measures the ability of a fluid to pass through the connected pathways of a saturated porous material under a pressure gradient. Basically, a material with high numbers of pore pathways or corridors in its pore network will be more permeable due to the low resistance to fluid flow under the pressure gradient. As a result, permeability is linked to durability since it determines the penetration of deleterious substances into the concrete body that can lead, for example, to corrosion in cases of reinforced concrete.

2.1.3 Sorptivity

Sorptivity can be described as the tendency of a porous medium to transmit a fluid only by capillary action without any pressure gradient. When a fluid makes contact with a dry porous material (e.g. concrete), moisture absorption by capillarity is going to take action.

2.1.4 Distinguishing between permeability and porosity

There is neither a direct nor inverse relationship between porosity and permeability. Figure 1 gives four very different examples: (a) shows an impermeable porous rock (e.g. shale); (b) a porous permeable rock; (c) a rock with very high porosity, but low permeability (e.g. pumice and clay) and (d) shows a low porosity but highly permeable rock (Baker. 1985).

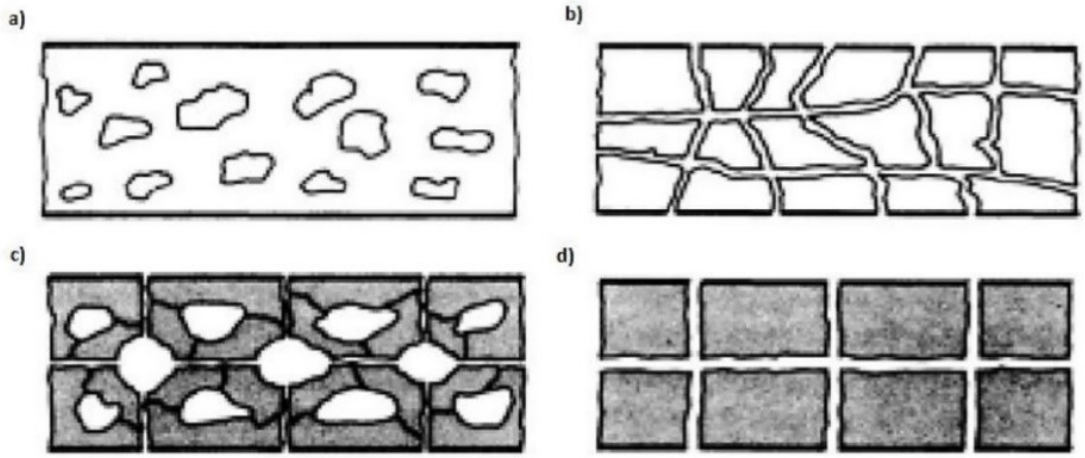

Figure 1. Types of porous media from Baker 1985.

From Figure 1, it is possible to identify that a pore network can become permeable if there is continuity and connectedness in the pores or void spaces. In addition, the pore size and width greatly influence the required pressure and resulting flow rate. The narrower the void spaces, the higher the pressure must be to force a fluid through the material. For durable concretes, the rate must be at the lowest possible level to prevent the possibility for intruded solutions (Heubeck, 2004). Figure 2 shows a modular relationship between porosity and

permeability (pore-tube model). Ideally, high performance concretes must have low porosity (ϕ) and low permeability (k) characteristics.

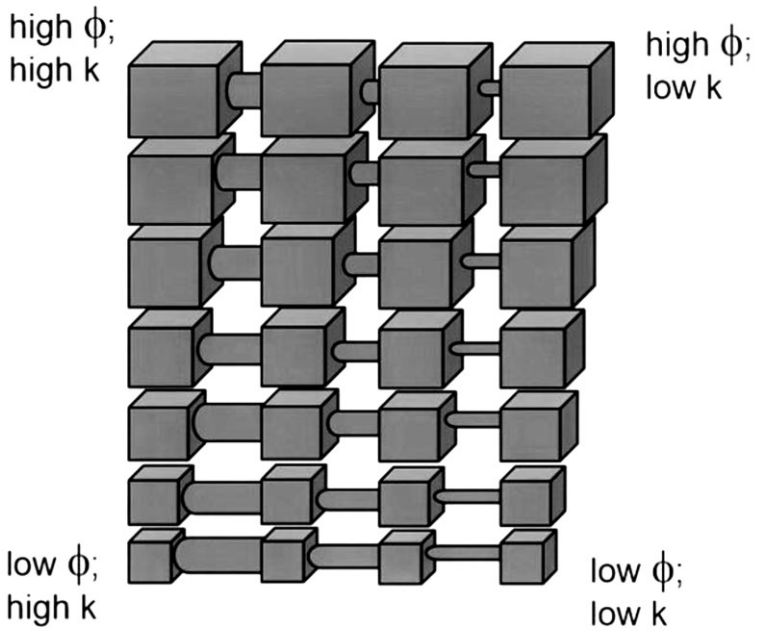

Figure 2. Porosity and permeability modular relationship

from (Heubeck, C. et al., 2004).

Generally, this is achieved when the water cement ratio is reduced and hence the space between the cement grains. Due to the hydration process, where chemical reaction between components of cement and water produce new solid phases (crystalline calcium hydroxide and cement gel) residual spaces are generally filled therefore decreased porosity is achieved.

Figure 3 shows the evolution of hardening cement paste. At early stages, cement paste is in a plastic state (cement grains immersed in water) where there are unhydrated cement particles (A). After one hour or more, there is a reduction in water due to hydration reactions, and subsequently, the void spaces between the cement grains are reduced, then the void pores in the cement paste are replaced by small voids termed "gel" pores (B). The remnants of water filled in space are known as capillary pores (large and small) but as the hydration reaction continues, particle packing efficiency will be increased diminishing or blocking the continuous capillary pores (C) until obtain a discontinuous pore network which lead to a less permeable and more durable concrete.

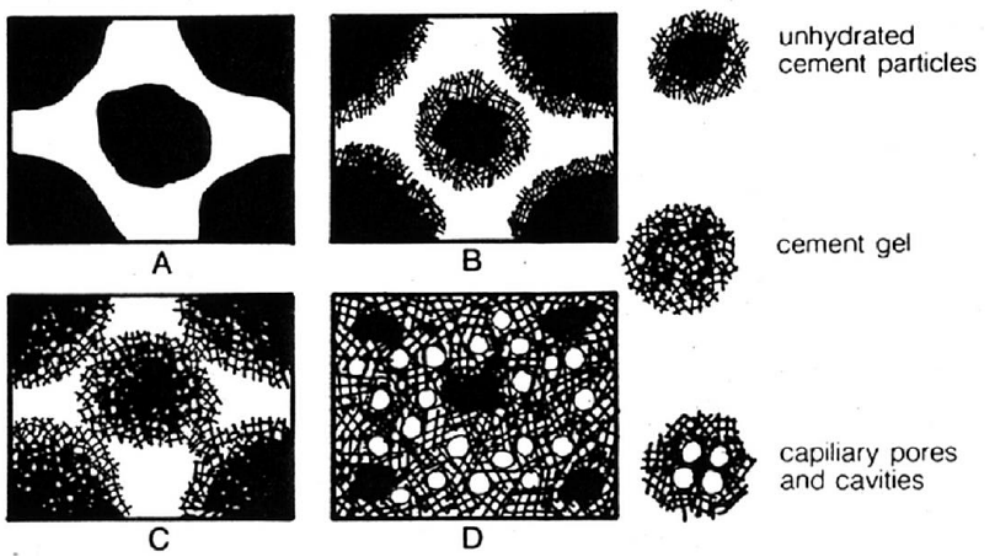

Figure 3. Hardening procedure evolution for cement paste from Powers et al., 1960.

It has been widely found that gel pores mostly influence the hydration progress, while the capillary pores mostly contribute to the water transport through the pore network (Powers et al., 1959). However, both of them are primarily controlled by the water to cement ratio, and concrete ingredients. Powers et al. (1959) identified the time required for achieving a discontinuous pore system with the approximate degree of hydration required. Table 1 illustrates that low water cement ratio concrete can achieve in less time and less degree of hydration a discontinuous pore system, avoiding the penetration and flow through the concrete body external substances carried by water or any fluids.

Table 1. Time required for achieving a discontinuous pore system

Powers et al., 1959.

Water cement ratio (w/c)	Time required	Approx. Degree of hydration required
0.4	3 days	0.5
0.45	7 days	0.6
0.5	14 days	0.7
0.60	6 months	0.95
0.70	1 year	1.0
>0.70	Impossible	>1.0

2.2 Electrical Methods for Concrete Durability

In this section, a review in the terminology plus the electrical methods developed through the years bearing on concrete's quality assurance are considered with special emphasis on

the Wenner four-electrode technique (Wenner, 1916). In subsequent sections, three groups of factors affecting test results are presented. The first group relates the factors that influence the probe spacing. The second group presents the influences of concrete mixtures, presence of steel reinforcing, effect of surface layer of different resistivity, and the effect of concrete non-homogeneity on resistivity. Finally, the last group shows the environmental effects such as temperature, moisture, and rainfall on electrical resistivity.

2.2.1 Background

During the 1920's and 1930's, due to concerns related to concrete durability, much interest was being taken with the measurement of concrete properties. While, significant efforts were made in order to measure permeability directly, the variability of replicate tests using water, solutions or gas showed that concrete is much more variable with respect to permeability rather than other properties such as strength. For instance, reproducible measurements of permeability can only be made if reproducible procedures are followed similar to testing for the 28 day strength of concrete with strictly controlled specimen preparation (Hooton. 1989). Regardless, true permeability tests have not been standardized and they are difficult to perform.

Concrete permeability can be measured indirectly through standard testing techniques; the majority of them are destructive and time consuming. However, during the most recent years, other techniques have been developed to indirectly measure this property in a non-

destructive manner, which are simple to use and not time consuming. Several studies were conducted showing it was possible to correlate concrete's durability with permeability, or in other words how easy fluids and/or gases can enter into or move through the concrete (Savas, 1999). This is due to the fact that permeability is affected by pore structure, water cement ratio (w/c), supplementary cementitious materials, temperature, moisture degree and other factors.

Electrical resistivity is the ability of concrete to resist electron transfer (Gowers and Millard, 1999). Electrical resistivity measurements on saturated concrete are easier to perform and can be related directly to permeability. In addition, such measurements have the advantage of being non-destructive. An electrical current passes through saturated pores containing ions from cement hydration (Shahroodi, 2010). A more tortuous path makes it more difficult for the electrons to pass through, resulting in higher electrical resistivity. Figure 4shows two examples of concrete pore networks; a) a network of connected capillary pores which generates a less resistive concrete and in b) disconnected capillary pores generating a more tortuous path leading to higher electrical resistivity.

Similar to permeability, concrete's resistance to electrical current and transport properties are related to its microstructure (porosity, pore connectivity and tortuosity), pore solution, and moisture content (Elkey and Sellevold 1995; Polder et al., 1995). When a voltage is applied, it creates an electric potential gradient that drives the flow of electrons through the concrete; for this reason, it is possible to characterize it as a physical parameter that can be used to indirectly characterize concrete's permeability and hence estimate its durability.

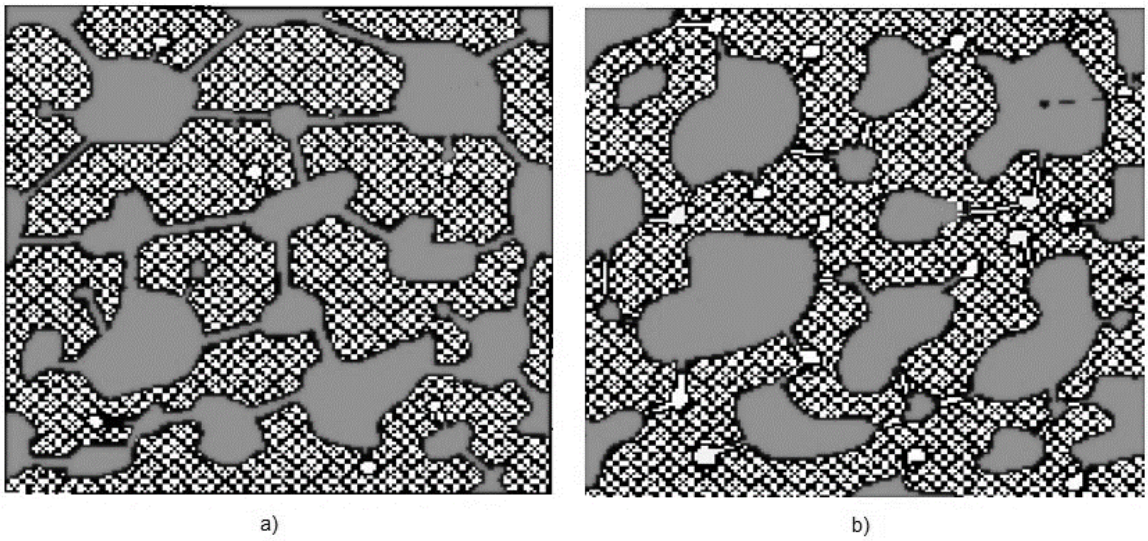

Figure 4. Pore network examples: a) connected pore network; b) not connected pore network by Neville et al. (1987).

Concrete is a composite material where aggregates and the cement matrix constitute the solid phase and water and/or admixtures the liquid phase. Electron flow is orders of magnitude higher in the liquid phase than in the solid phase. Therefore, an electrical circuit can be created, which can be linked to the circulation of fluids through the pore network. Table 2 shows the range of electrical resistivity values of common rock types. In a saturated concrete, the electrical resistivity values will be usually less than (10^3 Ω.cm) (Lopez and Gonzalez, 1993).

Table 2. Electrical resistivity of rocks by (Monfore et al., 1968).

Type of aggregate	Resistivity (kΩ-cm)
Sandstone	18.0
Limestone	30.0
Marble	290.0
Granite	880.0

Parameters such as chloride permeability and corrosion rate of reinforcing steel can be evaluated non-destructively by electrical resistivity, due to the fact that concrete is a semi-conductive material. As will be described in more detail later, electrical resistivity, as measured by AASHTO TP 95-11, can be used as an indication of concrete's ability to resist chloride ion penetration. Lower resistivity values indicate lower resistance to chloride permeability.

Electrical resistivity has also been correlated to the corrosion rate of steel reinforcements (Andrade and Alonso, 1996). Once corrosion is initiated, the corrosion rate is approximately inversely proportional to the electrical resistivity of concrete (Hornbostel et al., 2013). Moreover, electrical resistivity can be used to detect rebar corrosion. When this internal process starts, an electrical circuit is formed; a corrosion current passes through concrete from cathode to anode. Lopez and Gonalez (1993) found that steel corrosion is inversely proportional to resistivity over a wide electrical resistivity range. Table 3 shows the results obtained by Millard and Gowers (1991) where the electrical resistivity was measured on concrete samples with steel reinforcement. In the study, a

correlation between the corrosion level risk and resistivity was established. Low resistivity is related to a high risk of corrosion due to the concrete's poor ability to resist electron transfer; hence, the pore network is not complex and is permeable allowing water ingress more easily.

Table 3. Electrical resistivity values for rebar corrosion rate (Millard and Gowers, 1991).

Electrical resistivity (kΩ.cm)	Corrosion risk level
> 20	Low rate
10 - 20	Moderate rate
5 - 10	High rate
< 5	Very high rate

Electrical resistance is based on Ohm's law:

$$\mathbf{V = R.I} \quad [1]$$

Where, the voltage (V) is the force that drives the current through the material. It is called voltage or the potential difference between two elements. It is expressed in volts [V]. For instance, electrical circuits in homes have voltages of 120V/240V. The current (I) is the amount of electricity which flows through the material, is expressed in amps [A] or in milliamps [mA]. In common houses the electrical current is usually 100A or 200A. The Resistance (R) is the opposition to the flow of the current (ASP Construction 2003). The current will always seeks the easiest path; that is, the path which offers the least resistance. For materials such as copper or aluminum, the resistance may be low since electricity to

flow can pass easily through the material. For materials such as rubber, porcelain and fiberglass, the resistance is higher impeding the electricity flow. For porous materials, the resistivity is due to the pore network structure; granite has a higher resistance in comparison with sandstone, as was shown in Table 2.

Electrical resistivity ρ, is an intrinsic property that normalizes the measured resistance R and the geometry. For one dimensional flow of current, electrical resistance is normalized by the length, L, and cross sectional area, A, as shown in equation [2].

$$\boldsymbol{\rho = R\left(\frac{A}{L}\right)} \quad \text{[ohm·cm] or [Ω. cm]} \qquad [2]$$

Electrical conductivity is the material's ability to conduct an electric current, inversely proportional to electrical resistivity, as shown in equation [3].

$$\boldsymbol{\sigma = \frac{1}{\rho}} \quad \text{[S/m]} \qquad [3]$$

The following sections will introduce some of these electrical techniques explaining briefly the procedure, required testing setup, overall factors that can influence their use and finally, disadvantages of some of these testing techniques.

2.2.2 Electrical Conductivity Tests

The Rapid Chloride Permeability test indirectly measures the concrete's ability to resist chloride ion penetration. The test, designated as AASHTO T277 in 1983 by the American

Association of State Highway and Transportation Officials (AASHTO), was the first-ever test proposed for rapid qualitative assessment of chloride permeability of concrete (Chini et al., 2003). It was later adopted by ASTM International as a standard test method for electrical indication of concrete's ability to resist chloride ion penetration, designated as ASTM C1202 (2012). The main concept of the test is to monitor the amount of electrical current passing through a 50 ± 3 mm thick concrete slice with diameter ranging from 95mm to 102 mm over 6 hours. A potential difference of 60 V induces a direct current between two cells containing sodium chloride (NaCl) and sodium hydroxide (NaOH) solutions. Figure 5, shows the set up for the ASTM C1202 rapid chloride permeability test setup.

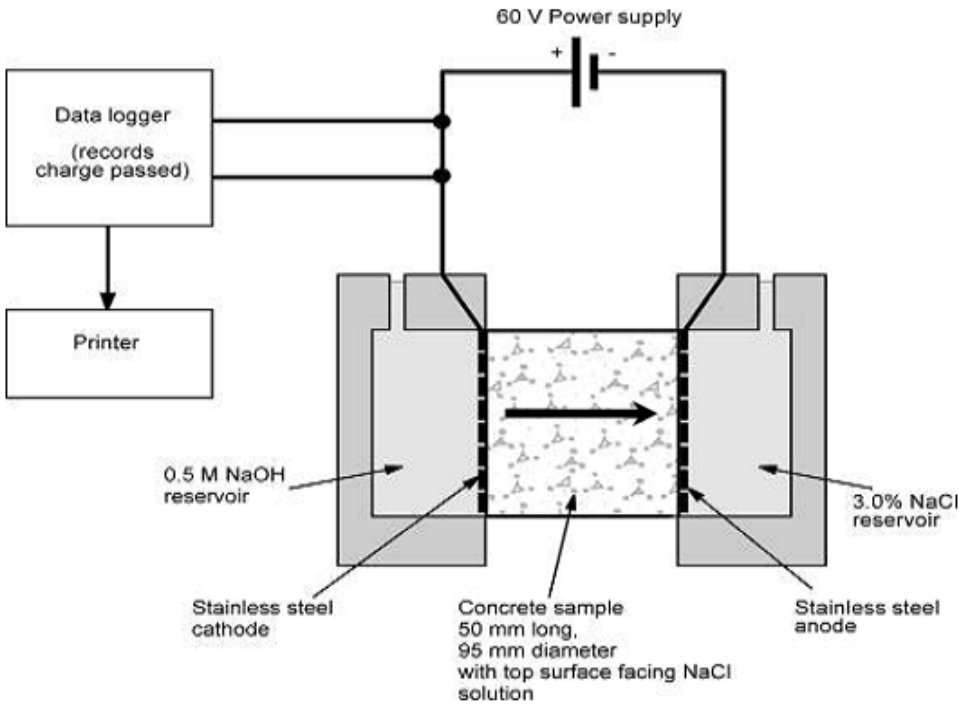

Figure 5. ASTM C1202-07 rapid chloride permeability test setup from Stanish et al., 1997.

Table 4 shows a classification of chloride ion penetrability based on the charged passed established by the standard (ASTM C1202, 2012). According to Chini et al. (2003), these values have been shown to be representative of chloride ion permeability, which is an indirect indication of the permeability of concrete.

Table 4. Chloride ion penetrability based on charge passed (ASTM C1202, 2007).

Charged passed (Coulombs)	Chloride Ion Penetrability
> 4000	High
2000-4000	Moderate
1000 - 2000	Low
100 -1000	Very Low
< 100	Negligible

Although this test is widely used, it is important to highlight some of its disadvantages found in the literature.

Disadvantages:

- For mixtures containing supplementary cementitious materials (SCMs), it is necessary to wait at least for 91 days in order to obtain a more stable pore solution chemistry and pore structure characteristics (Shi, 2004).
- The presence of reinforcing steel or other embedded electrically conductive materials may have a significant effect. Therefore, the test is not valid for specimen

with longitudinal reinforcing bars that can provide continuous electrical path between the two ends of the specimen (ASTM C1202, 2012).

- Temperature of the solution should be limited between 20 to 25 °C during measurements. As temperature increases, the reported RCPT level of permeability will be higher than the actual permeability level measured under the normal temperature (Bassouni et al., 2006).
- Although it is commonly referred to as the Rapid Chloride Permeability test, it neither measures chloride diffusion or water permeability, but electrical conductivity.

2.2.3 Electrical Resistivity Tests

In 2002, the Florida Department of Transportation (Kessler et al. 2008) started a research program to evaluate all available electrical indicators of concrete chloride penetration resistance in order to replace the most widely used method in the U.S., the Rapid Chloride Permeability (RCP) test (ASTM C1202, AASHTO T277). It was found that the surface electrical resistivity measured by an instrument called a Wenner probe without embedding any electrode into concrete presented the best option. Figure 6 shows the surface resistivity device set up used in the work research.

An advantage of electrical resistivity measurements is that, they can be performed in several ways non-destructively: using electrodes placed on a specimen surface, on opposite surfaces for cast specimens or cores taken from an existing structure, but also by

placing an electrode-disc or linear array or a four probe square array on the concrete's surface. A detailed description of the types of device techniques that can be used to measure this physical property will be detailed next.

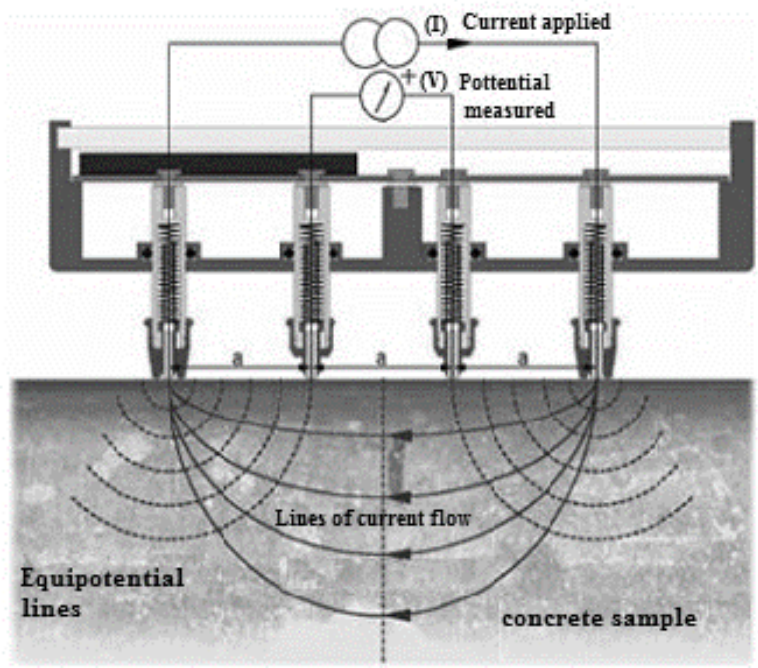

Figure 6. Surface resistivity device after Proceq SA manual (2013).

2.2.3.1 Bulk Electrical Resistivity Test

The bulk electrical resistivity test is generally used on cylindrical samples where two electrodes are placed on concrete opposite surfaces (Morris et al., 1996). Figure 7 shows the basic test setup, where an alternating current (AC) is applied, I and the potential voltage drop, P, is measured.

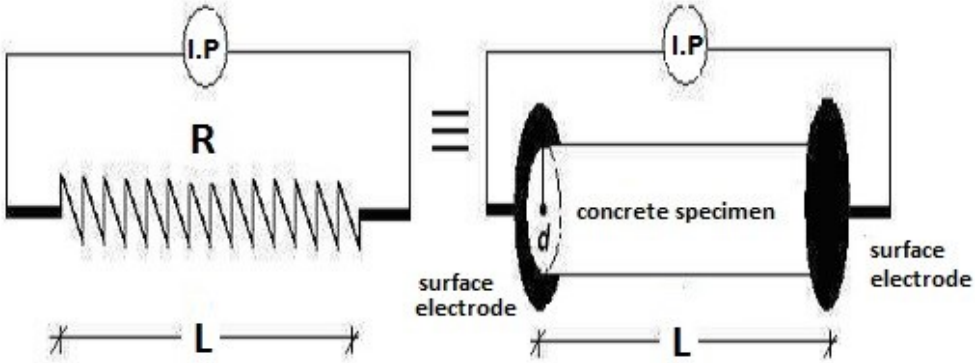

Figure 7. Bulk Resistivity setup after Shahroodi, (2010).

The electrical resistivity can be expressed as shown previously in equation [2], where, ρ is the electrical resistivity, L is the length of the sample, A is surface area of the specimen. Generally this technique is used in cylinders specimens or cores taken from existing structures.

Disadvantages:

- Unfortunately, the test is not suitable to directly measure the resistivity of any concrete element in the field, such as a column, wall or concrete beam unless the thickness is known and accessible. However, as the electron flow is undefined, equation 2 cannot be used to determine resistivity. In addition, Morris et al., (1996) reported that, the use can be complicated by the need for effective and uniform contacts between the end electrodes and concrete specimen end surfaces making it less accurate and poorly reproducible.
- It can be classified as a destructive technique due to the use of cores taken from an existing structure.

- Cylinders taken during casting may not accurately reflect the field concrete, so tests on cylinders are only indicative.

2.2.3.1 Surface Electrical Resistivity

The outer layer of any concrete cast in the field produces an external layer with different permeability in comparison with inner core concrete due to compaction, vibration, evaporation of water and curing. This outer layer is more susceptible to aggressive components of gases, water or chemical solutions after curing as it dries faster and results in the highest porosity which can lead to high possibilities for chemical reactions.

According to Kreijger (1984) this outer layer can be divided into three sub-layers, the first is the cement skin which is 0.1 mm thick, follow by a mortar skin of 5 mm thick approximately, then a concrete skin of approximately 30 mm thick or more. Generally, this layer is above the reinforcement. Figure 8 shows the composition of the outer layer or covercrete.

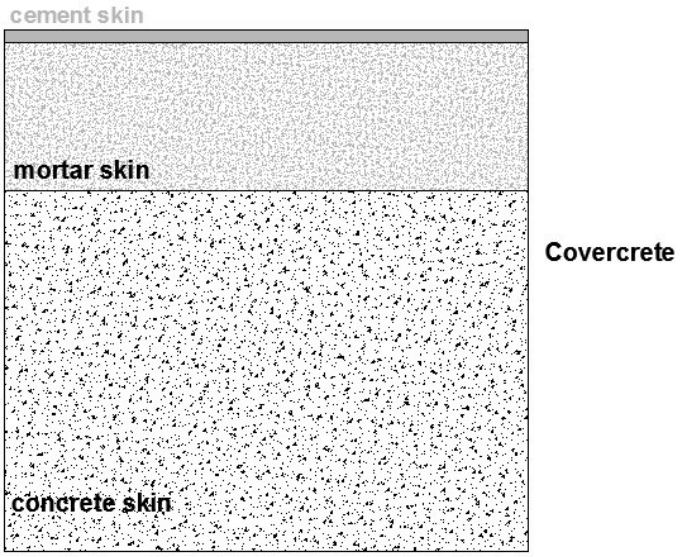

Figure 8. Covercrete layer composition (drawing without scale).

2.2.3.1.1 Surface Disc Test

This method involves an electrode placed on the concrete surface over steel reinforcement (rebar) and measures the resistance between the disc and the rebar. Figure 9 shows the setup of this test where a current I, passes through the covercrete and the surface electrical resistivity is measured between the rebar and the disc.

However, the test requires a connection to the reinforcement cage and full steel continuity (Polder et al., 2000) a requirement that makes it difficult, time consuming test to realize in the field due to the location of the steel rebar's must be known in addition to the covercrete thickness.

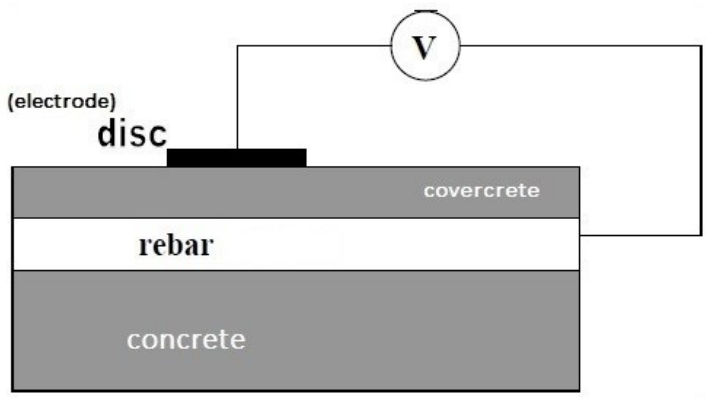

Figure 9. Setup of Surface disc test after Polder et al., (2000).

2.2.3.1.2 Four – Probe Square Array Test

This method also measures the in-place electrical resistivity non-destructively. In the device, the four probes are arranged in a square position; each electrode is spaced 5 to 10 cm. Figure 10 shows a representation of the device on a concrete sample.

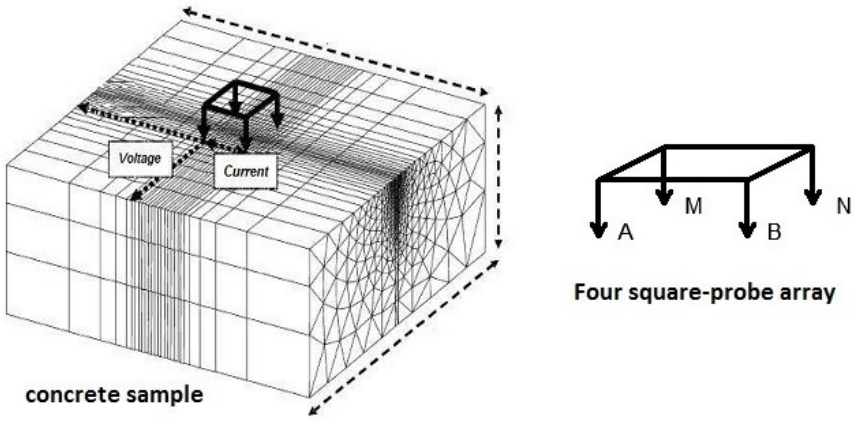

Figure 10. Setup of surface four square – probe array test after Lataste (2003).

The device works differently from the four-probe linear array device; in this case, two neighboring electrodes (A and B) introduce a known electrical intensity while the potential difference, ΔV created by the passage of the current in the material is measured between the two remaining electrodes (M and N) (Lataste et al., 2003).

2.2.3.1.3 Wenner Four Probe Line Array Test

The technique was first developed for the geologist's field in order to determine soil strata by Frank Wenner at the National Bureau of Standards in the 1910's and then adapted through time for concrete use. The Wenner four-electrode probe is an instrument where the electrodes are equally spaced on the surface of a saturated concrete element and its main function is to measure how easily charged species in the pore solution can be transported through the concrete under an applied electric field.

An alternating current (AC) is applied between the outer two electrodes and the voltage is measured between the middle two electrodes indicating the electrical surface resistivity of the element. The resistivity ρ of the concrete, for a semi-infinite geometry is the given by Millard et al. (1989).

$$\boldsymbol{\rho} = \frac{4\pi\, a\, R_C}{1+\left(\frac{2a}{\sqrt{a^2+4d^2}}\right)-\left(\frac{2a}{\sqrt{4a^2+4d^2}}\right)} \qquad [4]$$

Where a is the probe spacing, d is the depth of the embedded electrodes and R_c represents the concrete resistance. Figure 11 shows an example of embedded electrodes in a concrete sample.

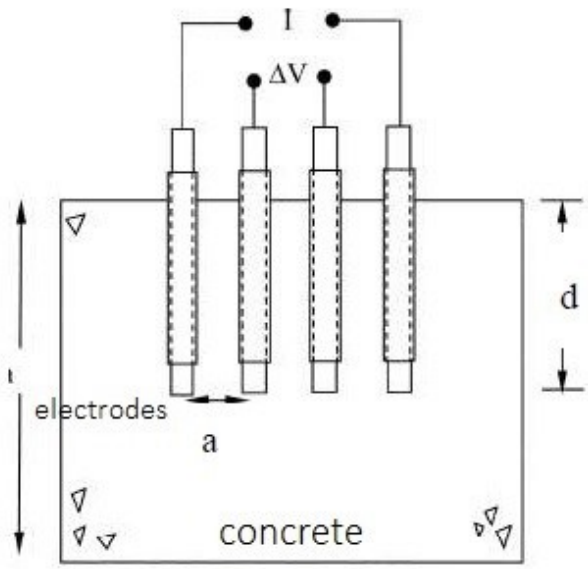

Figure 11. Embedded electrodes after McCarter et al., 2009

Moreover, if the electrodes are not embedded in the concrete specimen and the electrical resistivity measured at the concrete´s surface (d= 0), equation [5] can be simplified as;

$$\boldsymbol{\rho = 2\pi\, a\, \frac{V}{I}} \qquad [5]$$

Where a is the contact spacing in centimeters. Figure 12 shows a schematic representation of four-electrode resistivity test where the AC current is applied between the outer two electrodes and the voltage is measured between the middle two electrodes indicating the electrical surface resistivity of the element.

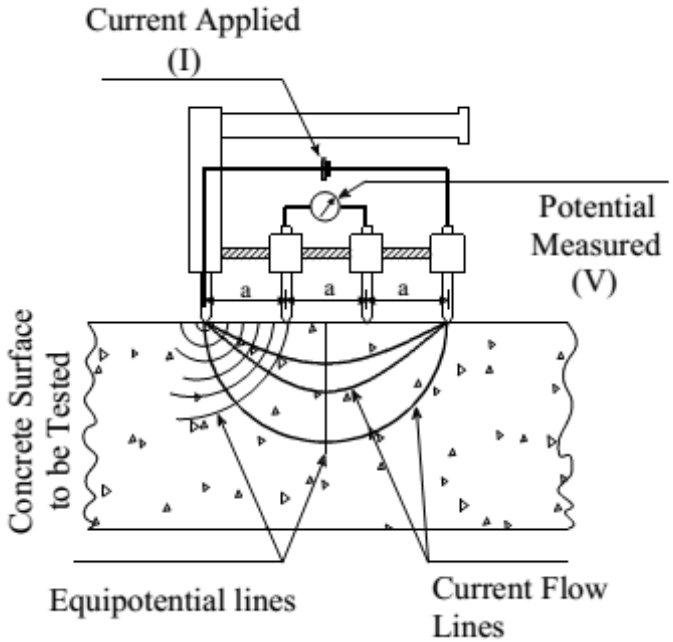

Figure 12. Schematic representation of four-electrode resistivity test by Kessler al. (2008).

Figure 13 shows the strong relationship found between the use of the Wenner four-probe line array with the Rapid Chloride Permeability (RCP) test of (R^2 of 0.95) for limewater saturated cylinders tested at 28 days (Kessler et al., 2008).

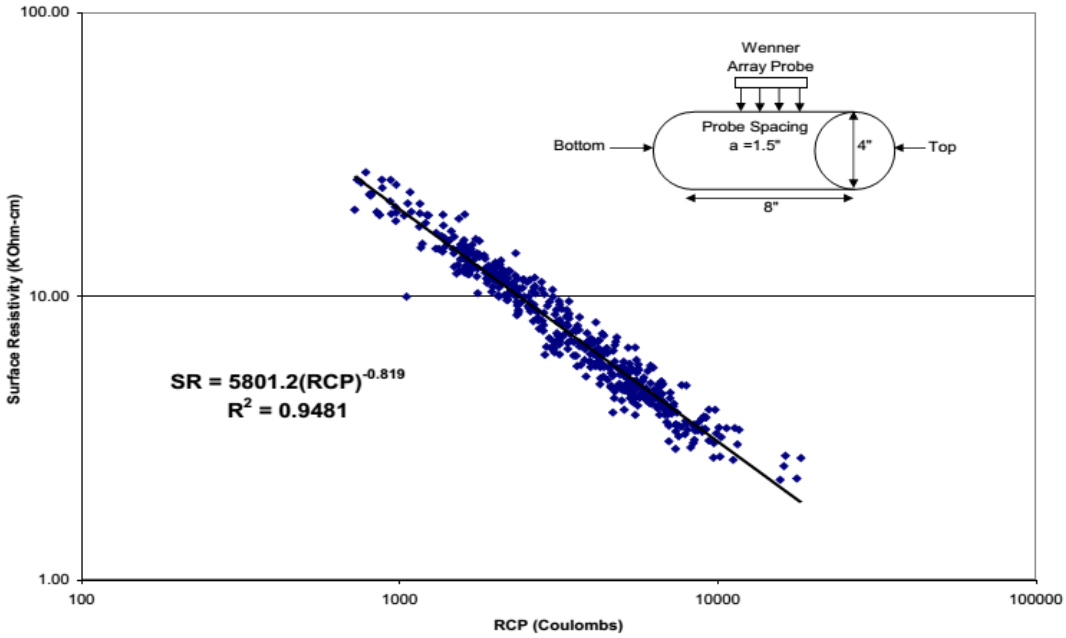

Figure 13. Correlation between Rapid Chloride Permeability and Surface Resistivity on saturated samples at 28 days reproduced from Kessler et al., 2008.

Additionally, with the use of this instrument it was possible to obtain a less time-consuming test, with a low coefficient of variation and it was found to be inexpensive compared with the RCP test, concluding that surface resistivity can be used as an electrical indicator of concrete chloride penetration resistance (Kessler et al., 2008). Later on, this statement was reinforced by Shahroodi (2010) and Rupnow and Icenogle (2011). Table 5 shows the correlation between electrical resistivity and chloride ion penetration implemented by AASHTO.

Table 5. Correlation between electrical resistivity and chloride ion penetration AASHTO, TP 95-11 (2011) reproduced from Yanbo, L. et al. (2014).

Chloride Ion Permeability	Surface resistivity (kΩ-cm) of 10x20cm cylinder, probe spacing a=3.81 cm (1.5in)	Bulk resistivity (kΩ-cm)
High	<12	<6.3
Moderate	12 to 21	6.3 to 11
Low	21 to 37	11 to 20
Very Low	37 to 254	20 to 134
Negligible	>254	>134

Note: The resistivity values presented here are corrected resistivity values after the correction geometry coefficient factor was applied. This correction geometry coefficient will be further explained in detail in section 2.3.4.

However, in practice this technique must be used with care or significant errors can be obtained on each reading. According to Gowers and Millard (1999), there are some principal sources of factors influencing probe spacing in the Wenner technique such as, geometrical constraints, surface contacts, concrete non-homogeneity, presence of steel reinforcing bars, effect of surface layer of different resistivity, effect of ambient environment conditions that will be described next.

2.3 Factors Influencing Probe Spacing in the Wenner Four Probe Technique

It was found there are some influences regarding use of resistivity measurements that easily can be avoided but some others are more complex. This first set of parameters is directly related with the use of the Wenner four probe device: the influence of the use of different probe spacing, the effect of surface contacts between the probe tips and concrete, the geometrical constraints found on cylindrical samples, and the specimen geometry.

2.3.1 Surface Contacts

Full contact between the Wenner four probe device and the surface must be applied to obtain reliable measurements. This is particularly important for the two inner contacts measuring the potential difference. An uneven electrical contact generates unreliable values. According to Gowers and Millard (1999), the use of a relatively low frequency and alternating current (AC) helps to minimize misleading values. The use of a direct current (DC) signal lead to problems due to polarization effects at the surface contacts.

2.3.2 Geometrical Constraints

Commonly, the dimensions of concrete elements being studied on site are large in comparison to the Wenner four probe electrode spacing, a. In this case, the assumption of a semi-infinite geometry does not lead to significant errors. However, if the dimensions of the concrete element are relatively small, such as cylinders or slabs samples, the current is constricted to flow into a different field pattern leading to an overestimation of the evaluation of the resistivity of the concrete. Figure 14 shows a schematic representation of resistivity measurements of concrete samples.

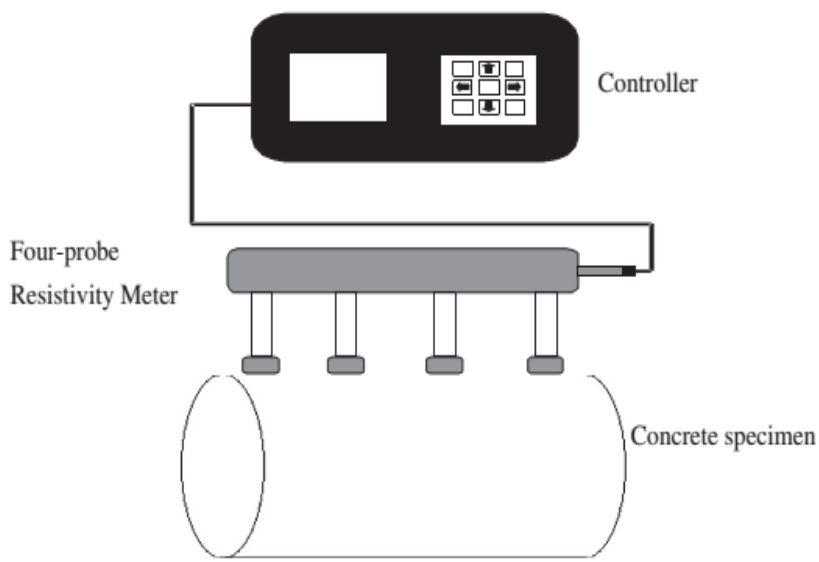

Figure 14. Representation of resistivity measurements of concrete samples from Chun-Tao et al. (2014).

According to (Gowers and Millard 1999) through experimental findings, the contact spacing should not exceed ¼ of the concrete section dimensions. The distance of the contacts from any element edge should also be at least twice the contact spacing. When the test is conducted on cylindrical specimens, the semi-infinite assumption is not valid as the large probe spacing and the small geometry generates a flow interfering with coarse aggregates, necessitating estimating a factor to account for the constricted flow in the material. Spragg et al. (2013a) established the following correction coefficient factor (k), equation [6], using the simulations developed by Morris et al. (1996).

$$\boldsymbol{k = 1.10 - \frac{0.730}{d/a} + \frac{7.34}{\left(d/a\right)^2}} \qquad [6]$$

The use of this correction is only needed when $d/a \leq 6$ or $L/a \geq 6$. According to Spragg et al. (2013a) and Liu et al. (2014), for a standard cylinder 10 cm x 20 cm, the correction coefficient value ranges from 1.8 to 1.9 when using the common spacing of 38 mm. Figure 15 shows the relationship between the correction coefficient k and cylindrical samples sizes by Morris et al. (1996).

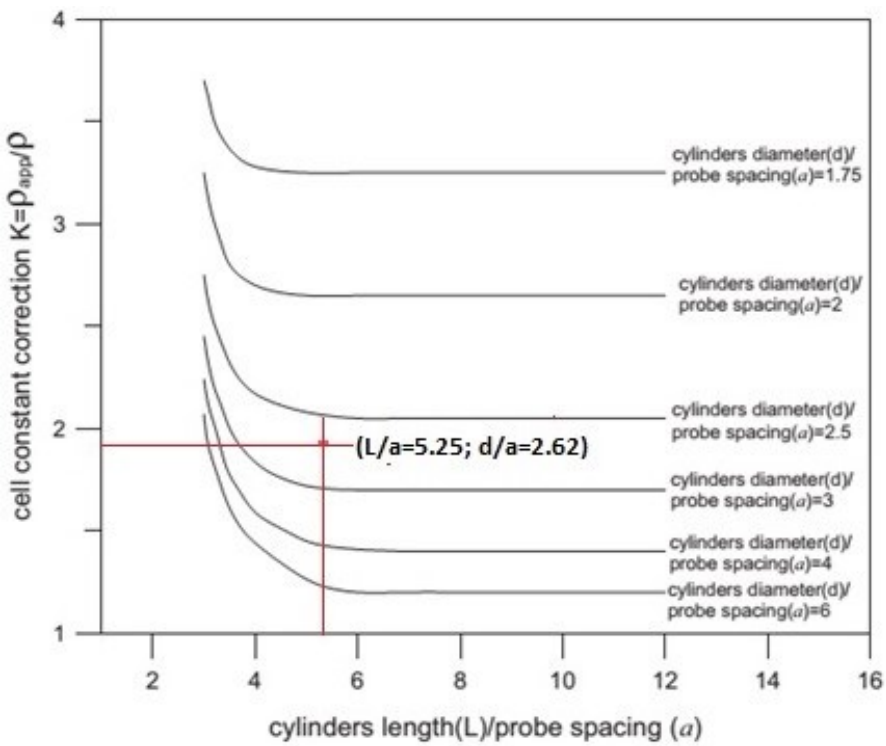

Figure 15. Relationship between the correction geometry factor (k) and standard cylinders (10x20cm) adapted from Morris et al. (1996).

Then, the real corrected resistivity (ρ_{real}) can be obtained using equation 7, where, (ρ_{app}) represents the apparent (measured) resistivity.

$$\boldsymbol{\rho_{real} = \frac{\rho_{app}}{k}} \qquad [7]$$

2.3.3 Probe Spacing

Many commercial devices are supplied with a stand for mounting the device and a variable spacing probe that allows probe spacing to be varied generally between 20 mm and 70 mm. This allows the device to measure concrete with larger aggregate sizes. In a study conducted by Shahroodi (2010), the surface resistivity was measured using different probe spacing in laboratory specimens both with standard cylinders (100 x 200 mm) and circular slabs (406 mm diameter x 75 mm). All the mixtures used a w/c range of 0.35 to 0.45 and for each mixture cylinders and slabs were cast, then the resistivity values were measured at 3, 7, 28, 56 and 91 days. Table 6 shows the values obtained at 91 days.

Table 6. Laboratory Mixtures after Shahroodi (2010).

Mixture Information		sample geometry	Surface resistivity (kΩ-cm) before cell correction				Surface resistivity (kΩ-cm) after cell correction				Average surface resistivity (kΩ- cm)
			Probe spacing (mm)				Probe spacing (mm)				
			25/20 *	30	40	50	25/20 *	30	40	50	91 Days
High Performance concrete - Silica Fume cement w/cm 0.35	HPC	cylinder	121.7	144.4	174.7	220.6	121.7	127.1	120.5	116.9	121.6
		slab	230.4	295.3	300.2	311.3	230.4	236.2	222.1	202.3	222.8
High Performance concrete - Silica Fume cement w/cm 0.35	HPC +	cylinder	114.7	132.3	160.3	208.3	114.7	116.4	110.6	110.4	113.0
		slab	154.3	194.3	230.7	254.6	154.3	155.4	170.7	165.5	161.5
Type I/II Portland Cement - Slag w/cm 0.40	PCSL 0.40	cylinder	48.3	57.3	65.3	88.6	48.3	50.4	45.0	46.9	47.7
		slab	54.8	75.0	81.4	99.0	54.8	60.0	60.2	64.4	59.9
Type I/II Portland Cement - Slag w/cm 0.45	PCSL 0.45 +	cylinder	30.3	35.4	45.8	60.9	30.3	31.2	31.6	32.3	31.4
		slab	28.4	43.1	54.6	65.9	28.4	34.4	40.4	42.8	36.5

* Note: 25mm spacing for the cylinders and 20 mm for the slabs.

The probe spacing was varied from 20 to 50 mm resulting increases in measured resistivity. However, using the correction coefficient factor (k), a reduction in the variation was observed. Also, it was found that at early ages (3 and 7 days) the use of a cell correction doesn't have an important reduction on electrical resistivity values, but at later ages, such

as 91 days, an important reduction and close tendency to a same value can be obtained using different probe spacing. If this correction is not done, the resistance measurements can vary by orders of magnitude (Spragg et al., 2013). Figure 16 shows the effect of the penetration depth using the Wenner probe device where a larger probe spacing leads to a greater electrical current penetration into concrete.

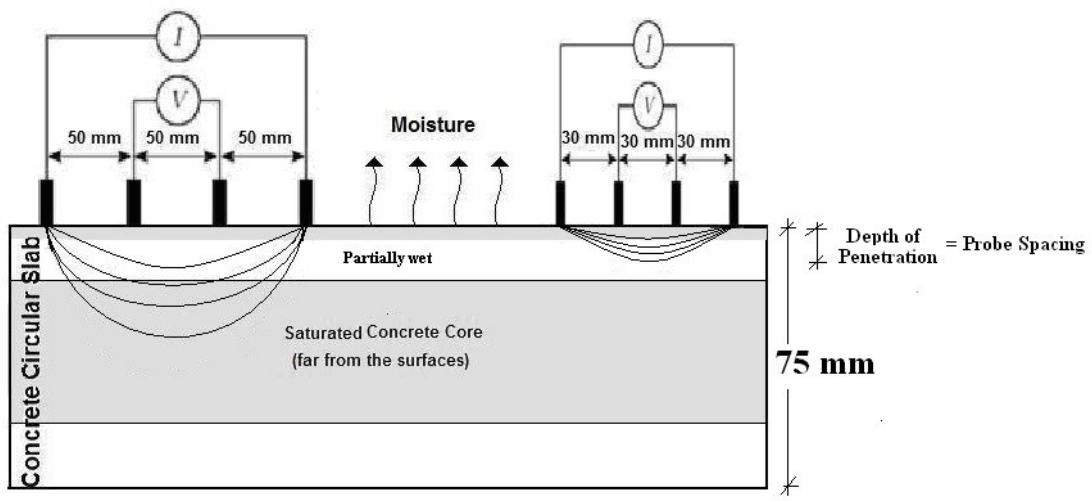

Figure 16. Probe spacing effect on the penetration depth using the four-line Wenner probe device reproduced from Polder (2001).

2.3.4 Specimen Geometry

Studies performed by Bryant et al. (2009) and Shahroodi (2010) confirmed the dependency of the measured resistance to the specimen geometry. Table 7 shows the laboratory mixture designs used by Bryant et al. (2009). All the mixtures were designed with an average w/c of 0.40 and for each mixture cylindrical specimens (10x20 cm) and

prisms or slabs (28x28x10.2 cm) were cast. Then, the resistivity values were measured at different ages (7, 14, 28 and 91 days). Although measurements were corrected for geometry, generally, cylindrical specimens present an average of + 24% higher electrical resistivity values in comparison with slabs at 91 days.

Only those samples containing Portland cement and diabase presented a different behavior where the slab's resistivity was higher. A similar behavior was estimated at 14 and 28 days; where without exceptions, all the cylinders specimens showed a higher resistivity values in comparison with slabs. Cylinders were higher by an average of 23% and 37% at 14 and 28 days, respectively.

Table 7. Corrected resistivity of cylinders and slabs (Bryant et al. 2009).

Mixtures Information		Geometry	Time (Days)			
			7	14	28	91
			Surface Resistivity (kΩ- cm)			
Type I/II Portland Cement	G	cylinder	-	13.58	16.31	21.18
		slab	9.35	8.43	14.81	23.07
Limestone Cement	LS	cylinder	-	17.44	30.06	28.61
		slab	21.16	14.86	20.54	27.42
Diabase	D	cylinder	-	15.63	22.14	21.41
		slab	10.08	14.99	19.02	52.27
Diabase - Slag	DSG	cylinder	-	29.06	39.55	60.49
		slab	15.87	21.64	30.55	48.21
Diabase - Fly Ash	DFA	cylinder	-	19.06	24.57	69.94
		slab	10.08	14.99	19.02	52.27
Diabase - Microsilica	DMS	cylinder	-	20.26	48.59	53.38
		slab	13.7	21.91	25.37	40.32

Table 8 shows the laboratory mixes design used by Shahroodi (2010) the real surface resistivity (ρ_{real}) after applying the correction geometry factor.

Table 8. Corrected resistivity of cylinders and slabs (Shahroodi 2010).

Mixtures Information		Geometry	Time (Days)			
			7	28	56	91
			Surface Resistivity (kΩ- cm)			
High Performance concrete - Silica Fume cement w/cm 0.35	HPC	cylinder	37.3	110.0	114.7	121.6
		slab	20.0	113.1	190.9	2228.0
High Performance concrete - Silica Fume cement w/cm 0.35	HPC +	cylinder	36.0	106.0	108.5	113.0
		slab	17.0	102.8	145.9	161.5
75% Silica Fume cement -25% Slag w/cm 0.40	SFSL 0.40	cylinder	30.8	93.6	99.7	107.2
		slab	16.1	90.8	127.3	140.8
Type I/II Portland Cement - Slag w/cm 0.40	PCSL 0.40	cylinder	16.0	32.2	35.7	47.7
		slab	8.2	25.5	37.9	59.8
Type I/II Portland Cement - Slag w/cm 0.40	PCSL 0.40 +	cylinder	10.5	20.8	29.8	40.7
		slab	6.4	22.3	30.7	51.9
Type I/II Portland Cement - Slag w/cm 0.45	PCSL 0.45	cylinder	8.7	20.6	22.7	39.5
		slab	4.9	18.1	24.6	42.0
Type I/II Portland Cement - Slag w/cm 0.45	PCSL 0.45 +	cylinder	8.0	19.1	25.6	31.3
		slab	4.5	15.7	24.8	36.5
100% Type I/II Portland Cement w/cm 0.45	PC 0.45	cylinder	5.0	9.8	12.0	15.2
		slab	3.0	8.7	12.8	23.7
100% Type I/II Portland Cement w/cm 0.45	PC 0.45 +	cylinder	4.7	7.4	10.2	11.9
		slab	3.0	7.7	11.1	19.5

The results obtained by of Shahroodi (2010) are different from the ones obtained by Bryant et al. (2009) described before. In this case, the slabs specimens showed an average 25.8% higher value in comparison with cylinder specimens after 91 days. The highest difference can be observed in the first three mixtures containing silica fume and slag with low water cement ratio (w/c 0.35). The same tendency was observed at 56 days although the difference was an average of 14.8% higher. Only at 28 days cylinders specimens presented

an average of 13% higher resistivity but only for the mixtures HPC+, SFSL 0.40, PCSL 0.40, PCSL 0.45 PCSL 0.45+ and PC 0.45.

Some alternatives can be presented as possible explanations for the difference in the two studies. The first one is the geometry correction coefficient described previously in section 2.3.2 in order to avoid the overestimation in the electrical values due to the size sample. Another factor is the surface texture, which is important according to Bryant et al. (2009). The cylinders are always tested on the cast surface along its height (more uniform and smoother) than the rough finished surface presented in the prism or slabs specimens. The variability can be reduced by abrading the surface to a smoother surface and/or material of the resistivity meter contact probes. Lastly, the variability associated with Wenner probe test arises mainly from factors as, the device, operator, material, production and curing process and they can be represented in the following expression (Equation 8, Spragg et al., 2013). Although in this research the variables were constant (device, operator, production and curing), in cases where this cannot be achieved, it is an important consideration.

$$\boldsymbol{\sigma_{total}} = \sqrt{\boldsymbol{\sigma^2_{machine}} + \boldsymbol{\sigma^2_{operator}} + \boldsymbol{\sigma^2_{material}} + \boldsymbol{\sigma^2_{production}} + \boldsymbol{\sigma^2_{curing}}} \qquad [8]$$

According to Spragg et al. (2013) it was estimated from laboratory conditions the variability of machine, operator, and material as 1.7%, 1.8%, and 3.4%, respectively due to the repeatability; matching with the findings of Rupnow and Icenogle et al. (2011).

2.4 General Factors Influencing Electrical Resistivity due to Concrete Mixture

According to literature, the parameters of concrete mixture, pore solution, supplementary cementitious materials, concrete's age, water to cement ratio (w/c), the presence of steel reinforcing bar, the effect of surface layer of different resistivity and concrete non – homogeneity or use of mineral admixtures or supplementary cementitious materials such as blast furnace slag, fly ash or silica fume basically affects the concrete porosity (pore structure) and workability of the mix. In the following section a detailed explanation of them will be presented.

2.4.1 Effects of Water Cement Ratio Effect on Surface Resistivity

A high percentage of porosity is caused by a higher w/c ratio, generating lower electrical resistivity. In addition, the degree of hydration affects resistivity as further hydration typically reduces the concrete porosity and how these pores are interconnected (Presuel-Moreno and Liu 2012).

Rupnow and Icenogle (2011) observed that generally an increase in w/c leads to a decrease in surface resistivity indicating a more permeable concrete. Table 9 shows the mixture designs used for this purpose.

Table 9. Mixtures design by Rupnow et al., (2011).

Mixtures Information		w/cm		
		0.35	0.5	0.65
		Surface Resistivity (kΩ- cm)		
100% - Type I/II Portland Cement	100 TI	21.0	9.5	8.0
80% PC - 20% Fly Ash Class C	80TI - 20C	22.0	15.0	12.0
80% PC - 20% Fly Ash Class F	80TI - 20F	28.0	15.0	14.0
50% PC - 50% Grade 100 Slag	50TI - 50G100S	30.5	49.5	41.5
50% PC - 50% Grade 120 Slag	50TI - 50G120S	34.0	40.0	39.0
95% PC - 5% Silica Fume	90TI - 10SF	42.0	24.0	22.0
90% PC - 10% Silica Fume	95TI - 5SF	29.0	15.0	13.0

However, for those concrete mixes containing slag, an anomalous behavior was observed. When the water cement ratio (w/c) was increased from 0.35 to 0.65, the surface resistivity values increased, which in terms of permeability means a less permeable concrete at 28 days.

2.4.2 Pore Solution in Cementitious Systems

Electrical resistivity measurements on porous material such as, rocks and ceramics had been widely measured over the last decades. However, there is a difference between them and concrete due to the microstructure and pore solution changes over time. For rocks and ceramic materials, these properties remain without significant changes through time (Spragg et al., 2013) since there is not a hydration process. The pore solution in cementitious materials forms when the water used in the mixing process reacts with cement. As a result, cement releases conductive ions, i.e., potassium (K^+), sodium (Na^+),

calcium (Ca^{2+}), hydroxide (OH^-), and sulfate (SO_4^{2-}) into the pore solution. (Barneyback and Diamond 1981; Elkey and Sellevold 1995; McCarter 1996). However, the amount of conductive ions released depends on the chemistry of the cement, the water used in the mixing process and the hydration degree of the cementitious materials (Spragg et al., 2013). Figure 17 shows a schematic representation of the ion conductivity in porous materials.

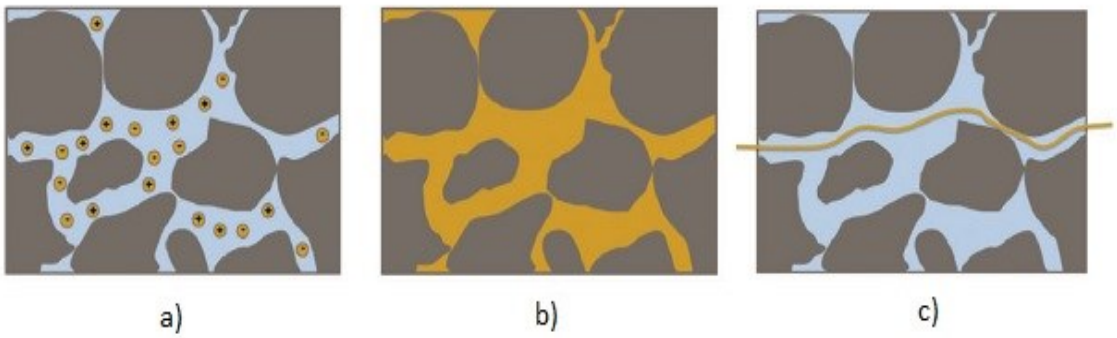

Figure 17. Conductivity in porous material, a) ions released in the pore solution; b) porosity; c) connectivity, reproduced from Spragg et al. (2013).

Porosity can be described as the volume of pores in the system and the connectivity characterizes the way pores are connected through the three-dimensional system or the concrete's pore network (Spragg et al., 2013).

2.4.3 Supplementary Cementitious Materials

The use of supplementary cementitious materials (SCMs) either in blended cements or as individual constituents in a concrete mixture have proven to improve the paste phase due to the reduction in capillary porosity generating a less permeable concrete with a more complex pore structure. In addition, SCMs reduce hydroxyl ions (OH^-), decreasing conductivity of the pore solution. Kessler et al. (2008) observed that as the percentage of Portland cement replacement increased with supplementary cementitious materials the surface resistivity value increased, indicating a less permeable concrete. Later on, this behavior was also observed in the studies conducted by Bryant et al., (2009), Presuel – Moreno et al., (2010) and Rupnow and Icenogle (2011).

2.4.3.1 Fly Ash Background

Generally known as a finely divided residue (a powder resembling cement) that results from the combustion of pulverized coal in electric power generating plants and is primarily silicate glass containing silica, alumina, iron, and calcium. Figure 18 shows the scanning electron microscope (SEM) of fly ash particles where all particles are solid spheres meanwhile ground materials, such as Portland cement, have solid angular particles (Kosmatka et al, 2002).

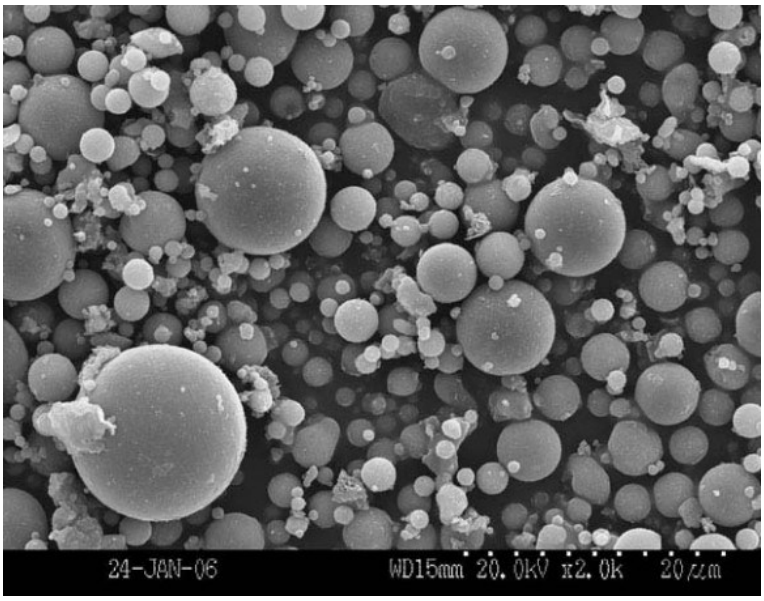

Figure 18. Scanning electron microscope of fly ash particles by Belviso et al., (2011).

2.4.3.2 Ground granulated blast-furnace slag Background

Ground granulated blast-furnace slag, also called slag cement, is made from iron blast-furnace slag; it is a non-metallic hydraulic cement consisting essentially of silicates and aluminum silicates of calcium developed in a molten condition simultaneously with iron in a blast furnace. The molten slag, at a temperature of about 1500 °C, is rapidly chilled by quenching in water to from glassy sand like granulated material. Figure 19 shows the scanning electron microscope (SEM) of slag particles with rough and angular shapes (Kosmatka et al, 2002).

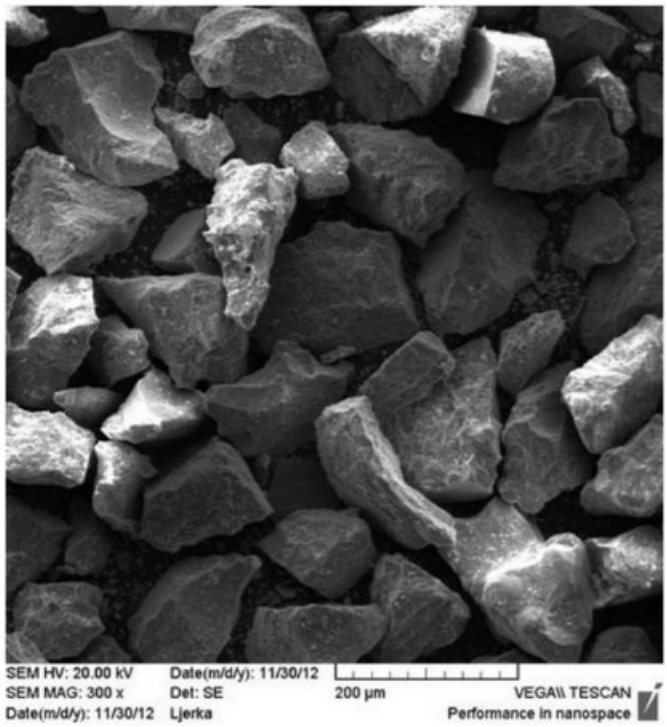

Figure 19. Scanning electron microscope of Slag particles by Rađenović et al. (2013).

Table 10 shows the laboratory mixture designs used by (Kessler et al., 2008). The surface resistivity was measured in cylinder specimens (10 x 20 cm) at different ages starting from 8 to 1092 days (3 years) in most of the cases. All the cylinders specimens contained a w/c of 0.35 and were without reinforced steel. It can generally be observed that the mixtures containing SCMs had higher resistivity than Portland mixtures (CPR01, 02, 03 and 12) at all ages. The only exception is one mixture (HRP2) at 14 days when the fly ash did not have sufficient opportunity to hydrate. Over time, the resistivity of the Portland mixtures increases slightly while those with SCMs increase quite significantly. This indicates the formation of secondary CSH and resulting in decreased porosity.

Table 10. Resistivity of the Laboratory Mixes after Kessler et al. (2008).

Laboratory Mixtures Design	w/cm	0,35						
		Surface Resistivity (kΩ- cm)						
	Days	14	28	56	91	364	546	1092
100 % - Type I/II Portland Cement	CPR01	6.1	6.9	7.5	7.8	9.6	10.6	12.8
100 % - Type I/II Portland Cement	CPR02	8.5	9.5	10.1	10.8	12.6	13.9	21.1
100 % - Type I/II Portland Cement	CPR03	5.5	5.9	6.2	6.6	7.2	8.9	14.1
72 % Type I/II POC - 20 % Fly Ash - 8% Silica fume	CPR08	13.8	24.3	33.1	38.9	56.5	65.2	69.8
90 % Type I/II POC - 10 % Metakaolin	CPR09	38.7	33.5	39.3	38.9	60.0	55.6	61.5
70 % Type I/II POC - 20% Fly Ash - 10 % Metakaolin	CPR10	34.6	31.7	37.6	43.5	85.3	90.3	113.8
100 % - Type I/II Portland Cement	CPR12	8.1	8.9	9.7	9.9	12.3	12.9	13.5
70 % Type I/II POC - 20% Fly Ash - 10 % fine fly Ash	HRP2	5.5	13.9	25.4	47.9	106.7	-	-
73 % Type I/II POC - 20 % Fly Ash - 7% Silica fume	TB2H5	16.2	29.8	56.7	82.09	90.7	-	-
50 % Type I/II POC - 10 % Fly Ash - 40 % Slag	TB4H5	15.6	19.6	34.5	42.9	54.4	-	-
50 % Type I/II POC - 30 % Fly Ash - 20 % Slag	TB5H5	11.0	20.4	35.7	51.2	91.9	-	-
40 % Type I/II POC - 20 % Fly Ash - 40 % Slag	TB6H5	14.1	25.5	40.9	52.4	79.4	-	-
40 % Type I/II POC - 40 % Fly Ash - 20 % Slag	TB7H5	9.1	17.6	28.9	45.0	80.3	-	-
30 % Type I/II POC - 10 % Fly Ash - 60 % Slag	TB8H5	22.0	36.0	49.6	62.9	66.3	-	-

Additionally, Shahroodi (2010) also observed that the mixtures containing slag showed a higher electrical resistivity after 10 days than plain cement concrete due to a denser and less porous pore system. According to Bassuoni et al. (2006) using silica fume as a blend alternative also lead to a higher density of cement paste generating a more tortuous path for the electrical charge passing through the pore system.

2.4.4 Concrete Age

The surface resistivity is affected by the age of the specimen due to dynamically changing connectivity of the pore structure and ionic concentration. The pore solution increases with

age generating higher electrical conductivity (lower resistivity) during the first 28 days (Nokken and Hooton 2006). Figure 20 shows the age effect on surface resistivity values for the laboratory samples tested by Kessler et al. (2008). Although resistivity increases with age for all mixtures, changes are more notable for mixtures containing supplementary materials. In the Figure, it is possible to see a relatively constant resistivity behavior value is obtained for mixes, CPR01, CPR02, and CPR03 after 91 days. Meanwhile, samples with supplementary cementitious materials, such as slag, the increase is significantly higher up to 91 days and continues increasing this time.

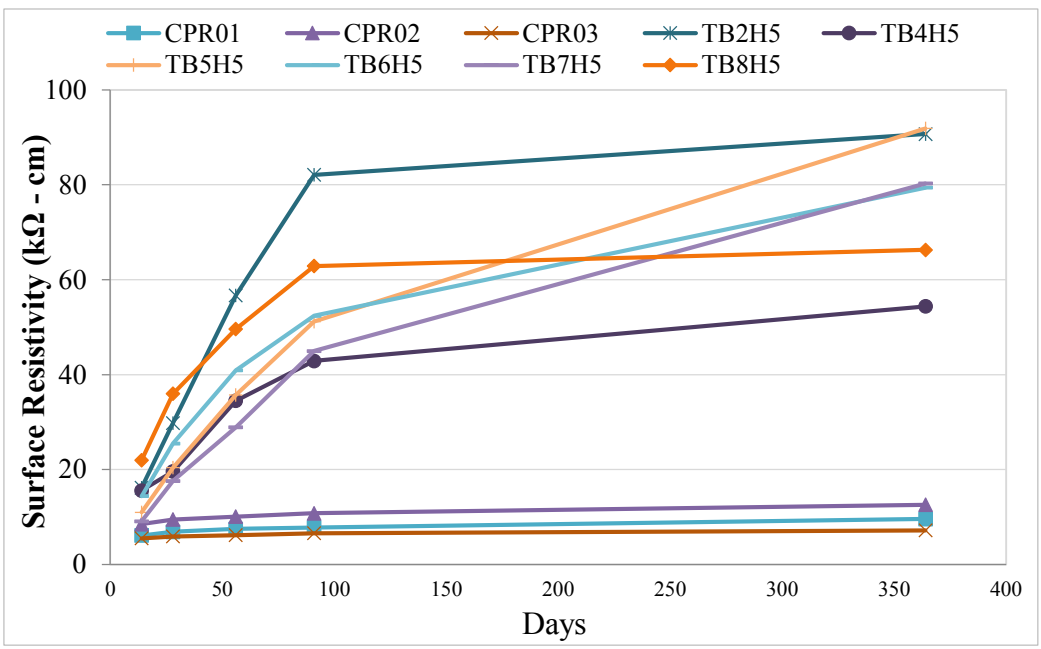

Figure 20. Effect of the age in concrete samples after Kessler et al., (2008).

According to Larsen et al. (2007), the surface resistivity generally increases over time. In a test conducted for the Norwegian Public Roads Administration, reinforced beams with electrodes at three different points (top, middle and bottom) with dimensions (3x0.15x0.30

m) were cast and then submerged half of the beam into sea-water. After 8 months, in June 1998, the beams were removed from this condition and the resistivity was measured using a frequency of 1000Hz. Later on, in January 2006, 2 days after removal from sea-water the resistivity was measured at the same three points. Although the season was different, hence the temperature for the three points, the study concluded that, when the concrete element is atmospherically exposed, the surface electrical resistivity increased approximately 2.8 times and when the concrete element is submerged, it increased 1.8 times.

2.4.5 Presence of Steel Reinforcing Bars

Electrical measurements in porous materials such as rocks, ceramics and cement materials can be described as:

$$\boldsymbol{\rho_T = \rho_0 \cdot \frac{1}{\varphi\beta}} \qquad [9]$$

Where ρ_T is the total resistivity, ρ_0 is the resistivity of the pore solution which is function of the ionic composition and concentration in solution, φ is the porosity of the system that is accessible to fluids, and β is the connectivity of the pores in the system (Dullien, 1992). Of course, this law is based on the assumption that the solid skeleton is non-conductive. In cases where steel reinforcement or steel fibers are used, or when lightweight aggregates are saturated with a low resistivity solution, it is not validated (Castro et al., 2012; Di Bella et al., 2012).

Gowers and Millard (1999) found that the measurement error was only significant if a measurement position was selected directly over a reinforcement bar. The error was not significant if the measurement position was orthogonal to a bar or located remote from a parallel bar. It was found that, even if resistivity measurements are taken directly over a bar, significant errors can be avoided if a contact spacing is used that is less than two-thirds the concrete cover to the rebar.

According to Presuel-Moreno et al. (2010), the presence of reinforcing steel (diameter of 5/8”) with a concrete cover more than 7.5 cm has a negligible effect on the surface resistivity value. However, in cases where the concrete cover is 5 cm (most common) or less, different resistivity values can be reached based on the Wenner probe location. In a concrete sample of (30 x 30 x 15 cm) with one steel rebar (5/8’’) located in the center of the specimen, several measurements were made at different places with two probe spacings (a) 3 and 5 cm (Figure 21).

The effect of rebar is most significant when the Wenner probe is exactly above the rebar (L1), where the resistivity value can be 6% lower than the concrete bulk resistivity when a, is equal to 3 cm, and 17 % lower when a, is equal to 5 cm. The resistivity is almost the same as the actual concrete resistivity when the Wenner probe is located in parallel at 5 cm of the rebar (L3) and 45 degrees (L4). When a measurement is done perpendicular to the rebar (L2), the resistivity is 2 % lower than the actual resistivity when a, is equal to 3

cm and 11% lower when a, is equal to 5cm. Table 11 shows the resistivity values obtained at different locations mentioned above.

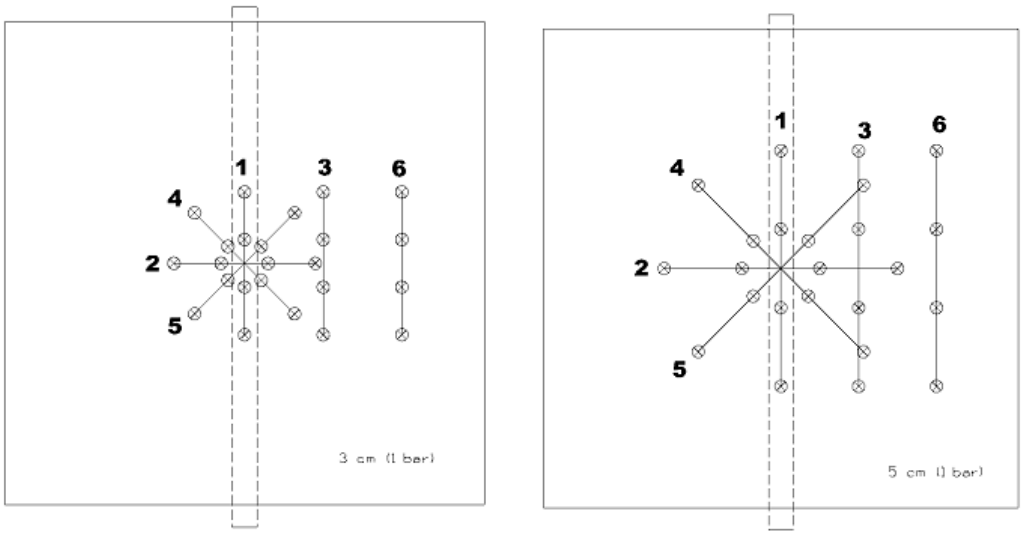

Figure 21. Measurement locations with one rebar, probe spacing of 3cm (left) and 5cm (right) (Presuel-Moreno et al., 2010).

Table 11. Resistivity values with one rebar by Presuel - Moreno et al., (2010).

a (cm)	L1	L2	L3	L4	L5	L6
	Bulk Resitivity = 1					
3	0.94	1.02	0.99	0.99	0.99	1.07
	6.0%	-2.0%	1.0%	1.0%	1.0%	-7.0%
5	0.83	1.11	0.99	1.0	1.0	1.26
	17.0%	-11.0%	1.0%	0.0%	0.0%	-26.0%

Moreover, concretes sample with four (4) rebar were also tested with different probe spacing (a = 3 cm, a = 5 cm) at different locations. Table 12 shows the relative values obtained from the study.

Table 12. Resistivity values with four rebar by Presuel-Moreno et al., (2010).

a (cm)	**L1, L4**	**L2, L5**	**L3, L6**	**L7, L10**	**L11, L12**
	Bulk Resitivity = 1				
3	0.99	0.98	0.96	0.98	0.97
	1.0%	2.0%	4.0%	2.0%	3.0%
5	0.97	0.93	0.8	0.92	0.89
	3.0%	7.0%	20.0%	8.0%	11.0%

Figure 22 shows all the locations in where surface resistivity was measured and from the study it is possible to say that, the closest values to the bulk resistivity are when the Wenner four probe is located at (L1,L4), (L2,L5) and (L7, L10), which are located further from the influence of the reinforcing.

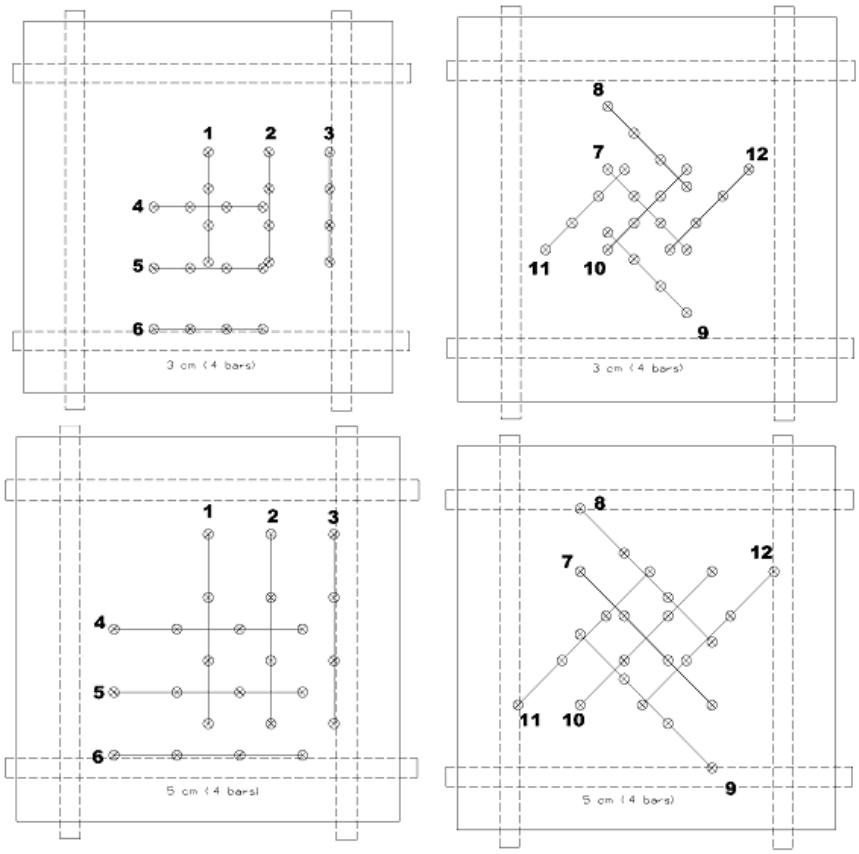

Figure 22. Measurement locations with four rebar, probe spacing of 3cm (above), 5 cm (bellow) by Presuel - Moreno et al., (2010).

2.4.6 Effect of Surface Layer of Different Resistivity

Generally, the samples taken from field exposed elements can behave unexpectedly in terms of resistivity. The surface parts (0-50 mm) have much higher resistivity values than their inner cores (50 – 100 mm) as was explained before in section 2.2.3. In addition, a relatively high-resistivity surface layer or covercrete can be formed by carbonation of the concrete. Subsequently, under certain environmental conditions such as rainfall, a second

low resistivity surface layer will be produced on top of the carbonation layer. However, a significant error can be avoided if the contact spacing is at least eight times the surface concrete layer thickness (Gowers and Millard., 1999).

2.4.7 Concrete Non – Homogeneity

The Wenner technique assumes that concrete is homogeneous, but aggregate particles possess a very high resistivity as was shown in section 2.2.1 (Table 2), and cement paste has a much lower resistivity. According to Gowers and Millard et al. (1999), from a series of repetitive measurements it was observed that the standard deviation did not exceed 5%, as long as the contact spacing was 1.5 times (or greater) as large as the maximum aggregate size.

2.5 General Factors Influencing Electrical Resistivity due to External Environment

A report presented by Gowers and Millard et al. (1999) mentioned that, no clear correlation has been found between the measurement of resistivity and either the ambient relative humidity of the air or the occurrence of rainfall. The only correlation made so far is for the temperature, which is inversely proportional to electrical resistivity. According to literature the parameters as rainfall, moisture and temperature and saturation degree can also influence resistivity measurements. A detailed explanation of them will be presented next.

2.5.1 Rainfall

According to Gowers and Millard (1999), an increase in the measured resistivity using the Wenner probe technique was observed after rainfall started indicating the double surface layer effect due to carbonation. One day later, after the concrete surface had dried, the resistivity measurements returned to their previous values for contact spacing of $a \geq 4$ cm. For smaller spacing, this was not the case; for this reason, it is recommended to use a contact spacing of $a \geq 4$ cm to minimize the surface wetting effects, even following 24 hours of dry weather.

2.5.2 Moisture Content and Temperature

2.5.2.1 Moisture Content Effect

From literature, it was found that moisture content plays an important role in concrete resistivity as electrical current in the concrete is carried through interconnected pore water. Basically, electrical resistivity increases with the decreasing moisture content and usually, an increase in temperature leads to decrease in resistivity, due to the change in the ion ($Na^{+,}$ $K^{+,}$ Ca^{2+}, SO_4^{2-} and OH^-) mobility such, ion – ion and ion- solid interactions mobility (Larsen et al., 2007; Presuel - Moreno et al., 2012; Liu et al., 2014).

Larsen et al. (2007a) measured resistivity under different moisture degree and air temperatures for discs of 45mm thickness from 8 mixtures with different binder characteristics and 90 days after casting. Figure 23 shows the effect of moisture degree (MD) on each sample where it is possible to see how the electrical resistivity increases with the decreasing moisture content. According to the data published in the study, the resistivity increases an average of 2 times higher when the moisture degree decreases from 88% to 77%. The change was more evident when moisture decreases from 88% to 66 %. In this case, the value obtained was an average of 6 times higher compared with the resistivity measured with a moisture degree of 88%. For all the mixtures, regardless of the type of binder used, the change in the moisture degree clearly influences the final resistivity value.

Once the concrete is placed in the field the only factor that it's possible to control is the saturation degree (SD). The saturation is the key factor in order to accomplish the electrical measurement, since a dry concrete may act more or less as an insulator ($\rho > 10^{11}$ Ω. cm).

Therefore, the resistivity measurements of the specimens with low moisture content are inappropriate (Chun-Tao et al., 2014). Meanwhile, saturated concrete may act as a semi-conductor (10 – 500 Ω. cm) (Lopez and Gonzalez 1993).

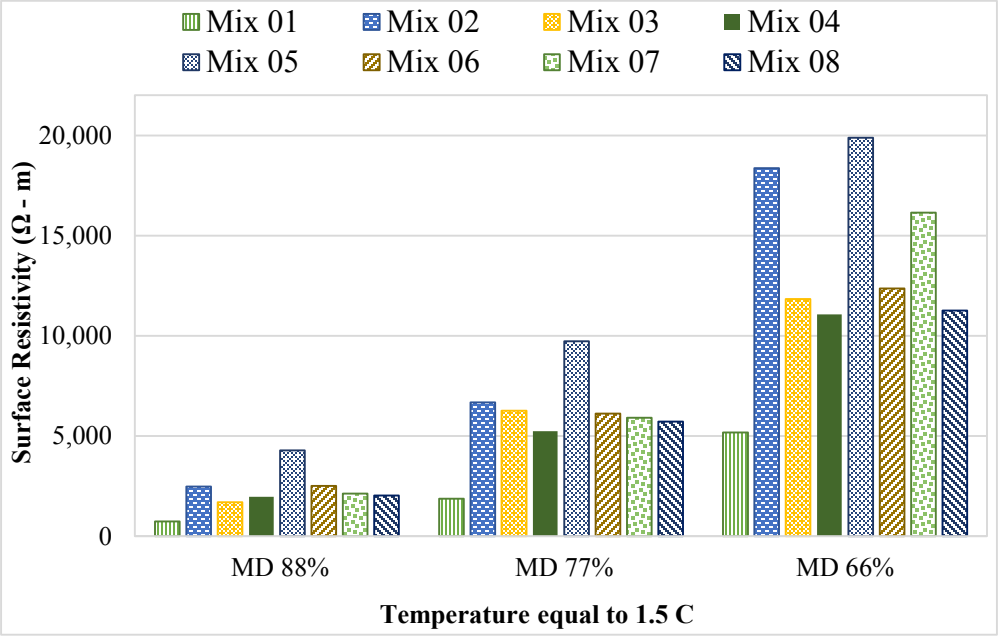

Figure 23. Moisture degree (MD) effect on surface resistivity after Larsen et al., (2007a).

2.5.2.2 Temperature Effect

Figure 24 shows the effect of temperature on the samples. It is possible to see how an increase in temperature leads to decrease in resistivity. From the data published in this study, the resistivity decreases an average of 2.20 times lower when temperature increases from 1.5 °C to 20.5 °C and almost 5 times lower at 40 °C.

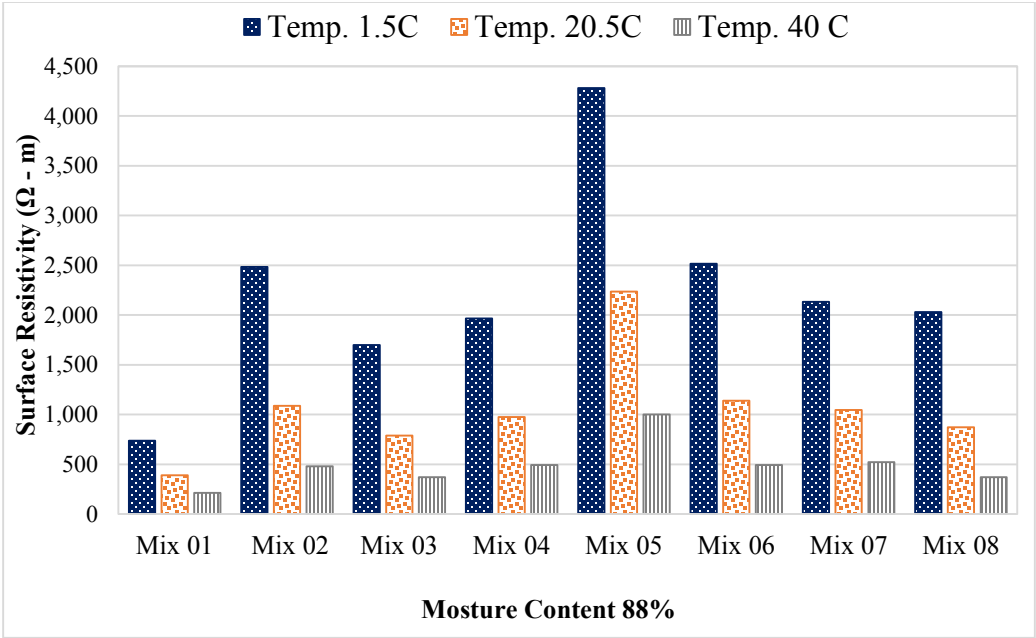

Figure 24. Temperature effect on surface resistivity after Larsen et al., (2007a).

Regarding to the effect of temperature, Elkey and Sellevold (1995) reported that for ordinary Portland cement (OPC) concrete, resistivity changes 5% per °C at 21 °C under 30% saturation, whereas it changes 3% per °C under 70% saturation. Equation 10 was developed in the study to describe the temperature effect on resistivity and it was used commonly to normalize the effect of temperature.

$$\boldsymbol{\rho_T = \rho_0\,[1 + \alpha\,.(\theta - T)]} \qquad [10]$$

Where ρ_T is the resistivity at temperature T (°C); ρ_0 is the resistivity at a reference temperature θ(°C); and α is a temperature coefficient (1/°C) value that according to literature can range from 0.022 and 0.035/°C. However, it was found that the equation [10] is only applicable over a limited interval of ± 5 °C to the reference temperature.

Liu et al., 2014 studied the electrical resistivity of water saturated and unsaturated concrete specimens to develop a methodology to normalize the resistivity values measured at different temperatures to the values at a reference temperature of 21°C, and to predict the resistivity variations due to temperature changes based on Arrehenius law [11].

$$\boldsymbol{\rho_T = \rho_o \cdot \exp\left[\frac{E_{a,p}}{R}\left(\frac{1}{T} - \frac{1}{T_0}\right)\right]} \qquad [11]$$

Where ρ_T is the resistivity measured at temperature T (K); ρ_o is the resistivity at a reference temperature T_0 (K); R is the gas constant (8.314 J $mol^{-1}K^{-1}$); and $E_{a,p}$ is the activation energy for resistivity (J/mol). The activation energy value $E_{a,p}$ quantifies the amount of thermal energy required to promote a mole of the ions that are part of the pore solution of concretes (such as Na^+, K^+, Ca^{2+}, SO_4^{2-} and OH^-) from equilibrium state to activated state (migrating ions) to carry a current flow under and electric field (Bockris et al., 2002).

In the study conducted by Liu et al. (2014) for 6 years, 200 concrete standard cylinders (10x20cm) from 54 mixtures divided in four groups with different types of aggregates and supplementary cementitious materials were used to analyze the influence as shown in Table 13.

Table 13. Type of cement and admixtures used by Liu et al., (2014).

Groups	Type of cement and blend mixures
I	Type I/II cement F1 and High Alkalinity (HA) cement with w/c of 0.41 and 19% Class F Fly Ash (FA).
II	Type I/II cement with different types/amounts of mineral admixtures such as Fly Ash, Silica Fume and Metakaolin and with a range of w/c (0.30 to 0.70).
III	Type I/II cement with Class F Fly Ash (FA) and Silica Fume (SF) with a w/c of 0.40.Limestone was used as coarse aggregate.
IV	Type I/II cement with Class F Fly Ash (FA) and Slag cement (GGBS) with a w/c of 0.41. Limestone was used as coarse aggregate.

The specimens were stored under different conditions: high relative humidity (RH) (95 to 100%) at a high temperature (38°C) in sealed containers, stored in tap water at 45°C, kept in a fog room with 100% RH, or in 95% for long periods of time (3 to 6 years). To achieve a variation of temperature, the cylinders were immersed in tap water tanks with a temperature range between 10 to 45°C. The water temperature was adjusted every 2°C for specimens in Groups I, II and III, and every 5°C for those in group IV. Once the samples were removed from water measurements were performed using a commercial four point Wenner probe. Using the following equation [12] it was possible to calculate the activation energy ($E_{a,p}$) for the different groups using the resistivity values obtained at different temperatures.

$$\boldsymbol{\rho = A \,.\, \exp\left[\frac{E_{a,p}}{R\,.\,(T+273.15)}\right]} \qquad [12]$$

Where A (Ω m) is the resistivity when T(°C); R is the gas constant (8.31 J/mol/K). Based on the activation energy ($E_{a,p}$) results, two trends where achieve to correlate concrete specimens with different mixture properties as shown in Table 14.

Table 14. Equations according to mixture properties by Liu et al., (2014).

Equations	Mixture properties
$E_{a,p} = 3.7738 \ln(\rho_{21}) + 9.7518$	Concrete with ≥ 20% fly ash Concrete with > 50% slag
$E_{a,p} = 6.0157 \ln(\rho_{21}) + 4.3121$	Ordinary portland cement (OPC) High alkalinity concrete Concrete with < 20% fly ash Concrete with ≤ 50% slag

With the correlations established, it was possible to develop an expression to normalize the temperature effect on resistivity for the two types of mixtures properties. The first two equations are those concretes with ≥ 20% fly ash or concretes with > 50% slag.

$$\boldsymbol{\rho_{21} = 10 \,.\, \exp\left[\frac{\ln(10/\rho_T)\,.\,T + 273.15 \ln\,(10/\rho_T) - 3.98755\,.T + 83.7385}{0.54312\,.\,T - 305.556}\right]} \qquad [13]$$

$$\boldsymbol{\rho_T = (\rho_{21}/10).\exp\left[1000.\ \frac{3.7738\,.\ln(\rho_{21}/10) + 9.7518}{8.314}.\ \left(\frac{1}{T+273.15} - \frac{1}{294.15}\right)\right]} \qquad [14]$$

The second set of equations are for those concretes with only ordinary Portland cement (OPC), high alkalinity, concretes with < 20% fly ash, concretes with ≤ 50% slag ≥ 20% fly ash or concretes with > 50% slag.

$$\boldsymbol{\rho_{21} = 10 \,.\, \exp\left[\frac{\ln(10/\rho_T)\,.\,T + 273.15 \ln\,(10/\rho_T) - 1.76405\,.T + 37.045}{1.45985\,.\,T - 324.808}\right]} \qquad [15]$$

$$\boldsymbol{\rho_T = (\rho_{21}/10).\exp\left[1000.\ \frac{6.0157\,.\ln(\rho_{21}/10) + 4.3121}{8.314}.\ \left(\frac{1}{T+273.15} - \frac{1}{294.15}\right)\right]} \qquad [16]$$

Where ρ_T (Ω m) is the measured resistivity at temperature T(°C). Then is necessary to calculate ρ_{21}(reference resistivity at 21°C) by plugging ρ_T and T into equations [13] or [15] according to the case to finally calculate resistivity at other temperatures by plugging ρ_{21} into equations [14] or [16] according the case. However, this methodology does not take into account the effect generated by moisture content an additional factor that can influence resistivity values. These temperature correlations were established using only standard cylinders specimen samples (Ø10x20cm).

2.5.3 Saturation Degree (SD)

Once the concrete is placed in the field the only factor that it's possible to control is the saturation degree. The saturation is the key factor in order to accomplish the electrical

measurement, since a dry concrete may act more or less as an insulator ($\rho > 10^{11}$ Ω. cm). Therefore, the resistivity measurements of the specimens with low moisture content are inappropriate (Chun-Tao et al., 2014). Meanwhile, saturated concrete may act as a semi-conductor (10 – 500 Ω. cm) (Lopez and Gonzolez 1993).

A characteristic example of saturation on a concrete bridge deck can be seen in Figure 25. It can be noticed that the duration of saturation is very brief; a) Several points have been measured (showing damp) and points that are going to be measured (paint dots) using the Wenner four probe device; b) Close view of the Wenner probe device over the concrete element; c) Another none destructive test (NDT) device called galvanostatic pulse measurement (GPM) used to measure corrosion rates over ponding saturate surface; d) An unreliable surface resistivity value is showed over a concrete element without saturation.

Figure 25. Ponding saturation examples a) Wenner-four probe ; b) Closed view of Wenner device; c) GPM device; d) Unreliable resistivity values, from Strategic Highway Research Program SHRP2, < http://www.ndtoolbox.org/content/bridge/er-description>

3 Laboratory and Work Practice Methodology

The objective of this work is to investigate issues involved in advancing the use of surface resistivity in the field. The development of a test method suitable for non-destructive field use to evaluate the potential durability of the surface layer or covercrete by determining the surface electrical resistivity would be a useful test. The following phases were established to analyze their influence on surface electrical resistivity:

- Phase One – Influence of Saturation Degree.
- Phase Two – Influence of Sample Storage under Different Solutions and Specimen Geometry.
- Phase Three – Analyses of Correlations to Normalize Temperature Effect on Site and influence of Curved and Plane Surfaces.
- Phase Four – Influence of Saturation Methods Techniques.

The phase one, two and four were completed under laboratory conditions at Concordia University. Phase Three was carried out at Concordia University, at University of Sherbrooke and directly on field over sidewalks cast for the City of Montreal (Ville de Montréal) located at North - East of Montreal, QC. Canada.

3.1 Phase One – Influence of Saturation Duration

Five binder combinations were investigated in this portion of the work in order to represent a wide variety of concretes from high performance to residential concretes; all but one of these combinations included the use of blast furnace slag. Rupnow and Icenogle et al., (2011) found that in concrete mixtures with slag, increasing of w/c gave increasing resistivity. As mentioned in the literature review, decreasing porosity achieved with lower water to cement ratios should lead to increased resistivity. Therefore, the laboratory mixtures for this phase are focused on mixtures containing slag in order to validate this behavior.

Table 15 shows the laboratory mixture designs used as well as fresh and hardened properties. Type I/II Portland (TI) and Portland-limestone (L) cement were used as the primary binders. The supplementary cementitious materials used were Grade 100 blast furnace slag (S) and Type F fly ash (F). Aggregates consisted of 14 mm coarse aggregate and natural sand. For each binder combination, five mixtures were made with w/c ranging from 0.32 to 0.64.

Chemical admixtures included air entrainer and water reducers were used to achieve target air of 5.0% and slump of 100 ± 10 mm. Slump and entrained air were measured at the time of casting using ASTM methods ASTM C1611 / C1611M - 14 (2014) and ASTM test C - 666 (2008) procedures A and B. As well, compressive strength was measured as the average of two cylinders using ASTM C39 / C39M - 14a (2014) at 56 days as is typical

for mixtures containing supplementary materials. The results of these tests are also given in Table 15.

Table 15. Phase One Mixture Designs and Properties.

Mixtures Design	w/c	Slump (cm)	Air Entrained (%)	Water (kg/m3)	Cement Type (kg)		Pozzolan (kg)		f'c 56 Days (MPa)
					Type I/II (TI)	Limestone (L)	Fly Ash (FA)	Slag (S)	
100 TI	0.40	9.0	6	186	433	-	-	-	45.30
	0.52	11.5	8	191	340	-	-	-	37.50
	0.52*	15.0	6	146	250	-	-	-	36.10
	0.60	20.0	4	188	288	-	-	-	26.50
50TI-50S	0.39	10.0	4.5	217	217	-	-	217	62.30
	0.52	23.0	8	170	170	-	-	170	40.00
	0.57	15.0	5	144	144	-	-	144	43.80
	0.63	11.5	7	125	125	-	-	125	34.80
50L-50S	0.32	16.5	5	150	-	217	-	217	49.70
	0.44	9.0	5	142	-	144	-	144	47.00
	0.48	15.0	4	177	-	170	-	170	49.80
	0.50	10.0	6	139	-	125	-	125	37.00
50TI-30FA-20S	0.36	11.5	7	172	215	-	133	88	48.30
	0.40	10.0	3	151	170	-	100	70	43.00
	0.53	18.0	5	169	144	-	86	60	28.30
	0.64	18.0	7	175	125	-	75	50	30.30
50TI-20FA-30S	0.37	10.0	4	174	215	-	88	133	51.00
	0.45	10.0	4	155	170	-	70	100	42.00
	0.53	15.0	5	169	144	-	60	86	28.10
	0.64	16.5	5.5	175	125	-	50	75	24.80

In the laboratory, one hundred (100) standards cylinders (10 x 20 cm) were cast mixture at standard temperature conditions (23 (+/-2) °C); five cylinders for every mixture. The cylinders were removed from their molds after one day and each specimen was marked in four locations, oriented at 90 degrees to indicate where to place the electrodes during the subsequent resistivity measurements. Figure 26 shows where the marks were located on every cylinder specimen. Every sample was stored in limewater solution maintained at 23

(+/-2) °C for 7 days after casting. The solution to sample volume ratio was less than or equal to 3:1, and the container was covered to prevent evaporation. Surface resistivity was measured upon removal from limewater. At this point, the cylinders were relocated to sealed containers with a small amount of water in the bottom to maintain high humidity (>85%).

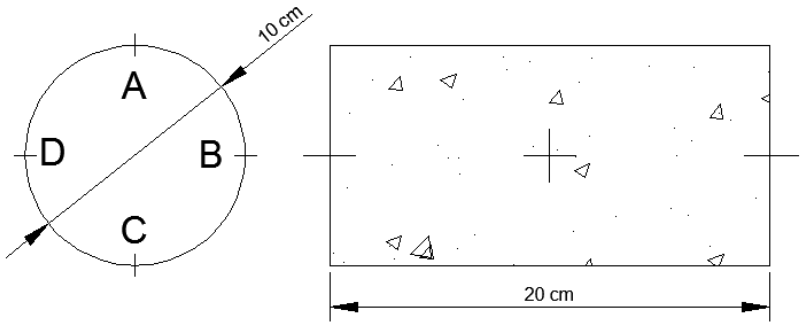

Figure 26. Marks for the four line electrodes locations.

Cylinders were removed from these containers at 28, 56, and 91 days to measure the surface resistivity over 3 days of limewater saturation. Previous research (Kessler et al., 2005) indicated that a decrease of surface resistivity of ~10% occurs between moist cured and limewater saturated conditions, the objective of this phase was to quantify the duration needed to achieve steady-state resistivity readings. Every specimen was removed from the limewater solution at intervals (1, 3, 6, 24, 48, and 72 hours), after this period they were returned to moist curing until the next test time.

A commercial brand Wenner four probe, Proceq Resipod, was used with 38 mm (1.5 inch) spacing to measure the resistivity. The standard cylinders were lightly wiped with a damp

rag prior to the measurements, which were completed within 5 minutes of removal from the solution. In all cases, two rounds of measurements were performed on each of the 4 lines, resulting in 8 measurements per sample.

3.2 Phase Two – Influence of Samples Storage under Different Solutions and Specimen Geometry

As an initial investigation on the influence of the immersion solution on the duration required for resistivity measurements, two set of mature concrete were investigated. The mature samples stored in air for long periods of time were examined in September 2013, February and August 2014. Two mixtures were tested; 75% Portland cement with 25% fly ash (75TI-25FA) saturated with tap water and 100% Portland cement (100TI) saturated with limewater. All cylinders were approximately 5 years old at the time of testing. The test cylinders, three for each mixture, were immersed in their respective solutions. The surface resistivity was measured more frequently in the first hour and thereafter at similar time intervals as in Phase One.

In order to further estimate the differences between samples saturated with tap water and lime water under laboratory conditions, an extra set of mixtures from the previous set of samples cast in Phase one (section 3.1) were chosen. Two using Portland cement and water cement ratio (0.40 and 0.50) 100TI to represent concretes commonly used in practice. The third mixture included supplementary cementitious materials as slag and fly ash

50TI30FA20S. For each mixture, a total of 6 standards cylinders (10 x 20 cm) and 4 circular slabs (30cm Ø x 10 cm) were cast. Figure 27 illustrates the samples' dimensions.

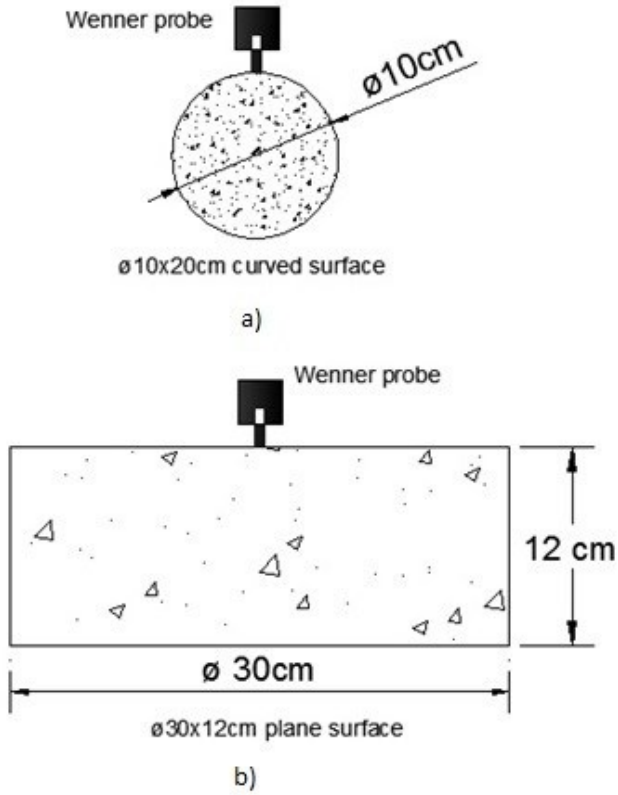

Figure 27. Geometry samples (a) standard cylinder (10x20cm) (b) circular slab (Ø 30x12cm) (Drawings without scale).

As in Phase 1, the samples were removed from the molds at 1 day followed by 6 days in either tap or lime water. However, in this phase the effect of tap water (TW) and limewater (LW) on surface resistivity was analyzed with half of the samples (three) of each mixture stored under tap and lime water solutions maintained at 23 (+/-2) °C for until 7 days after

casting. For those in limewater, the solution to sample volume ratio was less than or equal to 3:1. Surface resistivity was measured upon removal from both solutions.

At this point, the cylinders were relocated to sealed containers with a small amount of water in the bottom to maintain > 85% RH until 28 days when surface resistivity was measured upon removal.

The samples were then placed into these solutions and the resistivity measured at various durations at 7, 28, 56, 91, 119 and 155 days after casting. The results are presented and discussed in detailed in chapter four - section 4.2. In addition, to reduce the effect of the surface roughness of the slabs, special care was applied for the finishing of the top and bottom of each slab.

3.2.1 City of Montreal (Ville de Montréal) Samples

In addition to the samples cast for this research, other sets of samples were tested from a sidewalk project conducted by the City of Montreal (Ville de Montréal) and Sherbrooke University. Two cylinder sizes were cast for this project, Ø10x20 cm and Ø15x30 cm.

Table 16 shows the concrete characteristics of these. The samples were cast by the city in October 2013 and stored in a moist room at Sherbrooke University until testing. The testing consisted of removing the samples from the moist room and measuring resistivity at 4 orthogonal locations for two rounds.

Table 16. Concrete mixtures by city of Montreal

Mixture	General information
VdeMTL Temoin	73% GU, 27% GUb-SF(silica fume blended Portland cement), w/c 0.43, max. agg. size 20 mm
VdeMTL 25PV	75% GU, 25% glass powder , w/c 0.40, max. agg. size 20 mm
VdeMTL 10PV	90% GU, 10% glass powder , w/c 0.41, max. agg. size 20 mm

3.3 Phase Three – Analysis of Correlations to Normalize Temperature Effect on Site and the Influence of Curved and Plane Surfaces

The motivation in this section was to evaluate the correlations established by Liu et al., (2014) to normalize temperature effects for resistivity measured directly on site. The objective was to verify if it was possible to achieve a singular or very close resistivity value after applying the equations 15 and 16 developed by the study. The on-site resistivity was also compared to that of the lab specimens conducted at nearly the same age.

In addition to the lab specimens, the sidewalks themselves were tested. Figure 28 shows a map of Montreal with the sidewalk location highlighted. The sidewalks were cast with different blends and located on the same street (Av. Poutrincourt between Av. Louis Danton and rue Viel). Figure 29 shows the specific locations for the different concrete types. The color yellow represents mixture VdeMTL10PV, the red color is VdeMTL25PV and color green is mixture VdeMTL Temoin or (formule 3VM-10). Photographs of the sidewalks are shown on Figure 30.

Figure 28. Sidewalks location at North - East of Montreal, QC. CA.

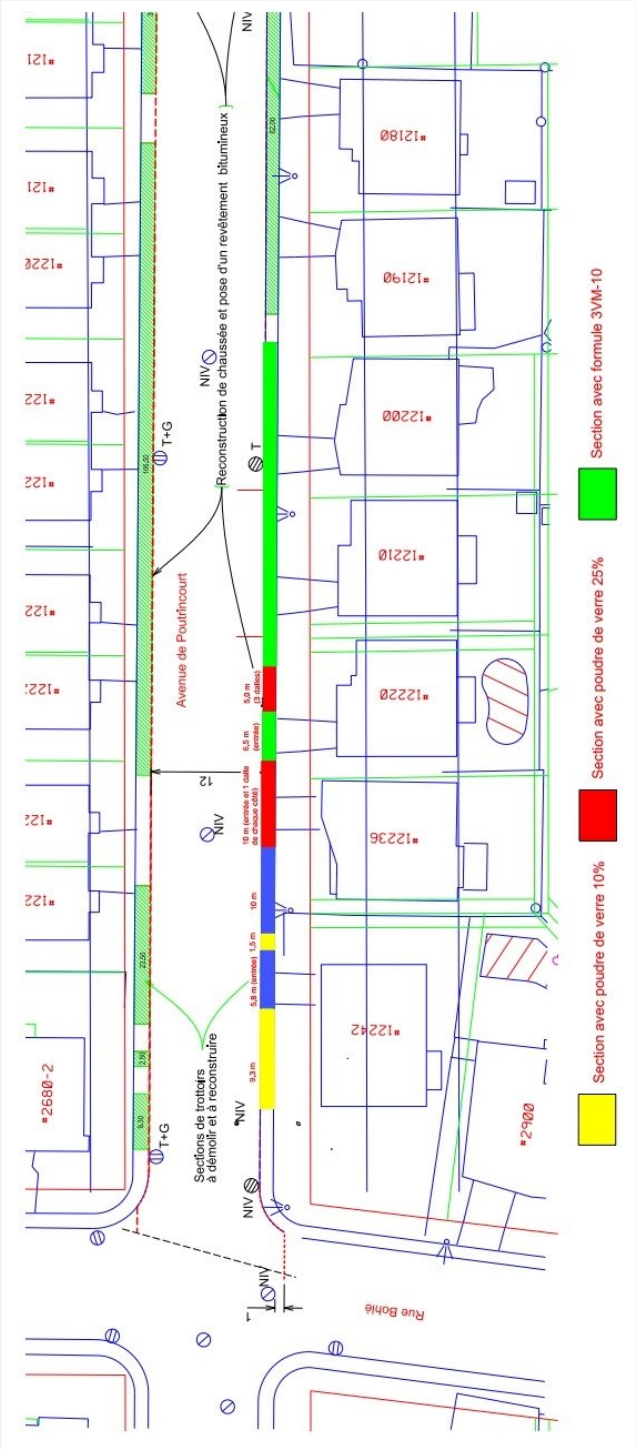

Figure 29. Sidewalks street location - Av. Poutrincourt between Av. Louis Danton and rue Viel, Montreal, QC.CA.

Figure 30. Sidewalks street view; a) VdeMTL10PV; b) VdeMTL Temoin or (formule 3VM-10) and c - d) VdeMTL25PV

According to Gowers and Millard (1999), an increase in the measured resistivity is usually observed after rainfalls, which indicates a double surface layer effect due to carbonation. Generally, it is recommended to wait for one day to obtain reliable values as well as using a probe spacing a ≥ 4 cm to minimize the surface wetting effects.

On each sidewalk, no evidence of carbonation was observed. Each measurement started after one hour the rain was over, until the excess of water had evaporated, but the sidewalk was still significantly wet. A total of 16 measurements per mixture were conducted directly on the sidewalks after rainfalls during two different days (September 11 and 13, 2014). The average rain precipitation was registered as 5-10 mm for both days.

The average concrete temperatures registered during these days were 10.5°C and 15°C, respectively using a handheld infrared thermometer. The probe spacing used was equal to 38.1mm (1.5in).

Each measurement started after one hour the rain was over, until the excess of water was evaporated in order to keep the area moisture. The average rain precipitation was registered as (5-10 mm). The average concrete temperatures registered during these days were (10.5°C and 15°C). The probe spacing used was equal to 38.1mm (1.5in).

Additionally, a comparison was established between the data obtained on field over the sidewalk, representing plane surfaces and the resistivity measured over the standard cylinders Ø10x20cm and Ø15x30cm, curved surfaces cast for the City of Montreal project described before in Section 3.2.1.

3.4 Phase Four – Influence of Saturation Methods Techniques

The motivation of this section was to establish a relation between different types of saturation methods used or alternatives that can be used on site to reach a similar degree of saturation found in laboratory conditions to obtain reliable surface resistivity values.

Basically, two types of saturation were analyzed in this Section, water pressure and ponding saturation, common techniques that are commonly used over concrete elements on site. In order to validate the different saturation methods, a simulation was established on circular concrete slabs (Ø30x12cm). Using the same three mixtures as for Phase 2 (100TI w/c 0.4 and 0.5, 50TI30FA20S w/c 0.40), two methods were used with tap water (TW); ponding and water pressure saturation. Tap water (TW) was used as primary source since can be found on any construction site project. Figure 31 illustrates a schematic representation of the circular slabs cast.

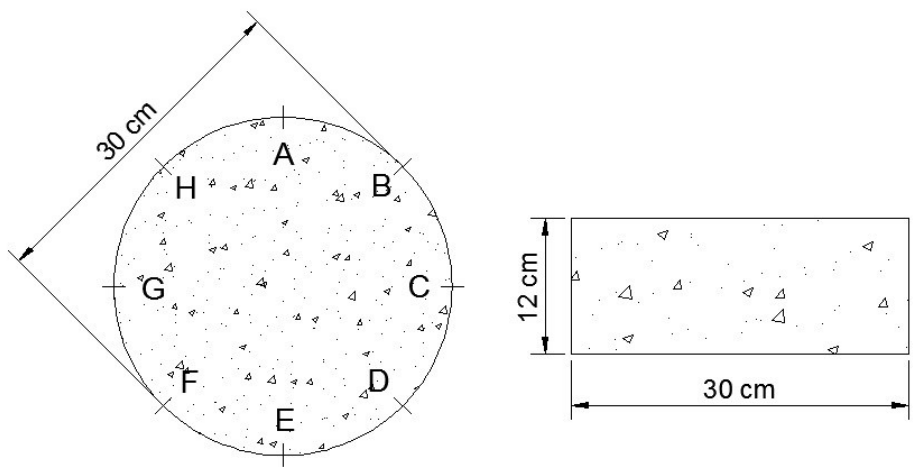

Figure 31. Circular slabs geometry Ø30x12cm (Drawings without scale).

The Wenner four probe device was placed on A-E, B-F, C-G, D-H, E-A, F-B, G-C and H-D directions twice to obtain an average resistivity value for each of the 12 circular slabs tested.

3.4.1 Water Pressure Saturation

To determine influence of water pressure on surface electrical resistivity at 125 days of casting, the same circular slabs Ø30x12cm samples described previously in Section 3.2 were tested after using a commercial water pressure machine - archer K3.690 in order to simulate a common practice on site to saturate concretes in a short period of time.

A total of four rounds of resistivity measurements were made at different times: after 10, 20, 30 and 40 minutes of continuous water exposure.

3.4.2 Ponding Saturation

To establish a comparison between the effect of fully immersed samples and ponding saturation, samples were saturated by surface ponding with tap water simulating common field practices.

A total of 12 circular slab samples Ø30x12cm were stored in air and tested at 205 days under laboratory conditions in order to achieve a relatively dry element. Then, for periods of time (10, 30 and 60 minutes), the samples were surface saturated (by ponding) to simulate a potential on site saturation practice. After this, they were immersed in tap-water until a constant resistivity value was achieved. Figure 32 shows a circular slab Ø30x12cm with 12.5 mm neoprene gasket on the edge to simulate ponding saturation.

Figure 32. Ponding saturation simulation on ø30x12cm samples.

4 Results of Phases

The following pages contain the results obtained for each phase; several comparisons were established in order to understand and analyze the influence of surface electrical resistivity when is influenced of several factors under laboratory and field conditions.

4.1 Phase One - Influence of Saturation Degree

For this part, the influence of saturation duration and its tendency at different ages (28, 56 and 91 days) was analyzed on five binder systems. All the electrical resistivity results presented include the correction geometry factor using equation [6] from section 2.3.2 and all the measurements were made with the same probe spacing, $a = 3.81\ cm$. As mentioned before, for the standard cylinders (10 x 20cm) the correction factor is 1.887. The results presented here are therefore 1.887 lower than measured.

4.1.1 Influence of Saturation 28 Days

At 28 days, five samples of each mixture were removed from the moist air curing and submerged into limewater. The results presented in this section represent the average of 40 measurements (8 per each of 5 cylinders) for each point. Generally, individual measurements did not vary by more than a few percent of the average (error bars are not shown here for clarity, but are shown in the Discussion Chapter). Figure 33 shows the surface resistivity values obtained at 28 days for 100TI at different saturation durations. Although, there is a significant decrease up to 6 hours; the resistivity values become relatively constant after 6 hours. An average difference of - 9.6% was observed between the first measurement and the last one (72 hours) with most changes occurring in the first 6 hours.

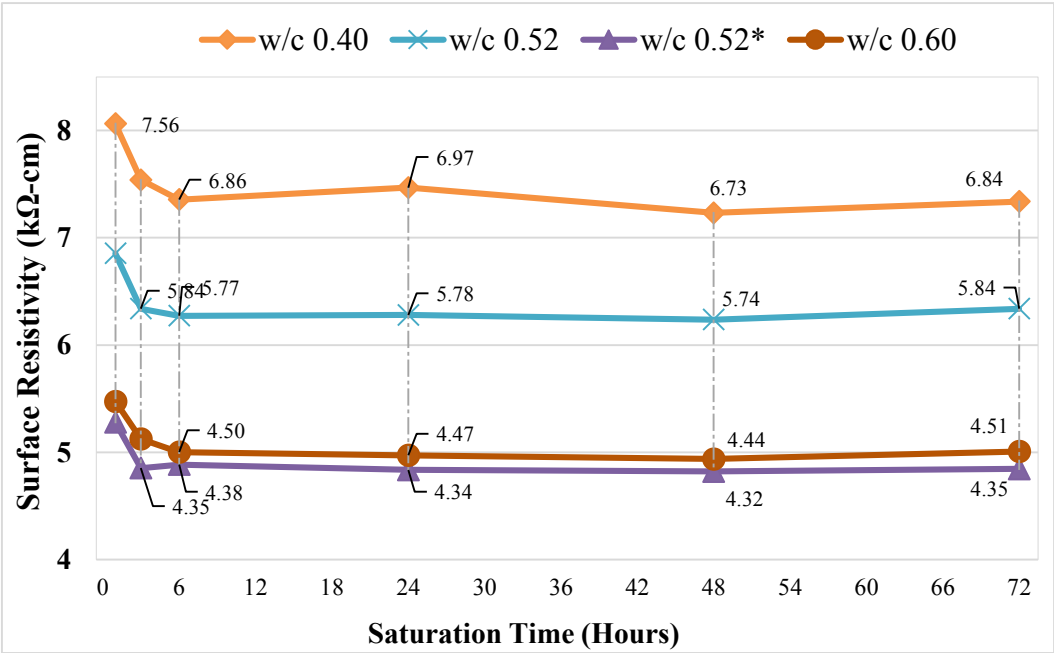

Figure 33. Resistivity Values against Saturation Time Mixture 100TI (28 days).

Figure 34 shows the values obtained for mixture 50L-50S. In this case, a significant decrease was observed in the three higher w/c ratio mixtures between 1 and 3 hours. After 3 hours, an overall increase in the resistivity value is observed in all the different w/c samples. An average difference of –0.07% was observed between the first measurement and the last one. A similar behavior was also observed for the 50TI-50S (–0.90%) and 50TI-30FA-20S mixtures (–0.58%), shown in Figures 35 and 36, respectively.

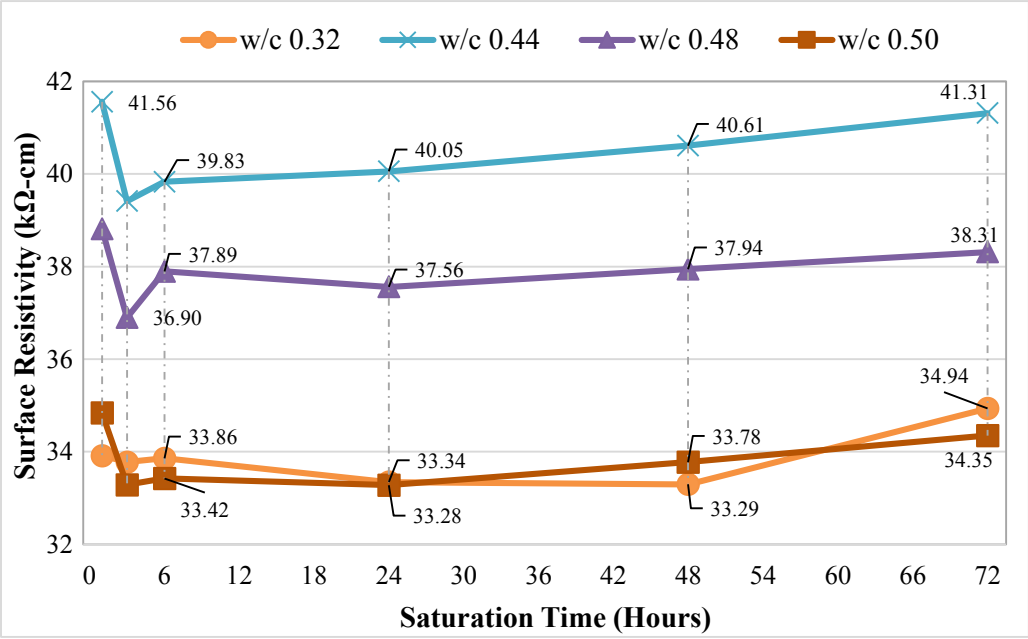

Figure 34. Resistivity Values against Saturation Time Mixture 50L–50S (28 days).

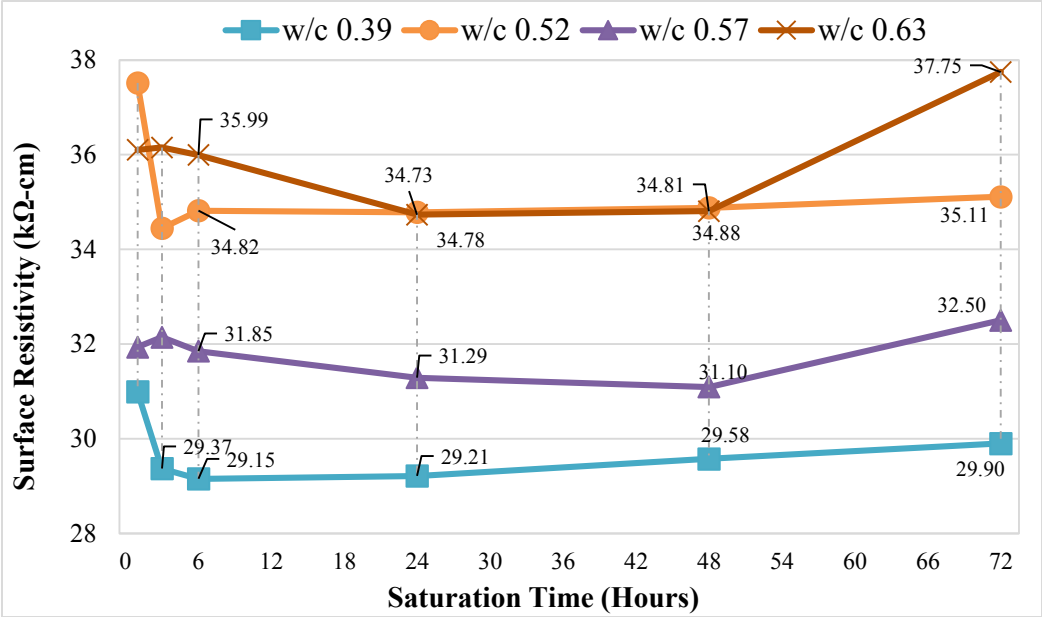

Figure 35. Resistivity Values against Saturation Time Mix 50TI-50S (28 days).

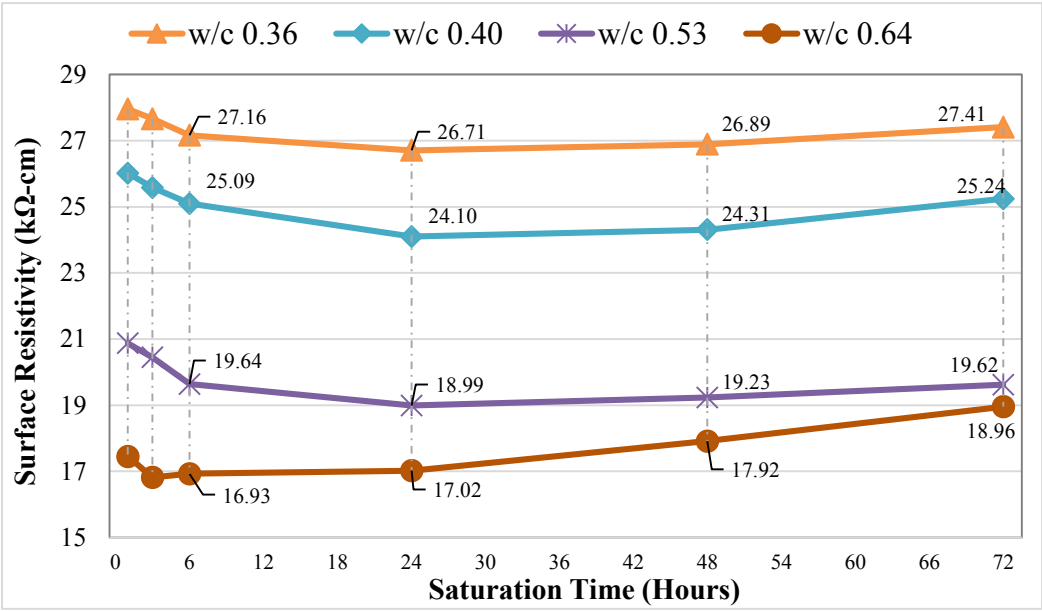

Figure 36. Resistivity Values against Saturation Time Mix 50TI-30FA-20S (28 days).

Figure 37 shows a different tendency for mixture 50TI-20FA-30S. All the w/c samples showed a very similar behavior. In this case, a lesser decrease was observed up to six hours, followed by an increase after 6 hours. An average difference of +9.4% was observed between the first measurement and the last.

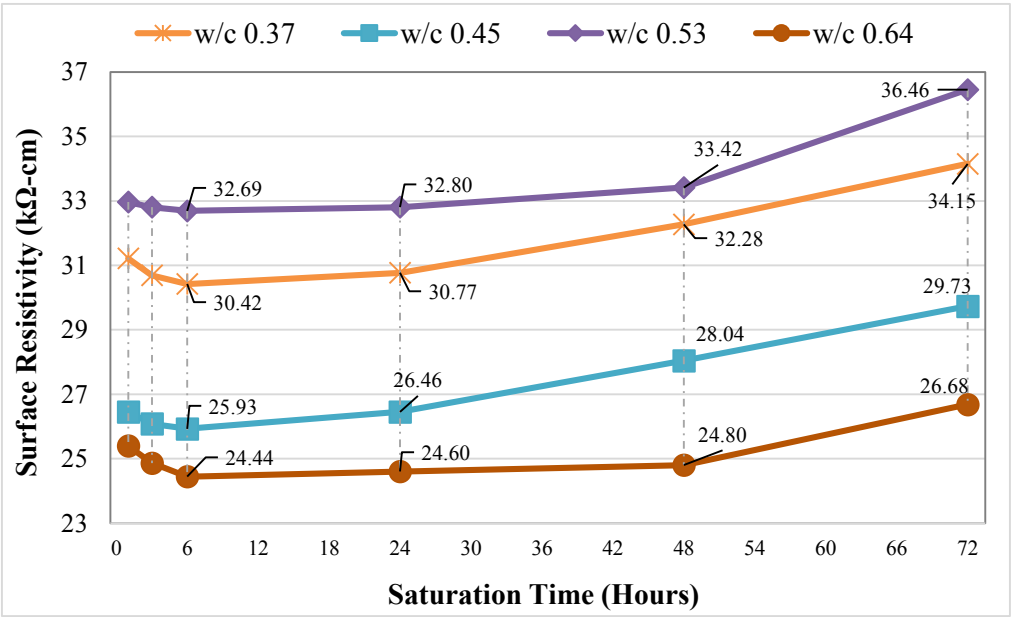

Figure 37. Resistivity Values against Saturation Time Mix 50TI-20FA-30S (28 days).

At 28 days, three different behaviors were observed in the 5 mixtures. However, there are two common tendencies in all the measurements for all mixtures. The first one is, after the first measurement where the sample was partially saturated after only one (1) hour immersion, a decrease in the surface resistivity was observed. After that, the surface resistivity has a general tendency to decrease up to 24 hours, but in some cases subsequently increase up to 72 hours.

In detail, for those mixtures containing only Portland cement, surface resistivity dropped up to 9.1% over 6 hours, but did not change substantially after this point. For the mixtures containing slag, increases in resistivity with time are observed. As mentioned in the literature review, resistivity is expected to increase as hydration proceeds. In this research, saturation was limited to 3 days in efforts to minimize any further hydration during testing which would cause an increase in resistivity, but it is possible that hydration effects in the slag mixtures are responsible for the observed increase. At 28 days, Portland cement mixtures achieve a high degree of hydration, while slag continues to react long after that stage. Interestingly, this effect can be seen regardless of w/c ratio.

4.1.2 Influence of Saturation – 56 Days

At 56 and 91 days, an additional measurement was included, 0 hour, which is the unsaturated sample measured directly from storage (>85 % relative humidity) since the last test (28 days) to determine the influence of storage condition and resistivity evolution after limewater saturation. Again, five samples of each mixture were removed from the moist air curing and submerged into limewater.

Figure 38 shows the surface resistivity values obtained at 56 days for 100TI at different saturation durations. In this case (as well as all others), there was a significant decrease in resistivity from the initial (0 hour) measurement to that at 1 hour. As mentioned in the procedures, samples were stored in humid conditions, >85% relative humidity. Again,

there was a significant decrease up to 6 hours; this initial decrease can be attributed to an increase in saturation as samples pass through from a partially saturated stage from the storage condition to gain saturation. From (1) one hour to 24 hours in all cases (w/c equal to 0.4, 0.50 and 0.6) an increasing tendency in resistivity can be seen, where samples are reaching a fully saturated stage until 24 hours. An average difference of -7.0 % was observed between the first measurement and the last one.

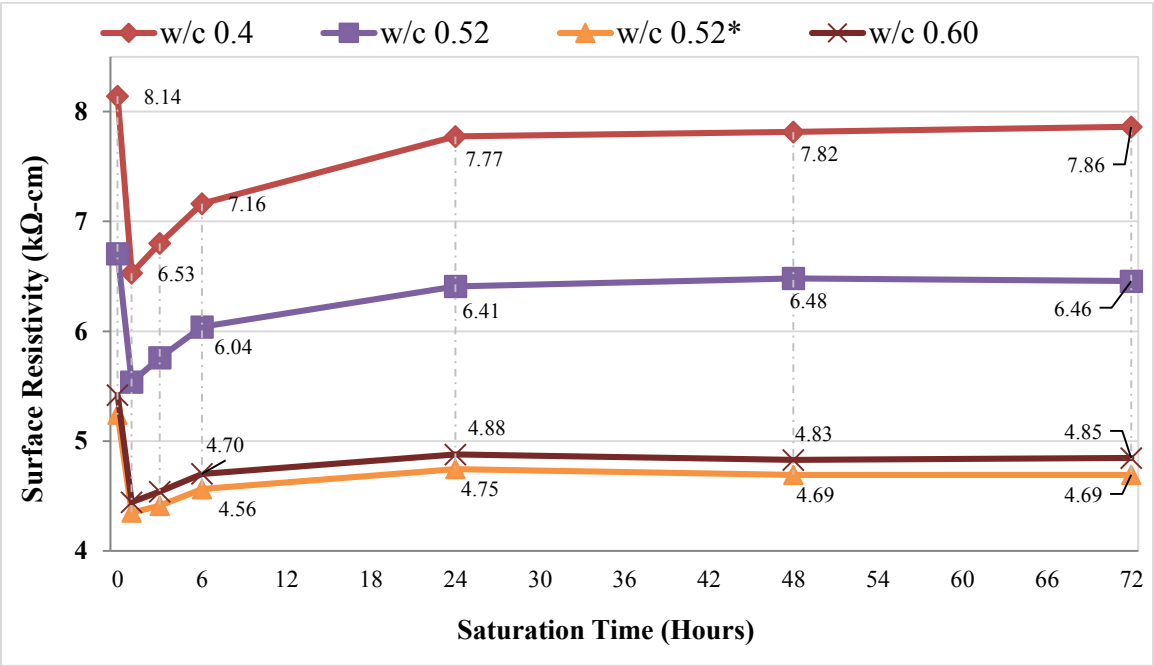

Figure 38. Resistivity Values against Saturation Time Mix 100TI (56 days).

Figure 39 shows the values obtained for 50L-50S. As for those samples with only Portland cement, a significant decrease is presented in the three higher w/c ratio mixtures between 0 and 1 hour. Then, a tendency for an increase in resistivity can be seen from 1 hour to 24

hours for the same mixtures. After 24 hours, the resistivity tends to reach an asymptotic value in all mixtures. An average difference of (–6.0 %) was observed between the first measurement and the last one.

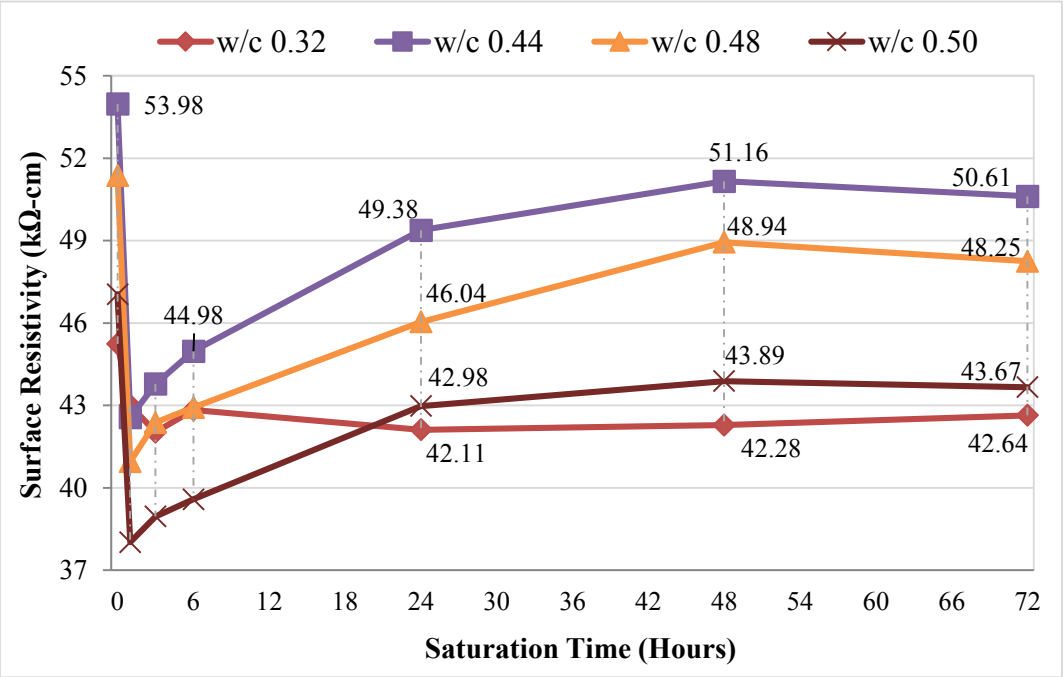

Figure 39. Resistivity Values against Saturation Time Mix 50L-50S (56 days).

For those samples with 50TI-50S in Figure 40 it can be see that, the only common behavior for the samples with different w/c (0.52, 0.54, 0.57, and 0.63) is after 24 hours where the resistivity values reach a reasonably stable level. An average difference of (–7.0 %) was observed between the first measurement and the last one.

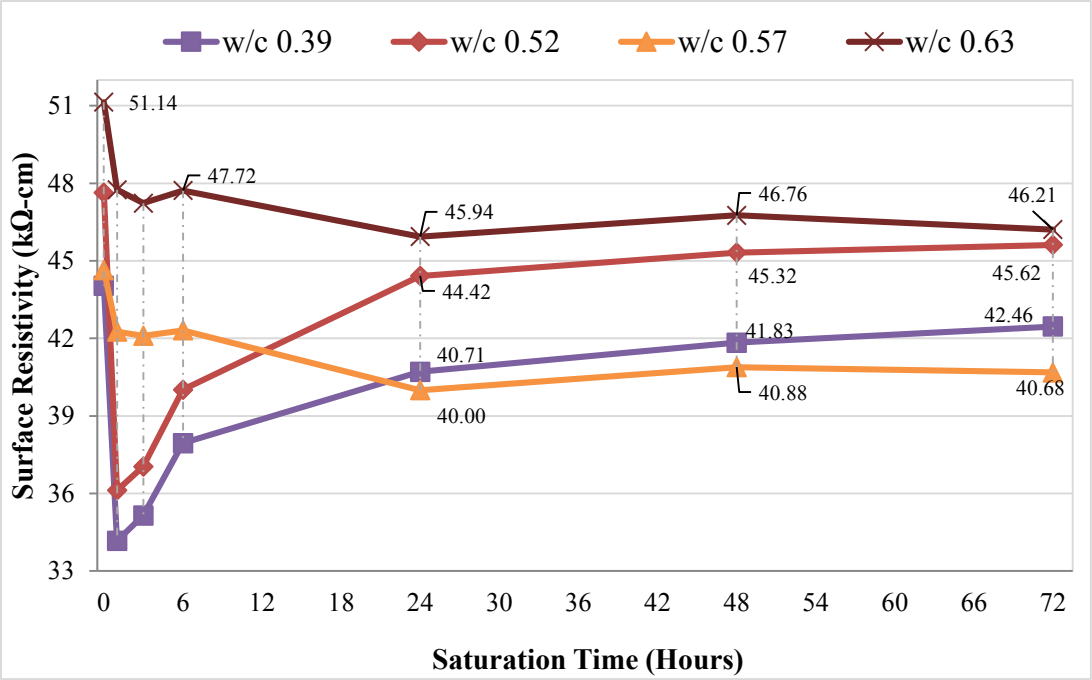

Figure 40. Resistivity Values against Saturation Time Mix 50TI-50S (56 days).

Figure 41 shows the tendency for mixture 50TI-20FA-30S. All the samples showed a very similar behavior. In this case, a lesser decrease was observed up to six hours. An average difference of - 9.0% was observed between the first measurement and the last. A similar behavior was observed for mix 50TI-30FA-20S (Figure 42).

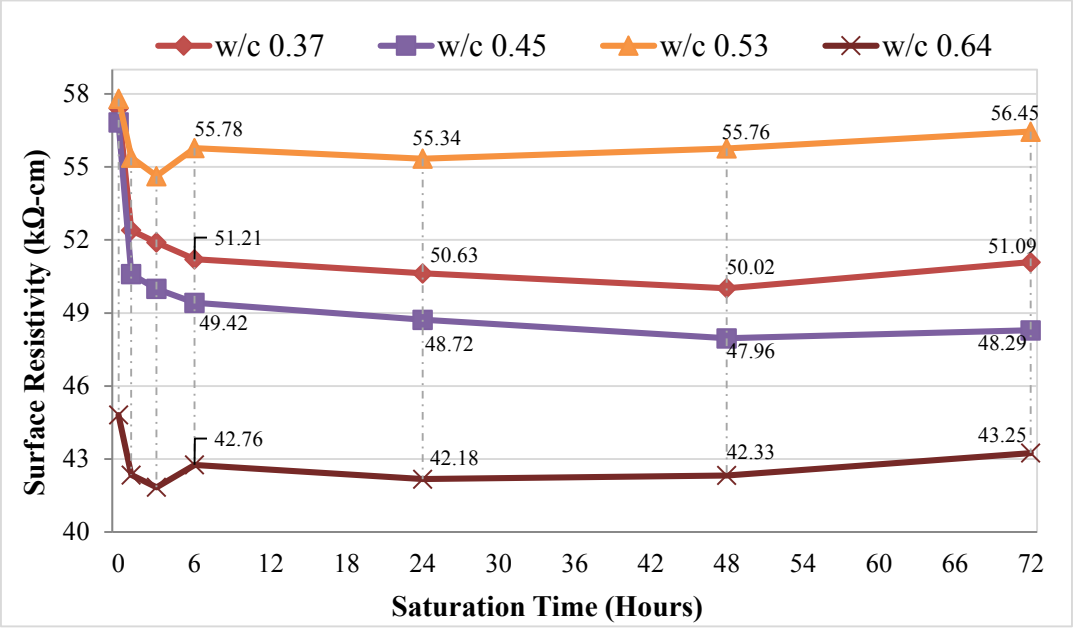

Figure 41. Resistivity values against Saturation Time Mix 50TI-20FA-30S (56 days).

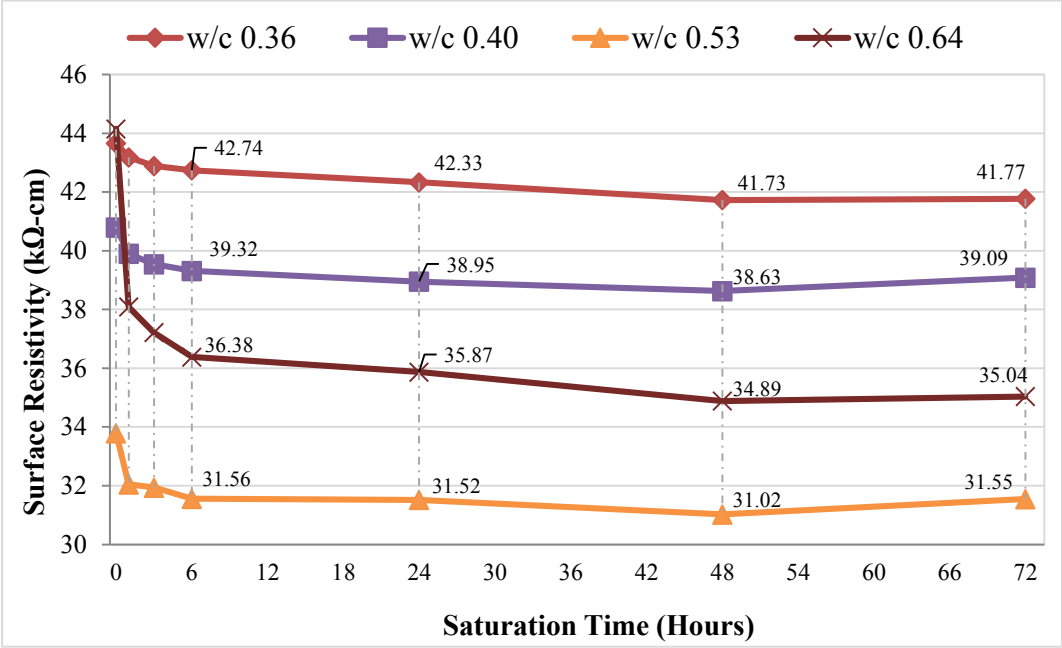

Figure 42. Resistivity values against Saturation Time Mix 50TI-30FA-20S (56 days).

4.1.3 Influence of Saturation – 91 days

Two of the five cylinders were tested for compressive strength at 56 days, leaving 3 cylinders for further resistivity testing. After 91 days, the surface resistivity test was performed again and it was observed that the resistivity behavior on the samples was very similar to the ones obtained 56 days.

Figure 43 shows the values obtained for 100TI at 91 days. There is a very marked decrease in resistivity on average 26% after one hour in limewater; at this age the pore network is not as dynamic as early stages. At this point surface resistivity is expected to increase as porosity decreases and tortuosity increases with additional binder hydration. For this reason, the transition between partially saturated and further saturation is more noticeable. After this time, increases were observed up to 6 to 24 hours depending on the w/c and then became relatively stable after 24 hours. The resistivity at 6 hours was approximately midway between that observed at 0 and 1 hour saturation. An average difference of -9.7% was observed between the first measurement and the last.

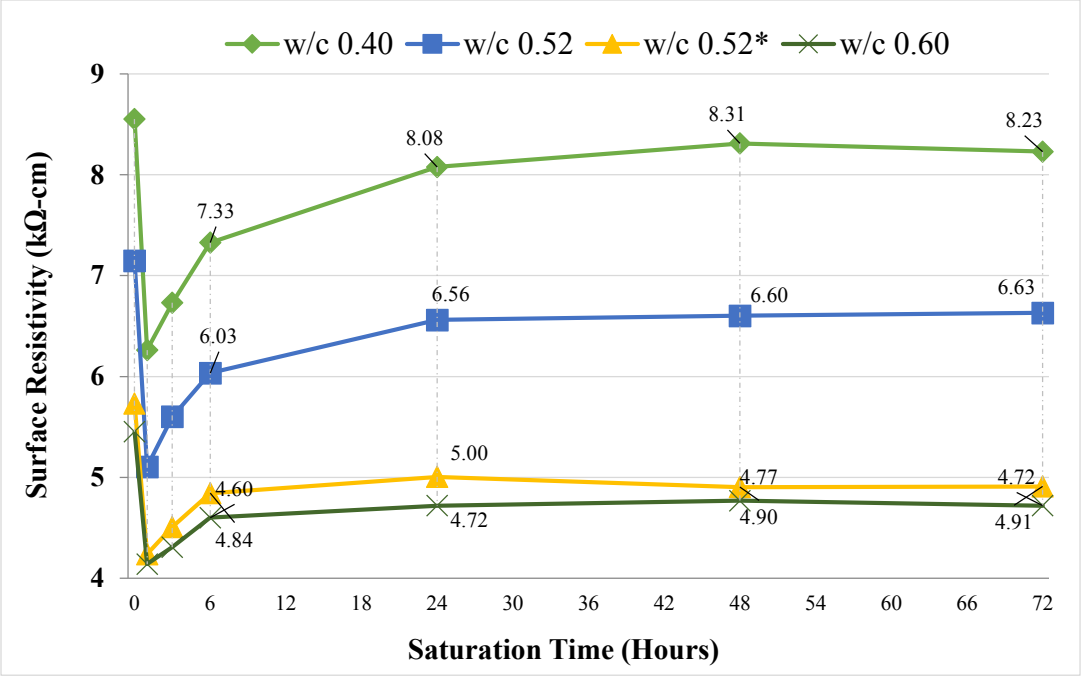

Figure 43. Resistivity Values against Saturation Time Mix 100TI (91 days).

Figures 44 and 45 shows the behavior at 91 days observed for 50TI–50S and 50TI-20FA-30S, respectively. Again, most changes were observed up to 6 hours and then the values were relatively stable after 24 hours. For the lowest two w/c, some small increases were observed between 48 and 72 hours. The magnitude of the drop between the initial measurement and that of 1 hour was similar to that observed in the 100TI mixture (on average -26.4%). An average difference of -6.1% was observed between the first measurement and the last.

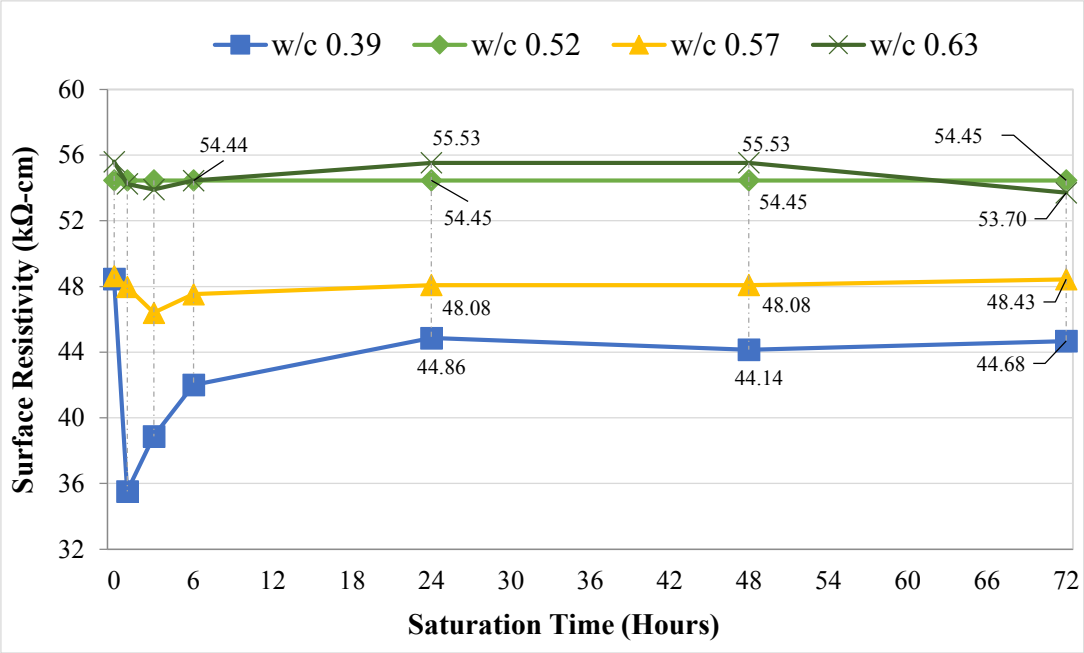

Figure 44. Resistivity Values against Saturation Time Mixture 50TI-50S (91 days).

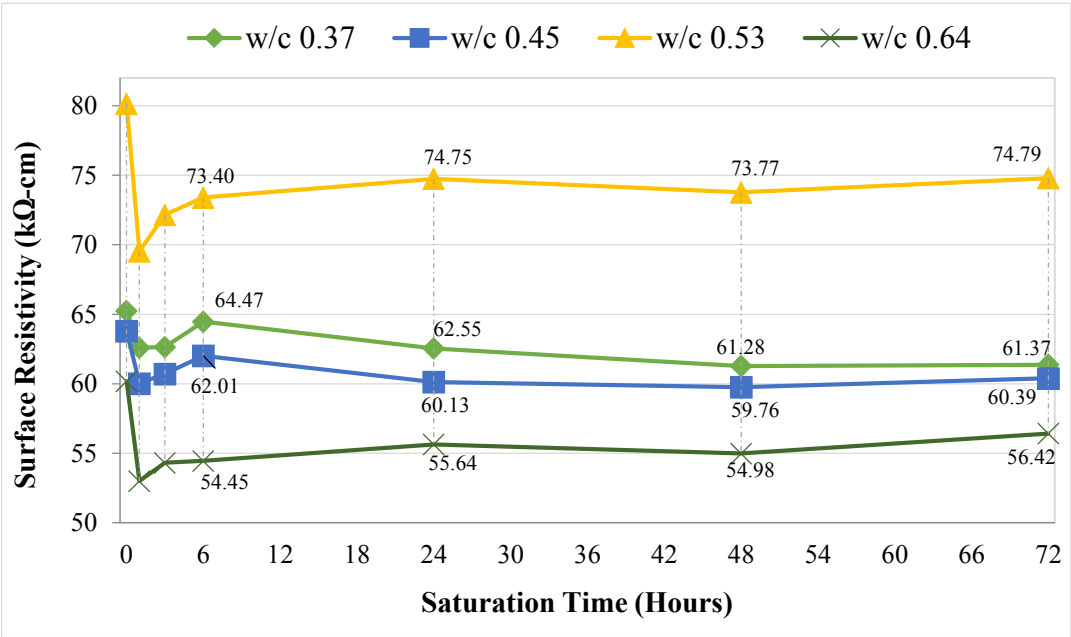

Figure 45. Resistivity Values against Saturation Time Mixture 50TI-20FA-30S (91 days).

Overall at 91 days, it was observed that some moderate increases in surface resistivity were observed between 1 and 24 hours for all the mixtures, but maintained relatively constant values after that time as was observed at 28 and 56 days.

4.1.4 Influence of Concrete Age and Supplementary Materials (SCMs) on Surface Electrical Resistivity

In this section, the influence of concrete age and supplementary cementitious materials influence on surface resistive were analyzed on the mixture samples cast in phase 1. Moreover, an estimation of the pore solution was estimated on each mixture using a free online software developed by Bentz (2007) is presented.

4.1.4.1 Influence of Concrete Age on Surface Electrical Resistivity

A comparison between the electrical resistivity increase over time for mixtures with water cement ratio equal or close to 0.40, 0.50 and 0.60 is presented in Table 17 which summarizes the surface resistivity values obtained through time for all the 20 mixtures tested. All results are those measured after 72 hours limewater saturation at the different ages. The bold values represent the multiplier from 7 days.

Table 17. Surface resistivity through time (days) for standard cylinders (ø10x20cm).

Standard cylinders (Ø10x20cm)		Surface Resistivity (kΩ-cm) after time (days)			
Mixtures	**w/c**	**7**	**28**	**56**	**91**
100TI	0.40	5.28	6.85	7.82	8.21
			+1.30	**+1.48**	**+1.56**
	0.52	4.47	5.78	6.45	6.60
			+1.29	**+1.44**	**+1.48**
	0.52*	3.60	4.47	4.85	4.74
			+1.24	**+1.35**	**+1.32**
	0.60	3.50	4.33	4.56	4.94
			+1.24	**+1.30**	**+1.41**
50TI-50S	0.39	6.25	34.92	45.12	54.45
			+5.59	**+7.22**	**+8.71**
	0.52	3.14	27.62	41.67	44.56
			+8.80	**+13.27**	**+14.19**
	0.57	4.76	28.51	40.52	48.20
			+5.99	**+8.51**	**+10.12**
	0.63	4.01	31.34	46.30	54.92
			+7.81	**+11.54**	**+13.69**
50L-50S	0.32	4.08	33.86	42.35	51.24
			+8.31	**+10.39**	**+12.57**
	0.44	9.04	40.66	50.39	62.80
			+4.50	**+5.57**	**+6.95**
	0.48	7.07	37.94	47.74	57.59
			+5.36	**+6.75**	**+8.14**
	0.50	5.55	33.80	43.51	51.59
			+6.09	**+7.83**	**+9.29**
50TI-30FA -20S	0.36	4.55	27.00	41.94	61.83
			+5.94	**+9.22**	**+13.59**
	0.40	3.89	24.55	38.89	56.07
			+6.32	**+10.01**	**+14.43**
	0.53	2.90	19.28	31.36	47.59
			+6.64	**+10.80**	**+16.38**
	0.64	2.73	17.96	35.27	47.07
			+6.59	**+12.93**	**+17.26**
50TI-20FA -30S	0.37	4.38	32.40	50.58	61.73
			+7.40	**+11.55**	**+14.10**
	0.45	3.01	28.08	48.32	60.09
			+9.31	**+16.03**	**+19.93**
	0.53	2.18	34.23	55.85	74.43
			+15.70	**+25.62**	**+34.15**
	0.64	1.93	25.36	42.58	55.68
			+13.12	**+22.04**	**+28.81**

For those samples with only Portland cement (100TI), the change is not as significant over time as can be observed for those with fly ash and slag. An increment of 1.56 times higher for the mixture 100TI w/c 0.40 was obtained between 7 to 91 days; for the mixture 50TI-30FA-20S w/c 0.40 increment of 14.43 times higher was obtained.

Figure 46 shows the average values obtained for all mixtures with a water cement ratio (w/c) close to 0.50. The electrical resistivity values obtained shows an accelerated resistivity increase especially for those containing fly ash and slag. Mixture 100TI (100% Portland cement) increases on average 1.48 times between the first measurement at 7 days and the last at 91 days. But for those mixtures with fly ash and slag, the increase is more significant; mixture 50TI- 50S during the same time the value increased on average 14.19 times higher, 50L-50S 9.29 times higher, 50TI30FA20S 16.38 and for those with 50TI20FA30S the value increased 34.15 times higher.

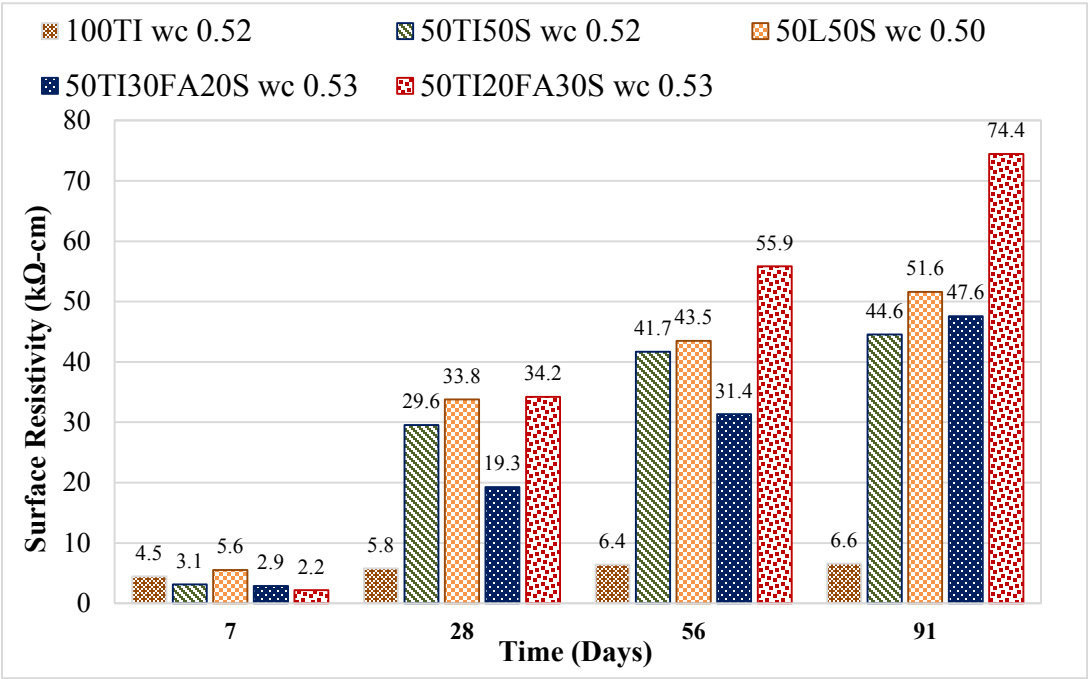

Figure 46. Resistivity increase over time for mixtures with w/c close to 0.50.

To verify the constant increase in surface resistivity, an extra set of samples was monitored on standard cylinder samples cast 5 five years previously (see Section 4.2.2 for the effect of saturation solution). The surface resistivity monitoring was conducted on standard cylinders (Ø10x20 cm) at three times over a period of 11 months. The samples stored in lab air between measurements.

Figure 47 illustrates the resistivity variation through three periods of time at three different saturation durations. The 0.40 w/c mixture contained 100% Portland cement and was saturated in limewater for the resistivity testing. Comparing the resistivity measured between September 2013 and August 2014, a 4.0 times increase was obtained, moving

from an average value of 12.30 kΩ-cm. to 49.47 kΩ-cm. Although these samples were approximately 5 years old at the time of the first resistivity measurement in September 2013, it can be seen that the resistivity is only about twice that observed in the similar Phase One mixture. It is postulated that the limewater absorbed during the 72 hour initial exposure initiated further hydration resulting in subsequently higher resistivity for the later measurements.

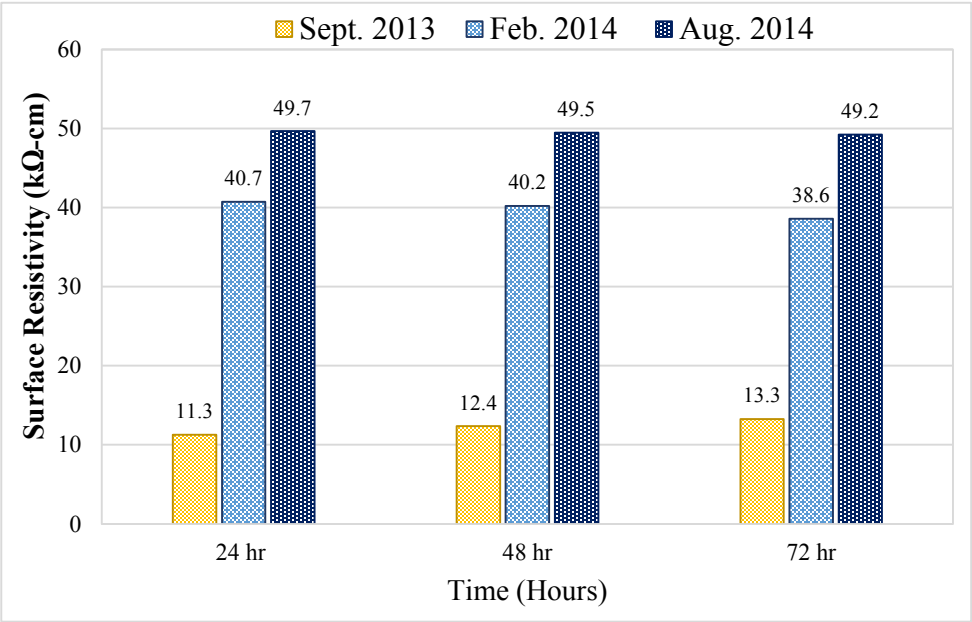

Figure 47. Resistivity variation through three periods of time – Mix 100TI.

For the Mixture 75TI-25FA a similar behavior was observed; Figure 48 illustrates the tendencies. Comparing again the resistivity measured between September 2013 and August 2014, the increase is less, only 1.6 times resistivity increases moving from an average value of 47.86 kΩ-cm. to 78.13 kΩ-cm. These samples were saturated with tap

water. The results indicate that the hydration process continues over time diminishing or blocking the continuous capillary pores to the extent that the pores are sufficiently segmented to prevent absorption of the solution which may be the reason why the surface electrical resistivity decreases between February and August 2014.

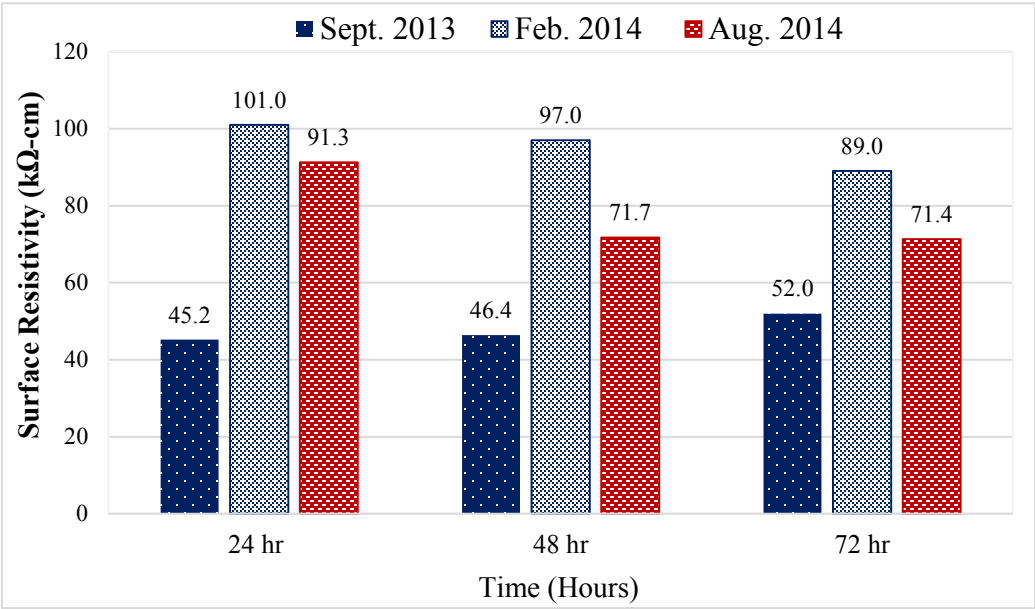

Figure 48. Resistivity variation through three periods of time – Mix 75TI – 25FA.

4.1.4.2 Influence Supplementary Materials (SCMs) on Surface Resistivity

It is expected that as the w/c increases, the surface resistivity should decrease indicating a more permeable concrete due to the greater porosity generated, leading to a lower tortuosity. The mixture with only 100% Portland cement (100TI) is a good example of this statement; Figure 49 shows the expected behavior. It can also be seen that resistivity increases with time as discussed in the previous section.

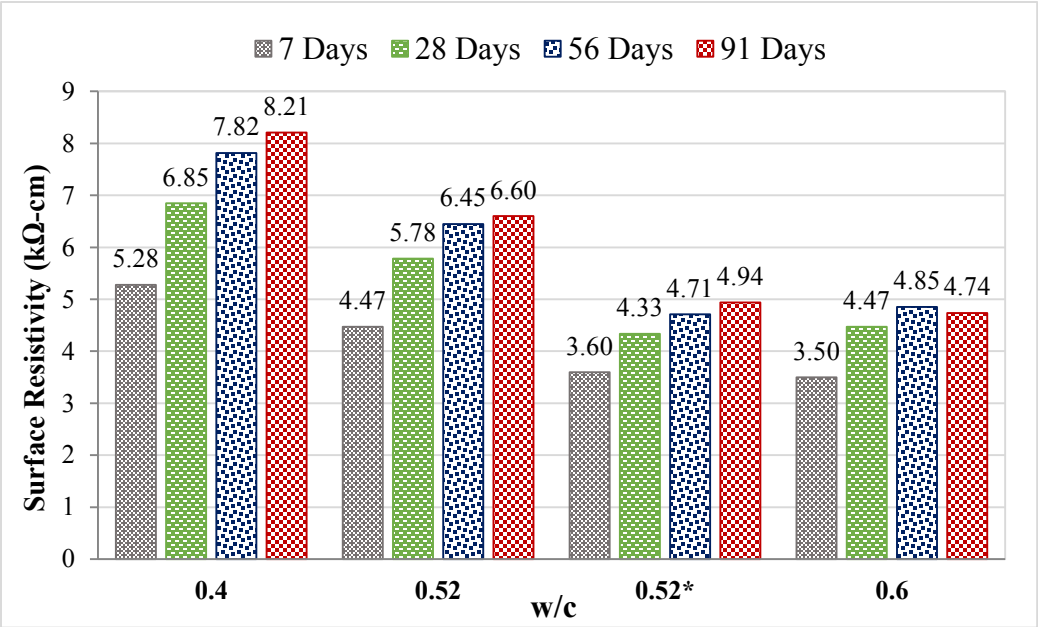

Figure 49. Resistivity Values for Mix 100TI within a range of w/c at different ages.

It is expected that supplementary materials will increase surface resistivity as was confirmed in this research. However, a different behavior with w/c was observed in those samples containing blast furnace slag. In this research, there was not a consistent decrease in resistivity with increasing w/c. Increasing water to cement ratio should decrease resistivity, but this was not consistently observed for the mixtures containing slag and agrees with the results of Rupnow and Icenogle et al. (2011). For those containing slag, 50TI-50S (50% Type I Portland Cement and 50% slag), 50L-50S (50% limestone cement and 50% slag), 50TI-30FA-20S (50% Type I Portland cement, 30% fly ash and 20% slag) and 50TI-20FA-30S (50% Type I Portland cement, 20% fly ash and 30% slag), a different behavior was observed as the water cement ratio was increased. This kind of behavior was more obvious after 56 and 91 days.

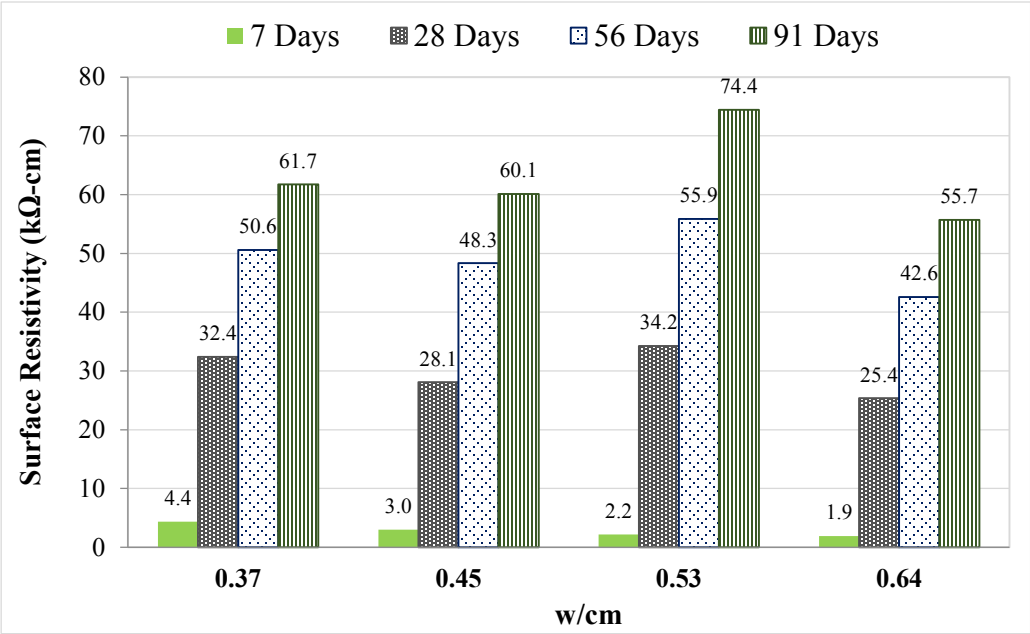

Figure 50. Resistivity Values for Mix 50TI-20FA-30S within a range of w/c at different ages.

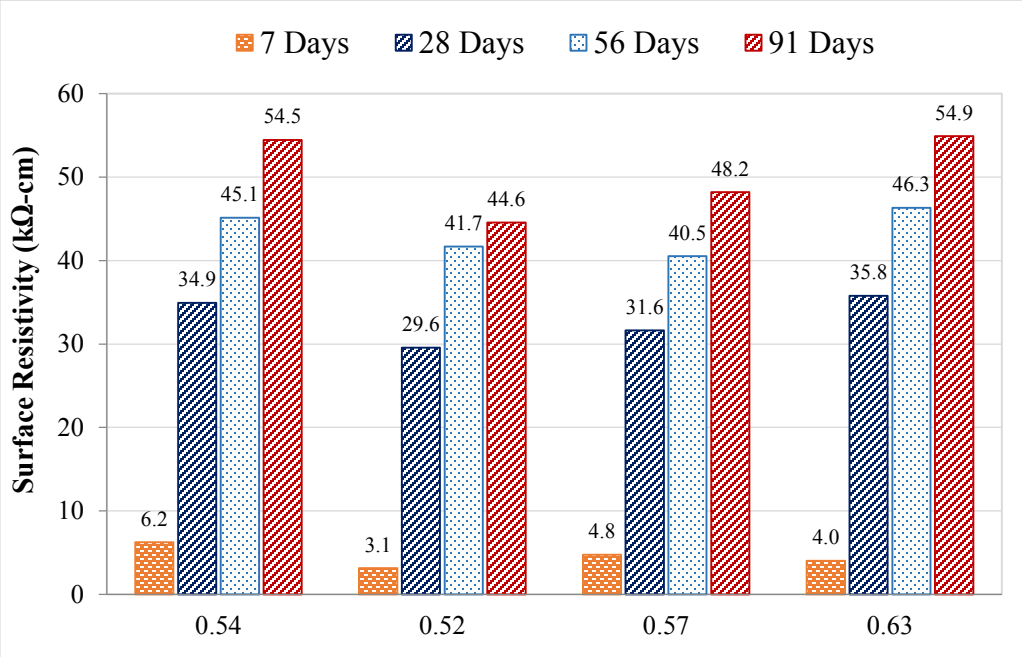

Figure 51. Resistivity Values for Mix 50TI-50S within a range of w/c at different ages.

Figures 50 and 51 shows the resistivity values do not decrease when the w/c increases for mixtures containing slag and fly ash. Only in the highest w/c ratios for some mixtures did resistivity decrease.

The effect of using SCMs generates a more complex and refined pore network; this was confirmed during the test conducted at 91 days with the standard cylinders (Ø10x20cm). The amount of water gain on every cylinder sample was measured at 91 days at the time of the final resistivity measurement. The mass of each cylinder was recorded after they were removed from storage conditions >85% RH, then again after 72 hours of saturation, once the constant resistivity value was obtained on each sample. Finally, they were dried at 110 ^{o} C for three consecutive days to measure the final mass. The mass gain was calculated as the 72 hour saturation minus the oven dry mass.

Figure 52 shows the relationship between water mass gain and surface resistivity when the w/c varies. It is possible to observe that mixtures networks without supplementary cementitious materials (SCMs) are less complex allowing more water flow through the concrete pore network, reason why resistivity is not affected once w/c is increased. PC represents Portland cement type I/II.

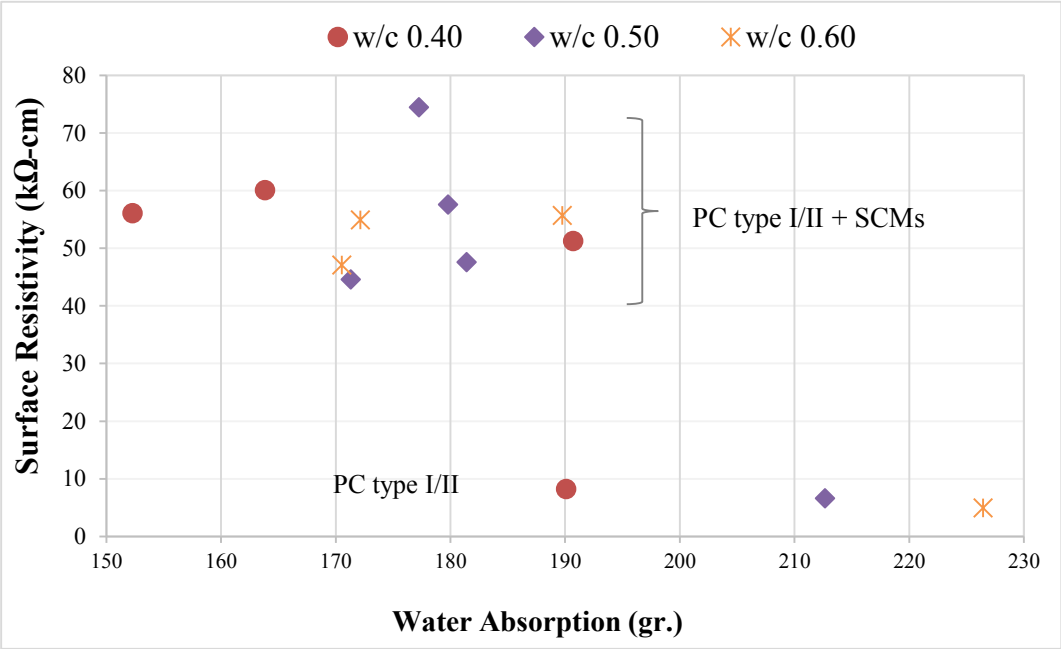

Figure 52. Relationship between water absorption and surface resistivity at 91 Days.

In this study it was established that, the porosity is highly reduced and this effect was clearly observed during the surface electrical measurements in where the highest values were obtained with the blends 50TI50S, 50L50S, 50TI30FA20S, 50TI20FA30S in comparison with those with only Portland cement (100TI) even though the w/c was increased due to a more complex, tortuous and less permeable pore network where the capillary pores are not connected making more difficult for the AC electrical current pass through the concrete sample. As the curing time passes, a secondary hydration reaction takes place when supplementary cementing materials (SCMs) are added. They react with the by-products of cement hydration. According to Powers et al. (1959), this kind of reaction increases the particle packing efficiency (durability) through diminishing or blocking the continuous capillary pores. Indicating that the pathway follow by the electrical

current is more tortuous due to the porous network reduction, where the possibility of chloride or sulphate attack, corrosion, or concrete degradation is minimized achieving negligible penetrability risk.

Besides the changes in porosity, the use of supplementary cementitious materials (SCMs) have an important influence on surface resistivity and compressive strength. A higher resistivity is related to higher compressive strength. According to the samples studied by Shahroodi (2010), lowering the w/c increases the compressive strength by 16% whereas the surface resistivity was increased by up to 60% at the same age.

4.1.4.2.1 Pore solution conductivity

The results indicate that surface resistivity values are clearly affected by the use of fly ash and slag. According to Nokken et al. (2006), at early ages the connectivity of the pore structure and pore size distribution is dynamically changing and the ionic concentration in the pore solution increases with age, generating higher electrical conductivity (lower resistivity) during the first 28 days.

As was mentioned before, pore solution chemistry in cementitious materials varies with mixture design and time. The National Institute of Standards and Technology (NIST) developed a technique to determine the conductivity of the pore solution using the concentration of different ionic species (Snyder et al., 2003).

Later on, the technique was programmed into a free web application by Bentz (2007) available at concrete.nist.gov/~bentz/poresolncalc.html. Modifying only the quantities of cement, water, type and amount of cementing materials used and assuming 80 % of hydration for each sample as input, it is possible to obtain an estimated pore solution conductivity of each binder. As the cement chemistry was unavailable, default values were used. Figure 53 shows the screenshot of the web application.

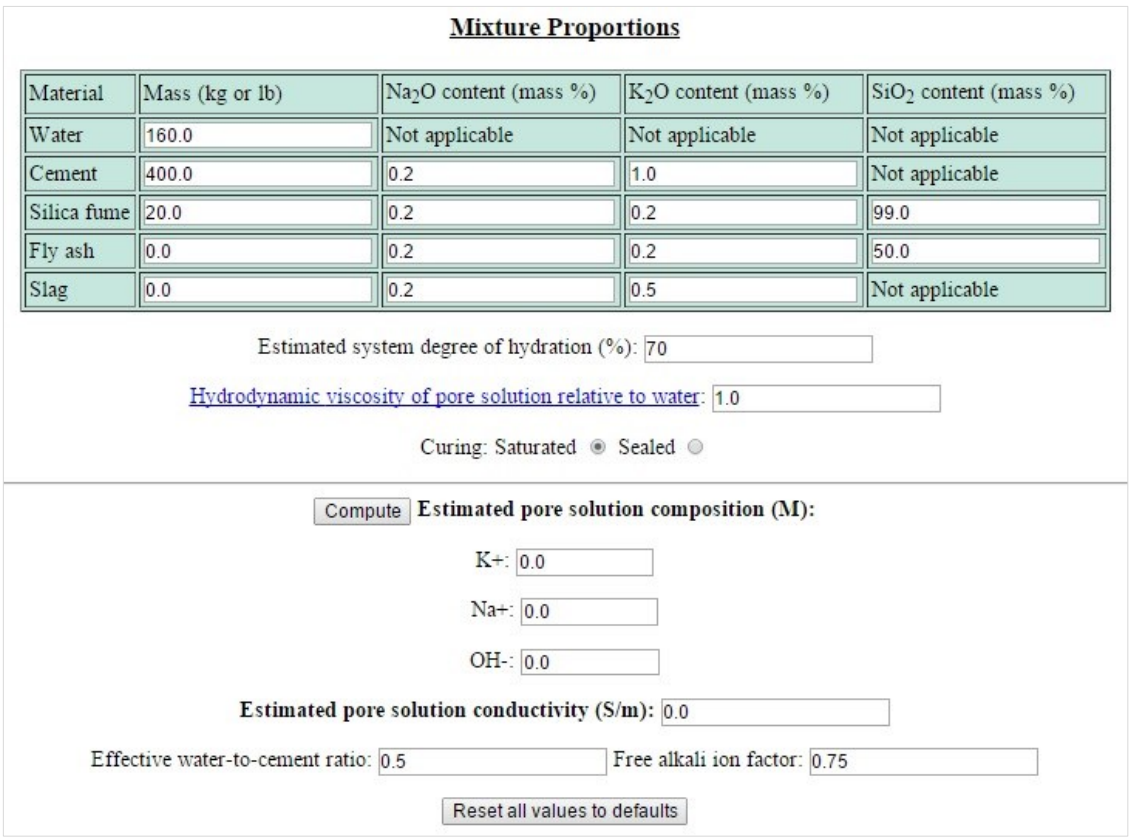

Mixture Proportions

Material	Mass (kg or lb)	Na_2O content (mass %)	K_2O content (mass %)	SiO_2 content (mass %)
Water	160.0	Not applicable	Not applicable	Not applicable
Cement	400.0	0.2	1.0	Not applicable
Silica fume	20.0	0.2	0.2	99.0
Fly ash	0.0	0.2	0.2	50.0
Slag	0.0	0.2	0.5	Not applicable

Estimated system degree of hydration (%): 70

Hydrodynamic viscosity of pore solution relative to water: 1.0

Curing: Saturated Sealed

Compute **Estimated pore solution composition (M):**

K+: 0.0

Na+: 0.0

OH-: 0.0

Estimated pore solution conductivity (S/m): 0.0

Effective water-to-cement ratio: 0.5 Free alkali ion factor: 0.75

Reset all values to defaults

Figure 53. Screenshot of the web application developed by Bentz (2007).

Table 18 shows the type of cement and supplementary cementitious materials used for the mixtures design for the cylinders samples cast in Phase One. The estimation of pore

solution conductivity and the measured final surface resistivity at 91 days from each mixture is given.

Table 18. Pore solution conductivity and surface resistivity at 91 days.

Mixtures Design	w/c	Air entrained (%)	Water (kg/m3)	Estimated Pore solution (M)			Estimated Pore solution conductivity (S/m)	Surface Resistivity at 91 days (kΩ-cm)
				Potassium (K^+)	Sodium (Na^+)	Hydroxide (OH^-)		
100TI	0.40	6	186	0.54	0.16	0.70	14.04	8.21
	0.52	8	191	0.37	0.11	0.49	10.11	6.60
	0.52*	6	146	0.36	0.11	0.46	9.66	4.74
	0.60	4	188	0.31	0.09	0.40	8.50	4.94
50TI-50S	0.39	4.5	217	0.22	0.07	0.29	6.23	49.94
	0.52	8	170	0.22	0.07	0.29	6.23	44.56
	0.57	5	144	0.22	0.07	0.29	6.23	48.20
	0.63	7	125	0.22	0.07	0.29	6.23	54.92
50L-50S	0.32	5	150	0.38	0.12	0.50	10.25	51.24
	0.44	4	142	0.22	0.07	0.29	6.35	62.80
	0.48	5	177	0.21	0.06	0.27	5.93	57.59
	0.50	6	139	0.19	0.06	0.25	5.47	51.59
50TI-30FA -20S	0.36	7	172	0.34	0.15	0.49	10.10	61.83
	0.40	3	151	0.29	0.12	0.41	8.67	56.07
	0.53	5	169	0.20	0.09	0.28	6.17	47.59
	0.64	7	175	0.16	0.07	0.23	5.02	47.07
50TI-20FA -30S	0.37	4	174	0.32	0.13	0.45	9.38	61.73
	0.45	4	155	0.27	0.11	0.38	7.97	60.09
	0.53	5	169	0.19	0.08	0.27	5.86	74.43
	0.64	5.5	175	0.15	0.06	0.21	4.74	55.68

Although the differences between the estimated pore solution conductivity on each mixture was not as significant as the surface resistivity, it is possible to notice that when the water to cement ratio is low, the estimated pore solution conductivity (S/m) is high as well values of individual conductive ions, Potassium (K^+), Sodium (Na^+), and Hydroxide (OH^-). The opposite happens when water to cement ratio is high, the conductivity and conductive ions are reduced. Figure 54 shows a comparison of the estimated pore solution conductivity and surface electrical resistivity at 91 days. For instance, those with only Portland cement

(100TI) the pore solution conductivity values were highest (lowest resistivity) but with the lowest resistivity values. However, if a comparison is established for those mixtures with fly ash and slag (50TI30FA20S and 50TI20FA30S) to mixtures with 100TI at similar water cement ratio (w/c), the pore solution conductivity is on average 1.78 times less but on average 10 times higher for electrical resistivity. Indicating an inverse relation between conductivity and electrical resistivity.

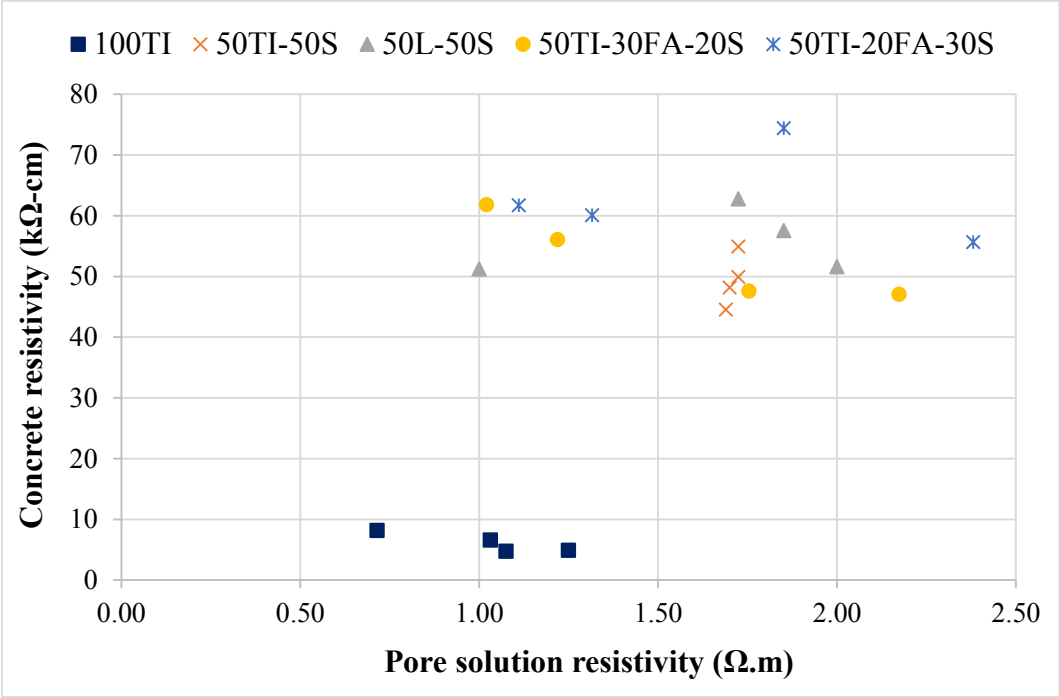

Figure 54. Estimated pore solution conductivity and surface resistivity comparison at 91 days.

4.2 Phase Two – Influence of Samples Storage under Different Solutions and Specimen Geometry

The motivation in this section was to determine the rate of change in surface resistivity in relation to saturation solution and geometry on a variety of concrete mixtures. Two types of specimen geometries were cast for each mixture, 6 cylinders (Ø10x20 cm) and 4 circular slabs (Ø30x12 cm) as shown in Figure 55.

Figure 55. Standard cylinders Ø10x20cm and circular slab Ø30x12cm.

4.2.1 Specimen Geometry

The methodology to measure the surface resistivity on the standard cylinders was performed as described in section 3.2. Except for the 7 day value, all measurements are presented after 48 hours in the respective solution. All the results for cylinders represent the average of 24 measurements (8 per each of 3 cylinders) for each point. For the circular slabs, each result presented represents the average of 32 measurements (16 per each of 2 circular slabs) for each point. In both cases, the geometry factor was applied to the measured values; 1.89 for the cylinders and 1.126 for the slabs. A comparison between the resistivity for three mixtures for the two types of geometries is presented in Table 19. Each value represents the average surface resistivity through time, starting at 7 to 155 days.

Table 19. Average surface resistivity values for Phase Two mixtures

Mixtures	w/cm	Geom.	Average Surface resistivity ((kΩ-cm) trough time (days)											
			7		28		56		91		119		155	
			Storage solution											
			LW	TW	LW	TW	LW	TW	LW	TW	LW	TW	LW	TW
100TI	0.40	Ø10x20	5.47	5.65	7.84	8.28	9.80	9.94	10.91	10.55	10.53	10.81	11.33	11.38
		Ø30x12	6.27	6.29	8.57	8.45	10.74	10.14	12.10	11.09	13.11	11.12	14.43	12.19
	0.50	Ø10x20	4.48	4.33	5.61	5.70	6.98	7.06	8.19	7.52	7.60	7.41	8.25	7.96
		Ø30x12	4.97	4.98	6.88	5.72	5.99	8.15	8.67	7.15	8.72	9.87	9.55	8.40
50TI30FA20S	0.40	Ø10x20	2.92	3.10	26.65	28.52	57.41	58.07	76.12	69.46	74.84	72.19	92.79	88.88
		Ø30x12	3.53	3.39	34.97	31.82	NA	66.36	72.89	74.41	77.80	84.93	96.36	106.23

Figure 56 shows in detail the values obtained at 28 days where the apparent resistivity (ρ_{app}) obtained directly from the specimens reveals a high difference for the two

geometries. However, once the (ρ_{app}) value is divided by the geometry factor a real resistivity (ρ_{real}) value is achieved, reducing the differences between the two geometries.

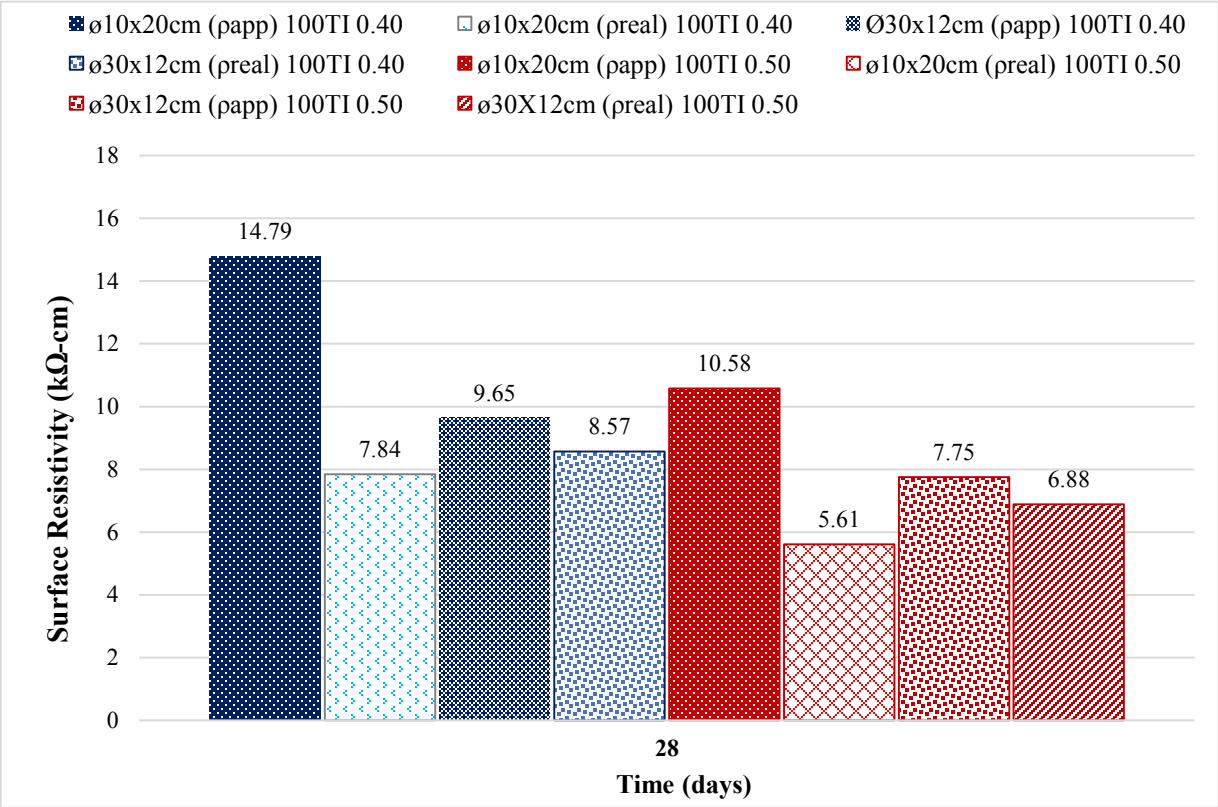

Figure 56. Effect of geometry factor before and after correction on mixtures 100TI with w/c equal to 0.40 and 0.50 at 28 days.

Table 20 summarizes the percentage differences between the resistivity values obtained directly (ρ_{app}) and after the geometry correction, where for the majority of the slabs samples (ø30x12cm) achieved a higher resistivity value after the geometry factor was applied. The percentage difference was calculated using the formula:

$$\%\,difference = \frac{\rho cylinder - \rho slab}{\rho cylinder} \qquad [17]$$

Table 20. Percentage differences before and after apply the geometry correction factor.

Mixes	w/cm	Geom.	Surface resistivity ((kΩ-cm) trough time (days)											
			7		28		56		91		119		155	
			ρapp	ρreal	ρapp	ρreal	ρapp	ρreal	ρapp	ρreal	ρapp	ρreal	ρapp	ρreal
100TI	0.4	ø10x20 / ø30x12	+33.5%	-11.4%	+39.1%	-2.0%	+39.2%	-1.9%	+37.3%	-5.1%	+38.6%	-2.9%	+43.3%	+4.9%
	0.5	ø10x20 / ø30x12	+31.5%	-14.8%	+40.1%	-0.5%	+31.2%	-15.3%	+43.2%	+4.9%	+20.5%	-33.1%	+44.1%	+6.3%
50TI30FA20S	0.4	ø10x20 / ø30x12	+34.7%	-9.5%	+33.4%	-11.6%	+31.8%	-14.3%	+36.1%	-7.1%	+29.8%	-17.6%	+36.7%	-6.1%

In Table 20, the cases where the slab has higher resistivity is represented with the symbol (-). In cases where the standard cylinders (ø10x20cm) presented a higher value, the symbol is (+). As shown in Table 20, the correction factor unified and reduces the gap between the two geometries but a percentage difference remains afterwards.

For planar surfaces, the proximity between the contact probes with the aggregates varies, it can be shorter in some cases due to construction practices (i.e. poor vibration) or due to the casting direction. As well, the Wenner four probe device location relative to the casting direction is different for the two geometries. Aggregates most often present higher resistivity in comparison with cement paste it can lead to higher resistivity results in comparison with curved surfaces. For planar surfaces, any segregation would be noticeable in regards to resistivity. However, on standard cylinders, segregation can appear

at the bottom of the cylinder but the Wenner probe device is located along the depth of the specimen.

4.2.1.1 City of Montreal (Ville de Montréal) Laboratory Samples

In addition to the samples cast for this research at Concordia University laboratory, another sets of samples were tested from a sidewalk project conducted by the City of Montreal (Ville de Montréal) and Sherbrooke University as was mentioned before in section 3.2.

All the samples were cast on October 2nd 2013 and afterwards stored in a fog room with a constant 99% RH at 21 ^{o}C. Figure 57 shows the surface electrical resistivity obtained 336 days after casting. The samples were measured directly from the fog room and not further saturated. Each value shown represents an average of a direct measurement from 22 cylinders (ø10x20cm) and 4 cylinders (ø15x30cm) mixture sample VdeMTL Temoin (GU), 8 cylinders (ø10x20cm) and 4 cylinders (ø15x30cm) for mixture samples VdeMTL 25PV and 10PV, respectively. In the same figure, (ρ app) represents the resistivity measured directly without the geometry correction factor and (ρ real) after the geometry correction factor (k) was applied.

All resistivity values were calculated to include the correction factor as mentioned in section 2.2.3 when $d/a \leq 6$ or $L/a \geq 6$. For ø10x20cm cylinders the correction value is 1.89 and for ø15x30cm, the correction value is 1.39. Again after the cell correction was

applied, a reduction in the difference between the two cylinders was achieved but the surface resistivity values were not the same.

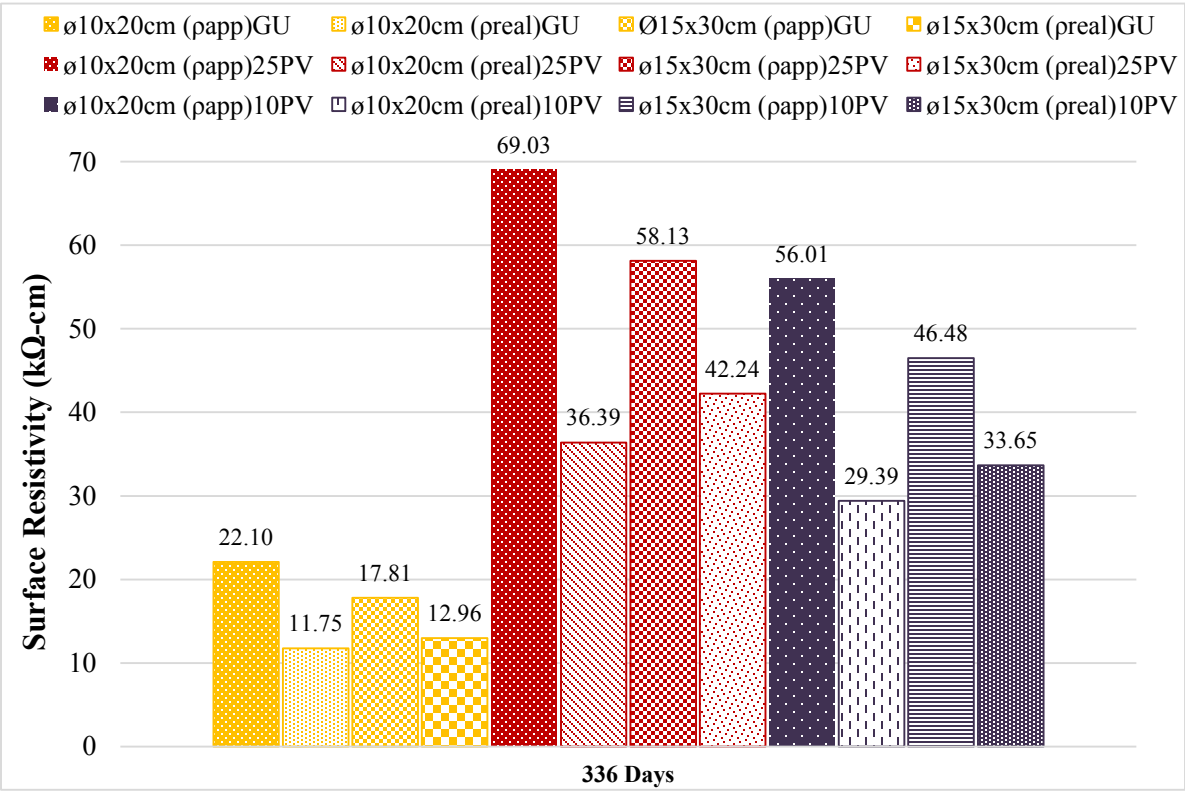

Figure 57. Effect of geometry factor Correction for City of Montreal

Table 21 shows more clearly the percentage difference achieved with these two sample geometries at 336 days after casting. As was found for this set of samples, the highest resistivity values were achieved for the larger sample (15x30cm) once the geometry factor was applied. (On the table, this is represented again with the symbol (-)).

Table 21. Average differences on specimen geometry from City of Montreal.

Mixtures	w/cm	Geom.	Surface resistivity (kΩ-cm) at 336 days			
			ρapp	Av. Diff	ρreal	Av. Diff
VdeMTL - 73% GU + 27 GU-SF	0.43	ø10x20	22.10	+24.1%	11.75	-9.3%
		ø15x30	17.81		12.96	
VdeMTL (25PV) 25% glass powder + 75% Type GU	0.40	ø10x20	69.03	+18.8%	36.41	-13.8%
		ø15x30	58.13		42.24	
VdeMTL (10PV)10% glass powder + 90% Type GU	0.41	ø10x20	56.01	+20.5%	29.41	-12.6%
		ø15x30	46.48		33.65	

From the two sets of geometries analyzed using the same probe spacing (38 cm), it is possible to determine that there is a clear influence of specimen geometry. In both sets, the sample with larger volume generally leads to higher surface electrical resistivity, even when corrected for geometry.

4.2.1.2 Layer contact surface

Using the circular slabs, the resistivity was measured on both sides (top and bottom) at 155 days. For all samples, the bottom surfaces developed a smoother surface in comparison with top surfaces. Table 22 shows the influence of this factor on the circular slabs after 155 days. On the table, the symbol (+) indicates that the bottom surface has lower resistivity value in comparison with the top surface. The percentage difference was calculated as $(\rho_{top}-\rho_{bottom})/\rho_{top}$.

Table 22. Average electrical resistivity and percentage differences between top and bottom layers from circular slabs.

Mixtures	w/cm	Electrical resistivity ((kΩ-cm) differences								
		Time	24 Hours				48 Hours			
		Type of surface	LW	% Diff.	TW	% Diff.	LW	% Diff.	TW	% Diff.
100TI	0.4	Top	14.18	+18.8%	11.93	+2.6%	14.43	+17.8%	12.19	-2.0%
		Bottom	11.93		11.62		12.25		12.44	
	0.5	Top	9.28	-4.5%	8.18	-14.1%	9.55	-3.4%	8.40	-13.2%
		Bottom	9.71		9.53		9.88		9.68	
50TI30FA20S	0.4	Top	91.58	-40.9%	105.23	-19.8%	96.36	-22.6%	106.23	-19.9%
		Bottom	154.94		131.19		124.45		132.64	

With only the exception for mix -100TI w/c 0.40, it was observed that the top surface had lower resistivity. The influence is more noticeable for the mixture with fly ash and slag after the specimen was fully saturated and less remarkable on those with Portland cement in comparison. For the Portland mixture with the lower water to cement ratio, the top surface had higher resistivity using limewater, but comparable values using tap water. Ideally, the smooth bottom surface should result in values closer to the cylinders presented in Table 19. As this is not the case, the curvature of the surface is of greater influence. According to the concrete's final use (sidewalks, pavement or structural elements), using any type of form after compaction, vibration, evaporation of water in and out of the concrete and curing is going to generate an external layer with different permeability in comparison with inner core concrete or other parts where the same manipulation didn't take place.

4.2.2 Sample Storage under Different Solutions

4.2.2.1 Initial Study of Saturation Solution on Mature Samples

As an initial investigation on the influence of the immersion solution on the duration required for stable resistivity measurements, two set of mature concrete were investigated. Figure 58 shows the resistivity values during the first one (1) hour for the mature samples measured in September 2013. Mixture 75TI-25FA was saturated in tap water and Mixture 100TI in limewater. The resistivity steadily decreased throughout this period. In the Figure, it is possible to observe an average difference of -15.16% between the first measurement and that at one hour for the mature sample containing fly ash. A similar behavior was observed for the Mix 100TI where the average difference was -29.3% between the first measurement and one hour.

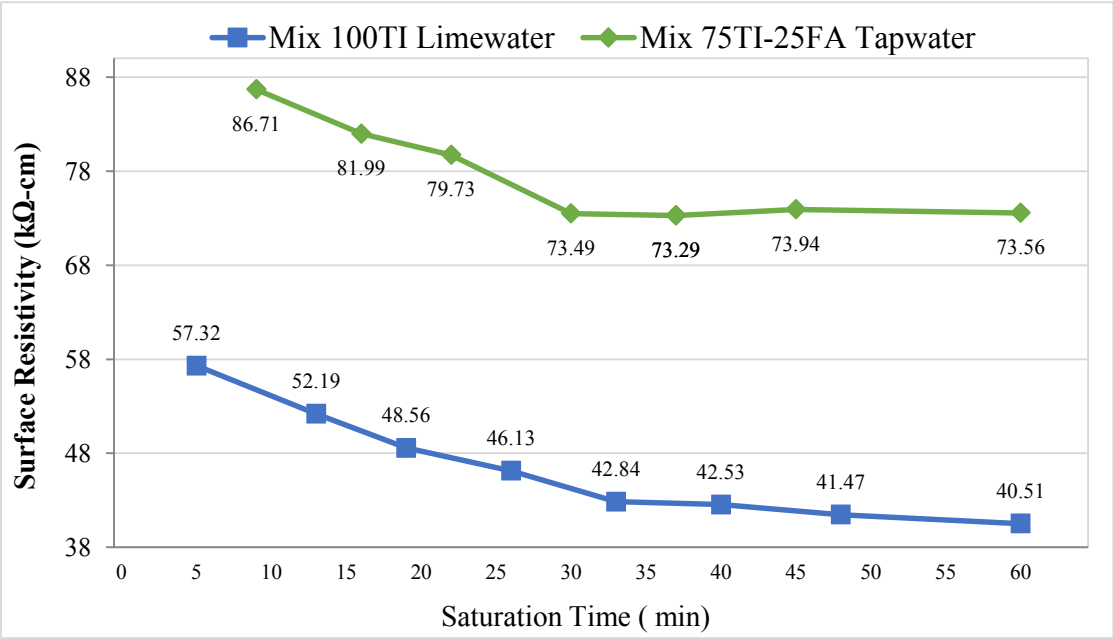

Figure 58. Resistivity values within the first hour – Mature Mixtures. Sept 2013.

Figure 59 shows the average results up to the full 72 hours measured for both mixtures. For Mixture 100TI, resistivity decreases rapidly and significantly up to 24 hours. It can be seen that after 24 and until 72 hours the resistivity increases slightly and an average difference of -76.86 % between the first measurement (5 minutes) and the last one (72 hours) was determined and a final average value of 13.26 kΩ-cm.

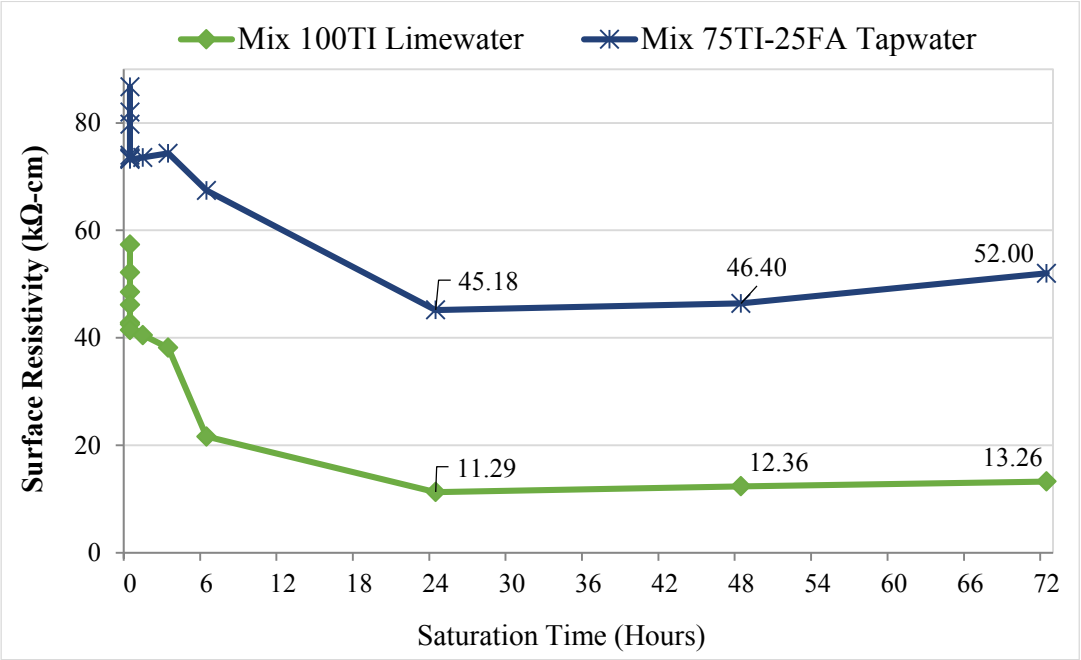

Figure 59. Resistivity values up to 72 hours – Mature Mixtures. Sept 2013.

A similar behavior was observed for the mixture 75TI-25FA, except that the resistivity increases somewhat after 24 hours and an average difference of - 40% between the first measurement (9 minutes) and the last one (72 hours) was estimated for a final average value of 52 kΩ-cm.

After a period of time chosen randomly in order to verify again this resistivity behavior, three months later the same test was conducted under the same conditioning factors. During the time before test, all the cylinders were stored under air laboratory conditions.

Figure 60 shows the resistivity values for the samples 100TI and 75TI-25FA during the first one (1) hour and after 11 measurements. In the Figure, it is possible to observe that the average difference increase for both samples, -56.35% between the first measurement and the last for the Mix 100TI and - 45.90% for the Mix 75TI-25FA, between the first measurement and the last one.

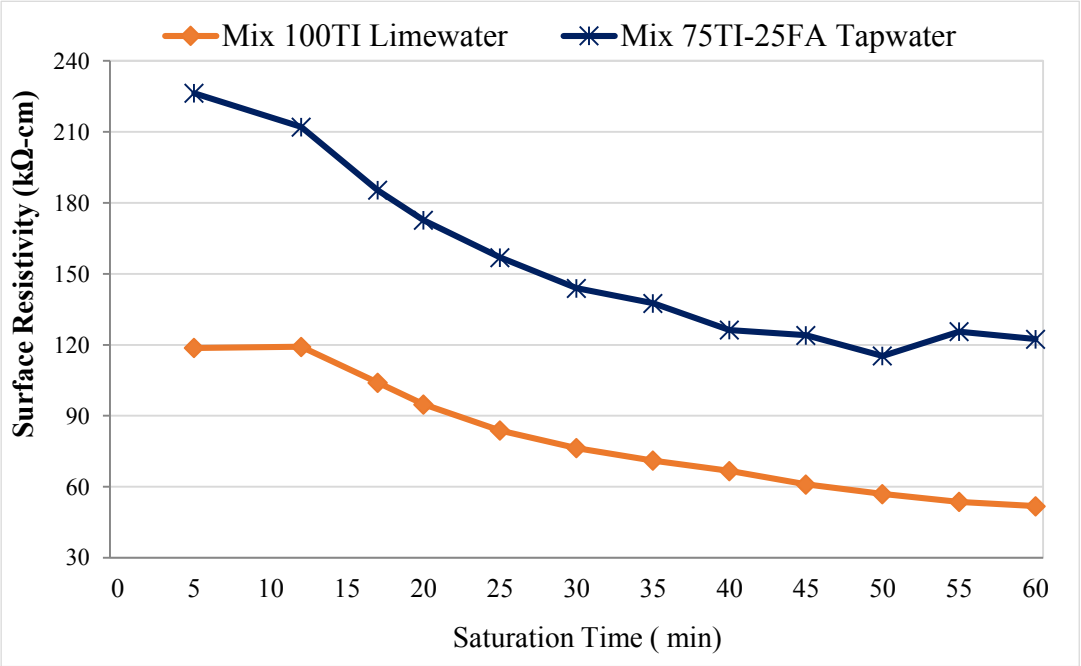

Figure 60. Resistivity values within the first hour – Mature Mixtures. Feb. 2014.

Figure 61 shows that the resistivity value stabilizes after 24 hours for both concretes. There is a representative increase in the final resistivity value at this time after a small period of

three months related to the continuing hydration process. For those samples with Mixture 100TI the resistivity increases from 13.26 kΩ-cm to 38.60 kΩ-cm and for Mixture 75TI-25FA from 52 kΩ-cm to 89 kΩ-cm.

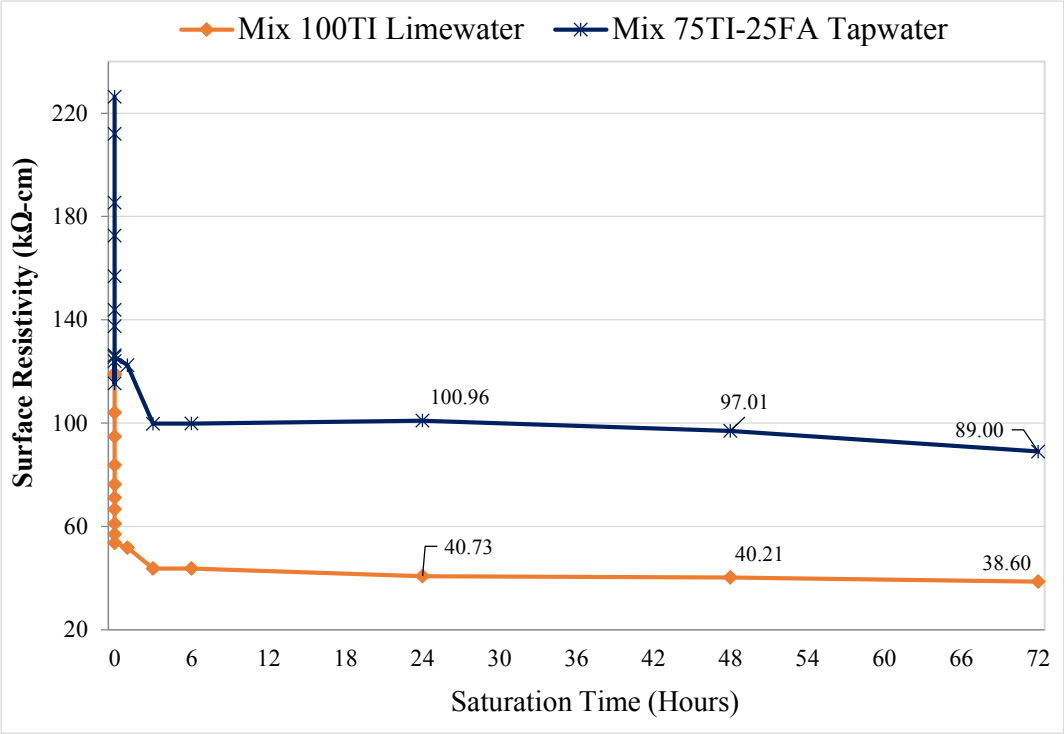

Figure 61. Resistivity values up to 72 hours – Mature Mixtures. Feb. 2014.

Finally, after 11 months the same procedure was followed for both mixtures. The same tendency was observed after different degrees of saturation.

4.2.2.2 Influence of Saturation Solution on Phase Two Samples

Table 23 shows the influence of these two solutions on the surface electrical resistivity analyzed in this study, limewater and tap water are represented as LW and TW,

respectively where at initial ages, 7 and 28 days, there is not a significance influence for the type of storage solution. At 56 days, tap water tends to result in higher resistivity. However, after 56 days, it is possible to observe a higher resistivity with the limewater solution.

Table 23. Influence of storage and specimen geometry on electrical surface resistivity.

Mixture samples		w/c	Time (Hours)	Surface Resistivity (kΩ-cm)									
				0		1		3		24		48	
			Geom.	LW	TW	LW	TW	LW	TW	LW	TW	LW	TW
7 Days	100TI	0.4	ø10x20									5.47	5.65
			ø30x12									6.27	6.29
		0.5	ø10x20									8.99	4.33
			ø30x12									4.97	4.98
	50TI30FA20S	0.4	ø10x20									2.92	3.10
			ø30x12									3.53	3.39
			Time (Hours)	0		1		3		24		48	
				LW	TW	LW	TW	LW	TW	LW	TW	LW	TW
28 Days	100TI	0.4	ø10x20							7.70	8.10	7.84	8.28
			ø30x12							8.48	8.54	8.57	8.45
		0.5	ø10x20							5.45	5.60	5.61	5.70
			ø30x12							6.82	5.62	6.88	5.72
	50TI30FA20S	0.4	ø10x20							25.22	27.23	26.65	28.52
			ø30x12							33.65	31.74	34.97	31.82
			Time (Hours)	0		1		3		24		48	
				LW	TW	LW	TW	LW	TW	LW	TW	LW	TW
56 Days	100TI	0.4	ø10x20							9.86	9.78	9.80	9.94
			ø30x12							10.65	10.34	10.74	10.14
		0.5	ø10x20							7.09	7.06	6.98	7.06
			ø30x12							6.12	8.20	5.99	8.15
	50TI30FA20S	0.4	ø10x20							56.93	58.01	57.41	58.07
			ø30x12								67.48		66.36
			Time (Hours)	0		1		3		24		48	
				LW	TW	LW	TW	LW	TW	LW	TW	LW	TW
91 Days	100TI	0.4	ø10x20	13.35	10.32	9.68	10.38	9.61	10.22	11.26	10.61	10.91	10.55
			ø30x12	15.46	10.88	11.89	10.79	11.52	10.66	12.24	11.07	12.10	11.09
		0.5	ø10x20		7.33	7.60	7.44	7.70	7.05	8.47	7.58	8.19	7.52
			ø30x12	10.45	7.02	8.03	7.03	8.73	7.00	8.83	7.23	8.67	7.15
	50TI30FA20S	0.4	ø10x20		71.39	64.66	68.65	64.13	64.22	77.20	69.86	76.12	69.46
			ø30x12	76.96	74.07	73.06	73.51	71.29	72.32	72.27	72.66	72.89	74.41
			Time (Hours)	0		1		3		24		48	
				LW	TW	LW	TW	LW	TW	LW	TW	LW	TW
119 Days	100TI	0.4	ø10x20	10.24	10.50	10.58	10.84	10.16	10.48	10.57	10.93	10.53	10.81
			ø30x12	13.49	10.86	14.06	11.03	13.13	10.67	13.60	11.32	13.11	11.12
		0.5	ø10x20	7.82	7.54	7.86	7.58	7.53	7.26	7.77	7.34	7.60	7.41
			ø30x12	10.21	8.06	9.47	7.82	9.13	8.06	8.89	7.89	8.72	7.78
	50TI30FA20S	0.4	ø10x20	88.00	79.69	76.74	75.30	74.26	71.02	76.44	72.17	74.84	72.19
			ø30x12	86.26	89.58	70.03	87.72	75.74	86.35	70.02	87.72	77.80	84.93
			Time (Hours)	0		1		3		24		48	
				LW	TW	LW	TW	LW	TW	LW	TW	LW	TW
155 Days	100TI	0.4	ø10x20	11.36	11.63	11.77	11.55	12.33	11.79	10.91	10.97	11.33	11.38
			ø30x12	14.72	12.40	15.14	12.16	14.98	12.33	14.18	11.93	16.25	12.19
		0.5	ø10x20	8.90	8.30	9.19	8.10	9.34	8.20	8.21	7.83	8.25	7.96
			ø30x12	10.24	8.15	10.12	9.72	9.65	8.99	9.28	8.18	9.55	8.40
	50TI30FA20S	0.4	ø10x20	108.17	97.57	106.02	92.03	102.19	88.36	95.29	87.49	92.79	88.88
			ø30x12	97.22	99.07	93.90	109.60	94.32	110.72	91.58	105.23	96.36	106.23

Table 24 summarizes the average percentage differences between the two solutions. At 91 days, the highest percentage differences were observed in 100TI w/c 0.50 for both geometries. For those samples stored in limewater solution, the surface resistivity value was higher.

Table 24. Average Percentage Differences between Lime Water (LW) and Tap Water (TW) After 48 Hours Immersion.

Mixes	w/cm	Geom.	Days											
			7		28		56		91		119		155	
			Storage solution											
			LW	TW	LW	TW	LW	TW	LW	TW	LW	TW	LW	TW
100TI	0.4	Ø10x20		+ 3.2%		+ 5.1%		+ 1.1%	+ 4.6%			+ 3.0%		+ 0.5%
		Ø30x12		+ 0.3%	+ 1.0%		+ 4.3%		+ 8.9%		+ 16.0%		+ 15.7%	
	0.5	Ø10x20	+ 3.4%			+ 2.1%		+ 0.8%	+ 12.1%		+ 4.0%		+ 4.1%	
		Ø30x12		+ 0.2%	+ 17.3%			+ 25.9%	+ 17.8%		+ 11.0%		+ 11.9%	
50TI30FA20S	0.4	Ø10x20		+ 5.6%		+ 7.0%		+ 1.5%	+ 9.1%		+ 4.6%		+ 6.2%	
		Ø30x12	+ 4.1%		+ 7.3%					+ 1.3%		+ 14.3%		+ 11.1%

From the results obtained, the use of tap water is feasible for saturation purposes in the field. At early ages (7, and 28) there is not a clear major influence neither tap water nor limewater. Therefore, for quality control tests conducted prior to this stage, no correction would likely be required. However, at or after 56 days, the use of limewater with volume ratio less or equal to 3:1 leads to surface resistivity on average 12% higher at 91 days, 8.9% higher at 119 days and 9.5% higher at 155 days than that measured on those submerged continuously in tap water.

4.3 Phase Three – Analysis of Correlations to Normalize Temperature Effect on Site and the Influence of Curved and Plane Surfaces

As mentioned in Section 3, the motivation in this section was to evaluate the correlations to normalize temperature effect established by Liu (2014) as well as to evaluate geometry effects.

4.3.1 Evaluation of Correlations to Normalize Temperature Effects

A total of 96 measurements were conducted directly on the sidewalks after rainfall on two different days (September 11 and 13, 2014). Sixteen measurements were performed for each mixture on each day; Figure 62 indicates how the measurements were taken twice at different locations over the sidewalks.

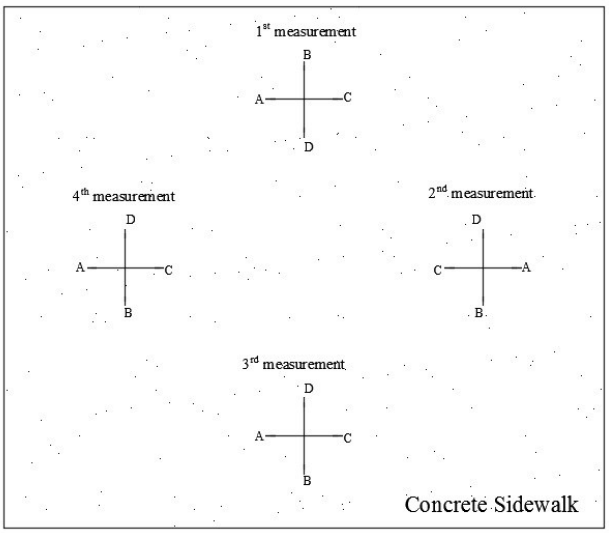

Figure 62. Wenner four probe pattern location over concrete sidewalk

Figure 63 shows the influence of temperature on surface resistivity. As the temperature decreases, surface resistivity increases. The word "site" represents the direct measurement on site and the word "after" means, after the temperature correction was applied, using equations 15 and 16.

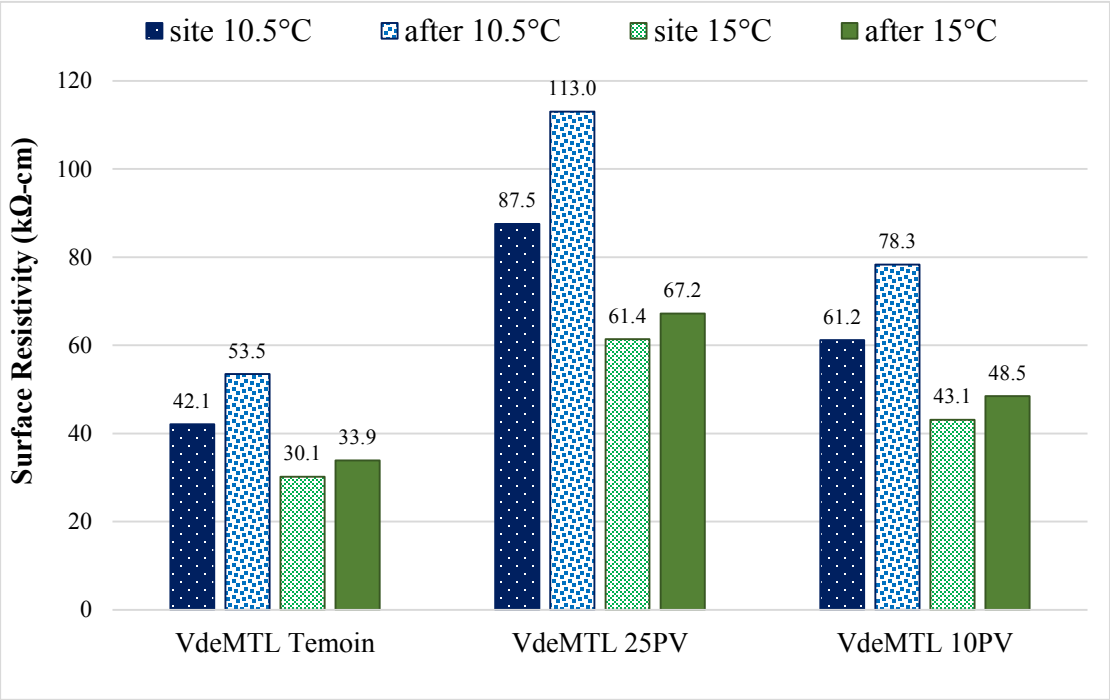

Figure 63. Differences between temperatures on mixtures samples.

Although the correlations established by Liu et al., (2014) to normalize the temperature effect on resistivity were used, it was not possible to achieve a common resistivity value for any of the mixtures tested. The correlations developed by Liu et al., (2014) were based on standard cylinder samples (Ø10x20cm). An important difference remains between the two temperatures on each sidewalks, where the resistivity measured at 10.5℃ was always higher; VdeMTL Temoin 57.7%, VdeMTL 25PV 68.1% and VdeMTL 10PV 61.6%. This

difference may be related to lack of full saturation. On site it was not possible to measure the saturation level on each sidewalk. A sense of the depth of water penetration and the uniformity of the water absorption was not possible to verify. Another factor may be the difference between curved and plane surfaces as seen in this research (as shown in section 4.2.1).

4.3.2 Differences between Curved and Plane Surfaces

On site, the dimensions of concrete elements being studied on site are large in comparison to the Wenner four probe electrodes spacing a, so it is possible to have the assumption that the current passes through a semi-infinite plane rather than a restricted and curved plane (Chun-Tao et al., 2014). Commonly most of the onsite measurements take place on planar surfaces, (bridge desks, beams, PCC pavements, etc.). For this reason, the determination of the onsite surface resistivity by cylinders generates a level of uncertainty. The motivation in this section was evaluating the resistivity differences on cylinders specimens (Ø10x20cm and Ø15x30cm) with curved surfaces against plane surfaces (sidewalks) with the same mixture properties.

The differences found between planar and curved surfaces can be seen in Figures 65, 66, and 67. All the values obtained for the cylinder samples were corrected using the geometry factor (k = 1.89 for cylinders Ø10x20cm, k = 1.39 for cylinders Ø15x30cm). The “Conc. Sidewalk” label represents the measurement made on site on the planar surfaces at the two

different temperatures. In Figure 64 each point represents the average value of 178 measurements for Ø10x20cm cylinder with a standard deviation of 0.67, 32 measurements for Ø15x30cm with a standard deviation (STD) of 0.59, and 64 measurement on each sidewalk at different temperature 10.5°C and 15°C with standard deviation of 2.27 and 1.98, respectively.

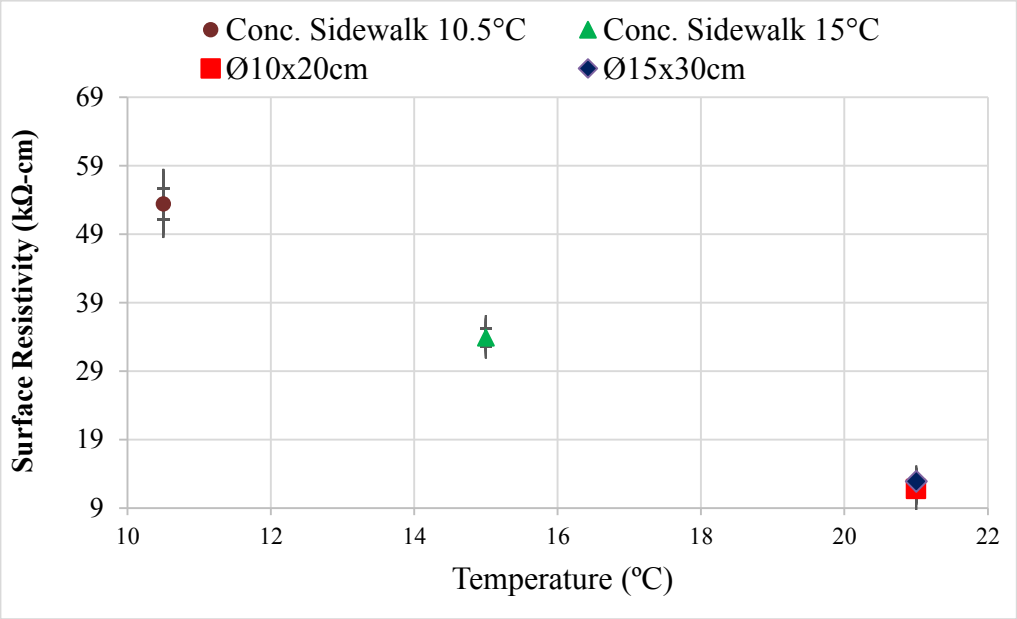

Figure 64. Differences between plane and curved surfaces mixture VdeMTL TEMOIN.

For Figure 65 each point represents the average value of 64 measurements for Ø10x20cm with a standard deviation of 1.97, 32 measurements for Ø15x30cm with a standard deviation of 2.46, and 64 measurements on each sidewalk at different temperature 10.5°C and 15°C with standard deviation of 5.29 and 2.08, respectively.

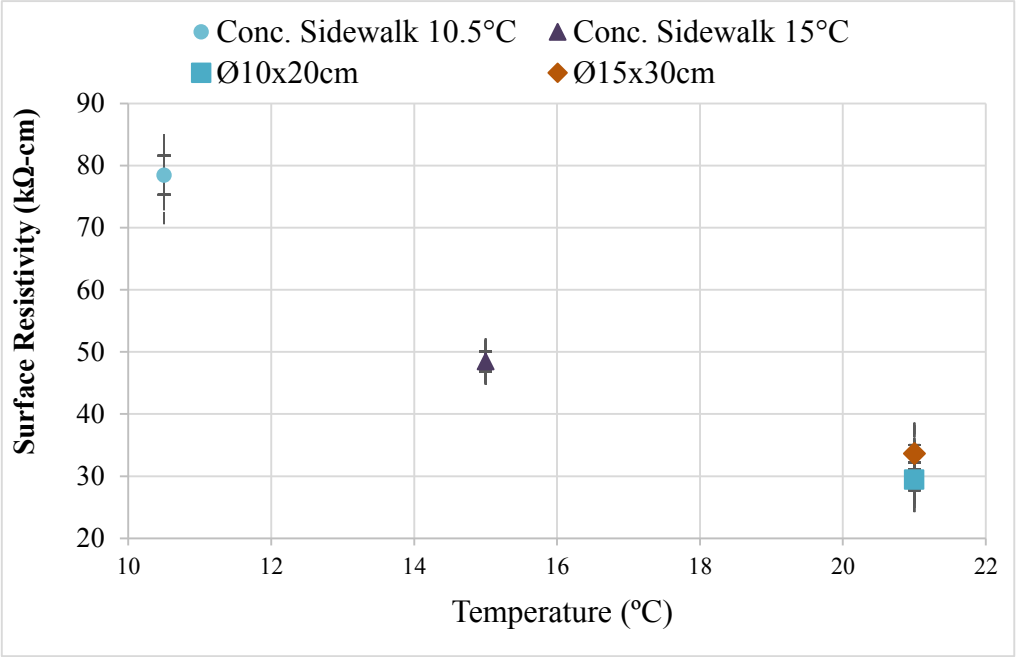

Figure 65. Differences between plane and curved surfaces mixture VdeMTL 10PV.

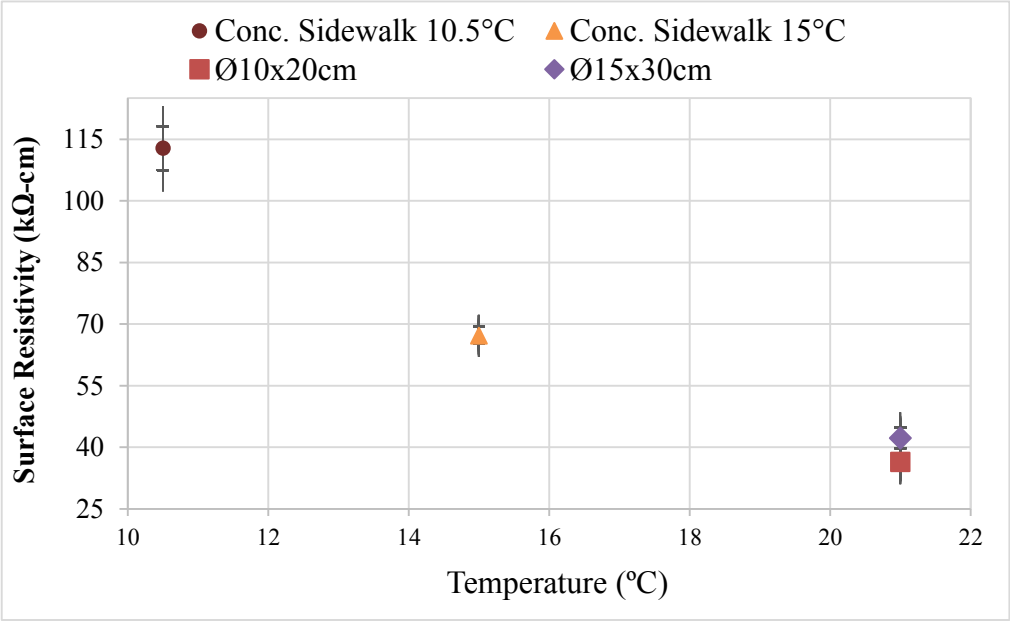

Figure 66. Differences between plane and curved surfaces mixture VdeMTL 25PV

On Figure 66 each point represents the average value of 64 measurements for Ø10x20cm with a standard deviation of 1.65, 32 measurements for Ø15x30cm with a standard deviation of 1.37, and 58 measurements at 10.5°C temperature with standard deviation of 3.10 and 72 measurements at 15°C temperature with standard deviation of 1.56.

For all laboratory samples and areas tested on site, it was found that although geometry and temperature corrections factor were applied there are significant differences on the resistivity values especially with the onsite measurements. The lowest resistivity values were always on Ø10x20cm samples. The Ø15x30cm samples had an average increase above the smaller cylinders for the three mixtures of 12.80%. Comparing the resistivity values between the Ø10x20cm samples and measurements taken on sidewalks at 10.5ºC, for VdeMTL TEMOIN the resistivity values increased 4.54 times higher, VdeMTL 10PV 2.66 times and VdeMTL 25PV 3.10 times higher. On the other hand, at 15ºC for VdeMTL TEMOIN the resistivity values increased 2.88 times higher, VdeMTL 10PV 1.65 times and VdeMTL 25PV 1.84 times.

The results indicate that it is necessary to improve how to saturate the sidewalk and verify the level of saturation onsite in order to achieve reliable values. As well, further work is needed to more accurately account for temperature. Finally, it is necessary to establish correlations between standard cylinder samples and directly placed site concrete for geometry corrections. What is important is to guarantee a similar curing process for both, plus to evaluate performance through time, comparing and then estimating how various measurements can be related.

4.4 Phase Four - Influence of Saturation Methods Techniques

4.4.1 Water Pressure Saturation

The results obtained in this section are presented in Figures 67, 68 and 69. In all mixtures, a similar behavior was observed; resistivity values without a significant increase or decrease after test time. A total of 16 measurements were made every 10 minutes on each sample for a total of 64 measurements in 40 minutes after 125 days of casting. The error bars can be seen the resistivity values at 10, 20, 30 and 40 minutes highlighting the minimal influence.

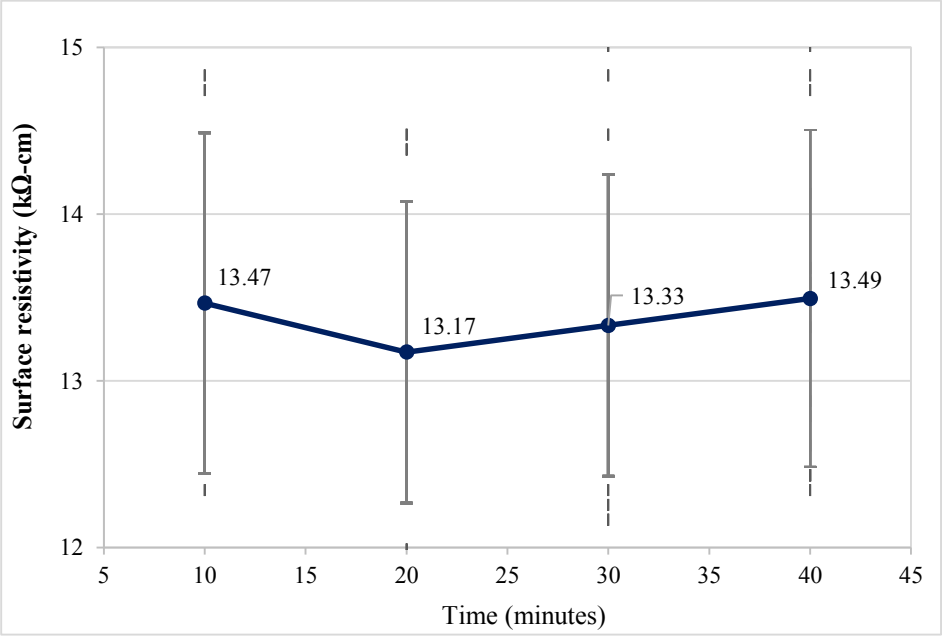

Figure 67. Water pressure saturation results mixture 100TI w/c 0.40

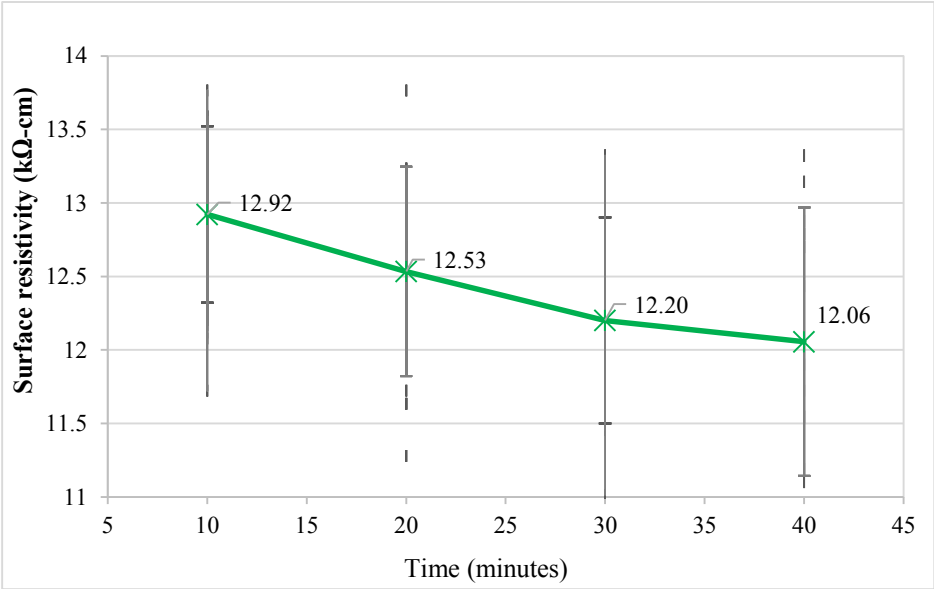

Figure 68. Water pressure saturation results mixture 100TI w/c 0.50

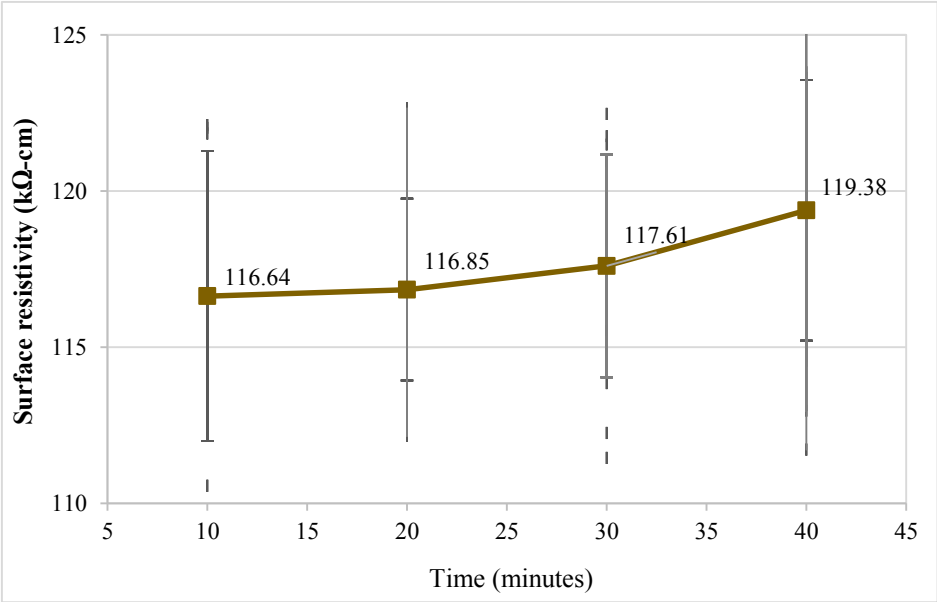

Figure 69. Water pressure saturation results mixture 50TI 30FA20S w/c 0.40

In addition to the samples tested using the pressured approach at 125 days. They were compared with samples where the surface resistivity was measured at 119 days by full immersion saturation after 24 and 48 hours. In Figures 70, 71, and 72 it can be seen the

differences from one approach to another. The pressurized water values are the same values shown before at 10, 20, 30 and 40 minutes.

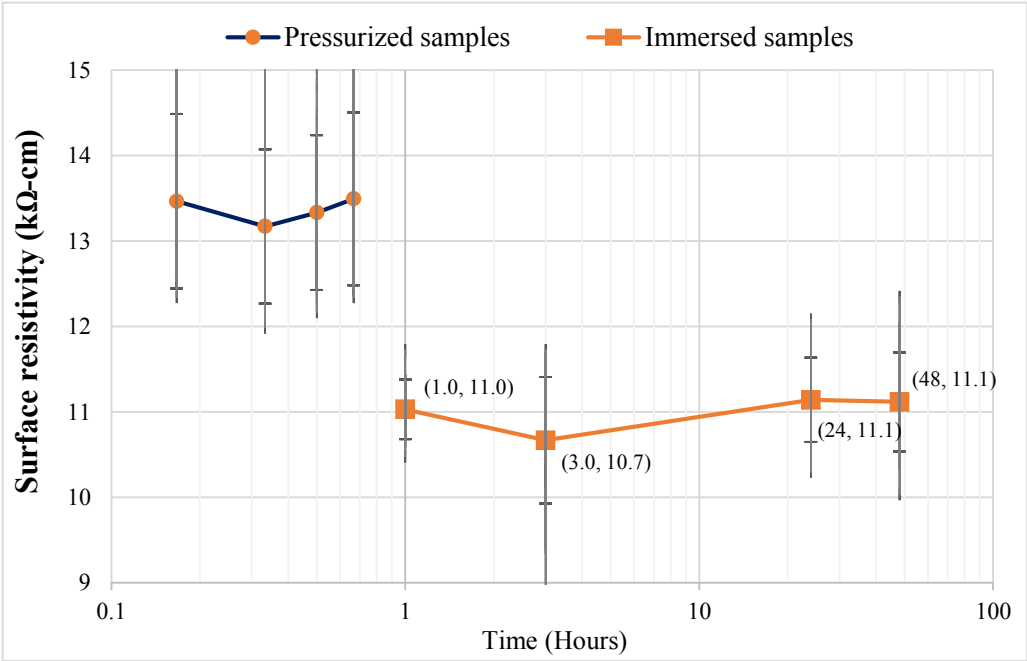

Figure 70. Comparison between immerse and pressurized water Mix - 100TI w/c 0.40

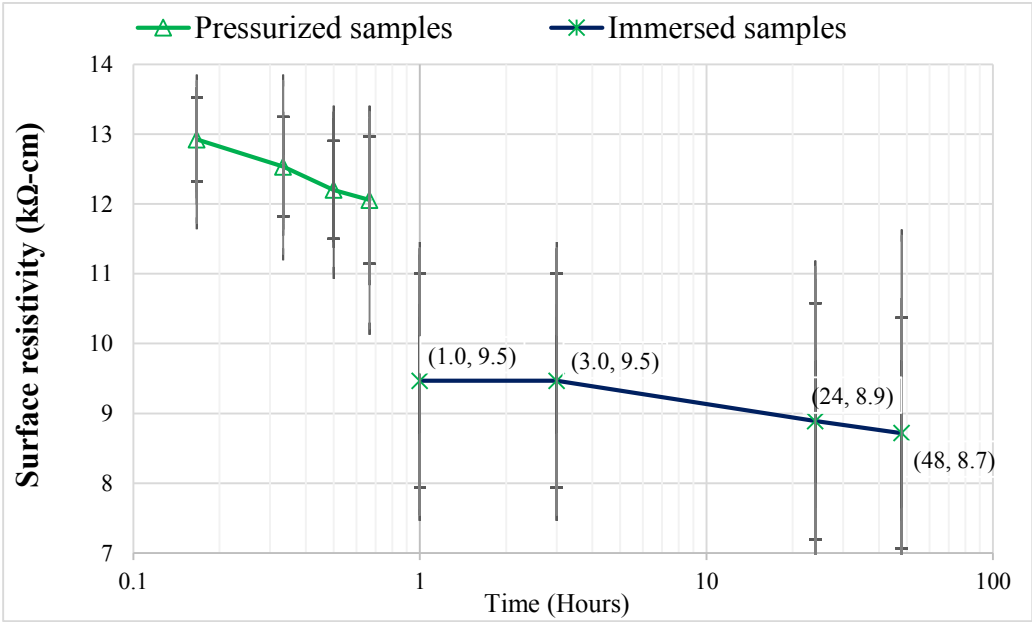

Figure 71. Comparison between immerse and pressurized water Mix -100TI w/c 0.50

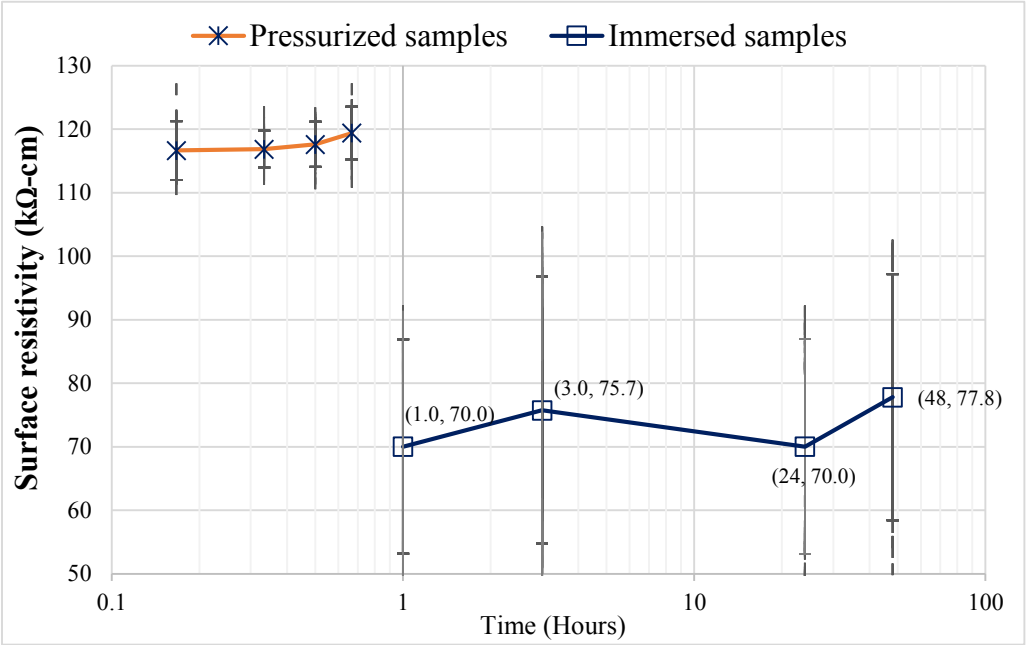

Figure 72. Comparison between immersed and pressurized water Mix-50TI30FA20S w/c 0.40

In all cases, the use of pressurized water presents on average higher resistivity; mixtures with 100% Portland cement w/c 0.40 and 0.50, on average +20% and +60% higher, respectively. For those with 50% Portland cement, 20% fly ash and 30% slag cement the increment was on average +38%.

The pressurized water method does not reveal important changes on surface resistivity values. After time passes, there is not a tendency of decreasing or increasing the resistivity value. The high pressure avoids proper surface saturation, due to constant water rebound occuring between the pressure hose and sample's surface making it difficult for the water to penetratethe sample by permeability or sorptivity, preventing reliable resistivity values.

Additionally, the amount of discharge water used during the test is excessively high making this approach difficult to implement in construction projects without water facilities.

4.4.2 Ponding Saturation

After the last testing at 155 days, all the circular slabs from Phase Two mixtures were stored in laboratory air conditions for 50 days to achieve a dry sample at 205 days. For periods of time (10, 30 and 60 minutes) the samples were surface saturated (by ponding with tap water) to simulate on site practices. After the resistivity measurements were completed, the slabs were fully immersed in tap-water for 72 hours. Surface resistivity was measured at 24, 48 and 72 hours of immersion. A total of nine samples were measured, three samples of each mixture. In all cases, an important decrease was observed in the surface resistivity between the first measurements at 10 minutes with the last one at 72 hours.

Figures 73, 74 and 75 shows the generalized decreasing behavior observed using ponding saturation. Each point represents the average results of 16 measurements at every time (10, 30, and 60 minute, 24, 48 and 72 hours) on each sample. The “x” axis is in a logarithmic scale in order to facilitate the view of measurements at 10 min and 30 min.

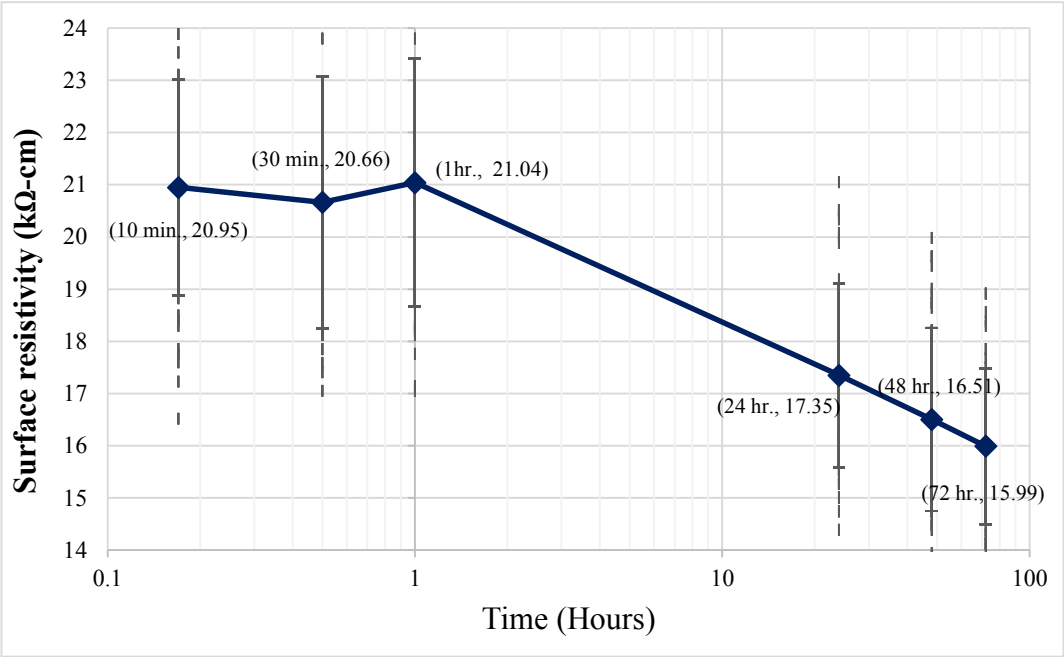

Figure 73. Ponding saturation Mix - 100TI w/c 0.40

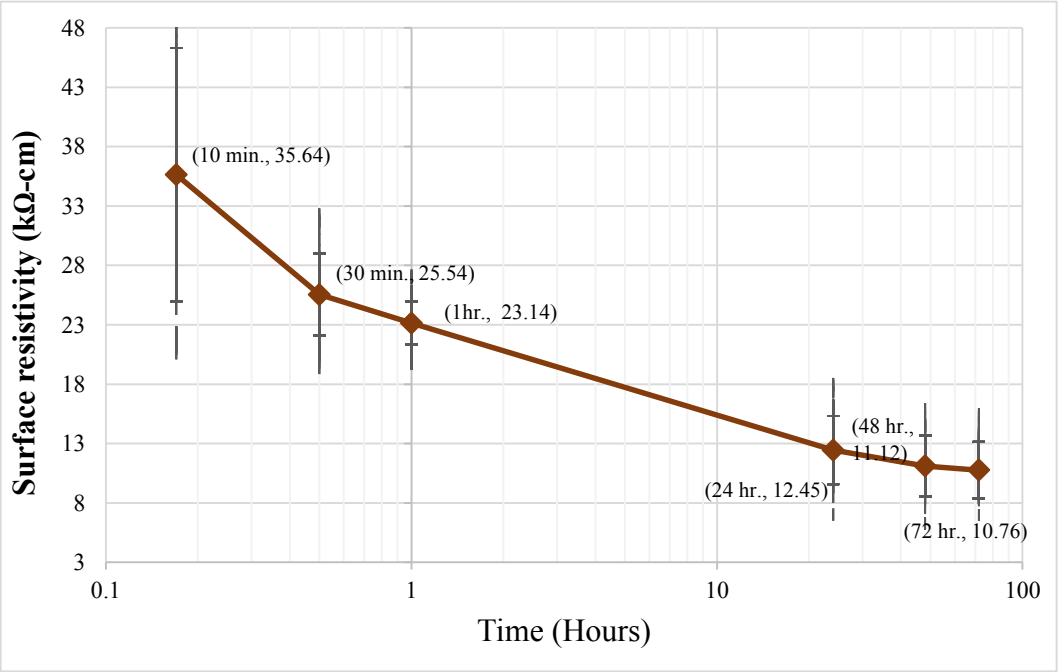

Figure 74. Ponding saturation Mix- 100TI w/c 0.50

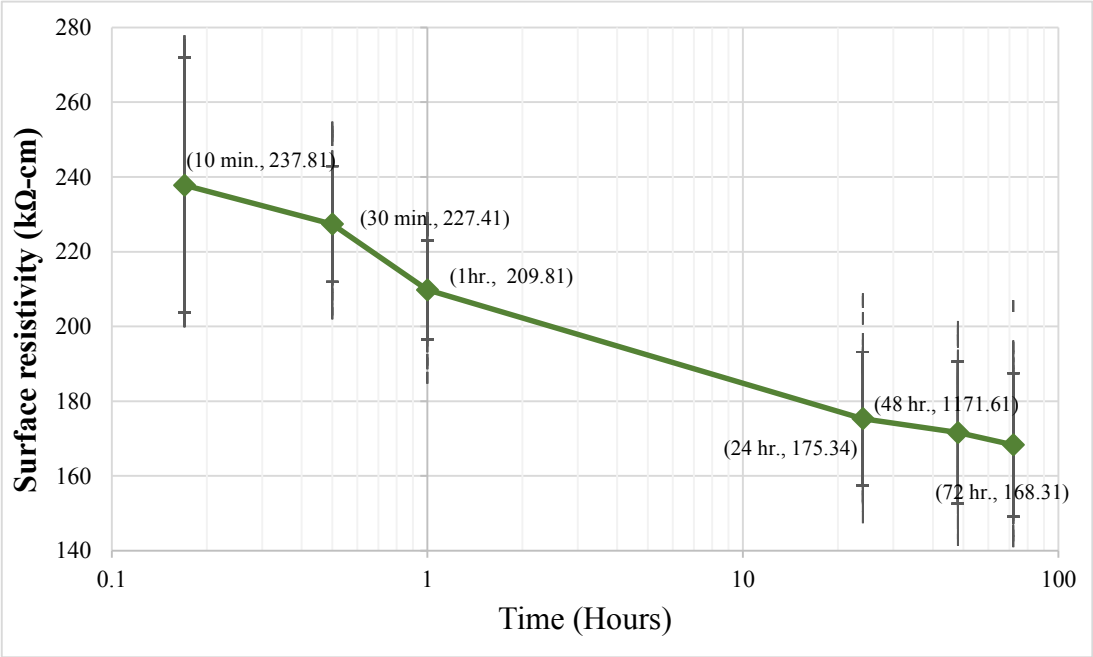

Figure 75. Ponding saturation Mix- 50TI30FA20S w/c 0.40.

In all cases, the use of ponding saturation after 10, 30 and 60 minutes presented significantly higher resistivity values than later measurements. In the following order, mixtures with 100% Portland cement w/c 0.40, the difference on average obtained between the first measurement at 1 minute and 72 hours was - 29%. For those with 50% Portland cement, 20% fly ash and 30% slag cement the decrement was on average - 41%. For those with 100% Portland cement w/c 0.50 the resistivity value decreased more than three orders of magnitude.

It can be seen in Figure 76 a comparison between the previous resistivity values obtained at 91, 119 and 155 days from where samples were stored at RH>85% and then fully immersed for 48 hours, and the values obtained at 205 days using ponding saturation. The differences between the measurement obtained after 1 hour and followed by those made after 24, and 48 hours shows less variation as the values obtained using ponding saturation.

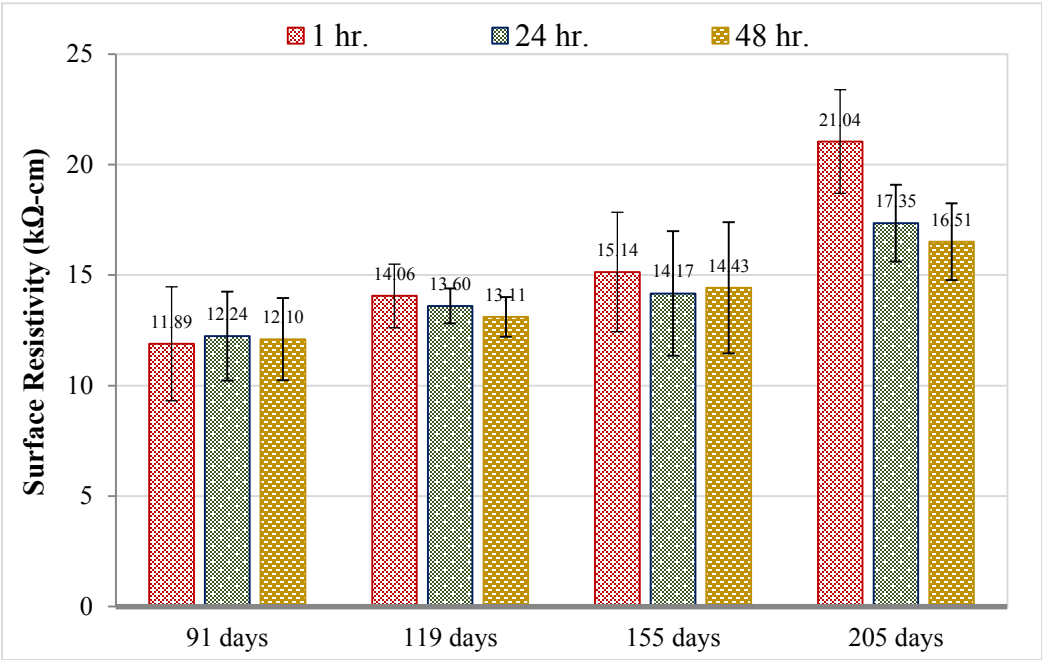

Figure 76. Differences through time in surface resistivity Mix - 100TI w/c 0.40.

For the mixture 100TI w/c 0.40 at 91, 119 and 155 days, it was estimated that the average percentage difference between 1 hour and 48 hours of saturation was – 2.4%, + 5.0% and +5.5%, respectively. Meanwhile, at 205 days the differences was +19.5%. The symbol (+) indicates that the value measured at one (1) hour is higher than the one measured after 48 hours.

For those with w/c 0.50 at 91, 119 and 155 days, it was estimated that the average percentage differences between 1 hour and 48 hours of saturation was + 1.5%, 7.0% and + 7.0 % respectively. Meanwhile, at 205 days the differences was + 49 % (Figure 77).

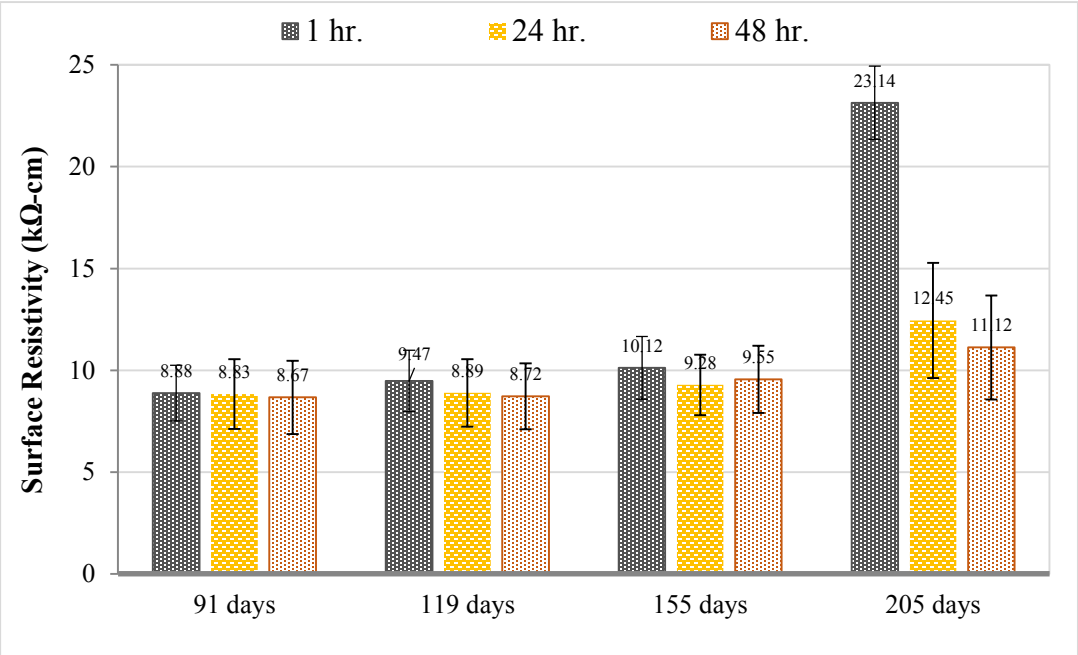

Figure 77. Differences through time in surface resistivity Mix -100TI w/c 0.50.

On the other hand, for mixture 50TI30FA20S w/c 0.40, the differences were + 0.70%, -5.5% and – 0.1% at 91, 119 and 155 days, respectively. At 205 days the difference was +17.30% (Figure 78).

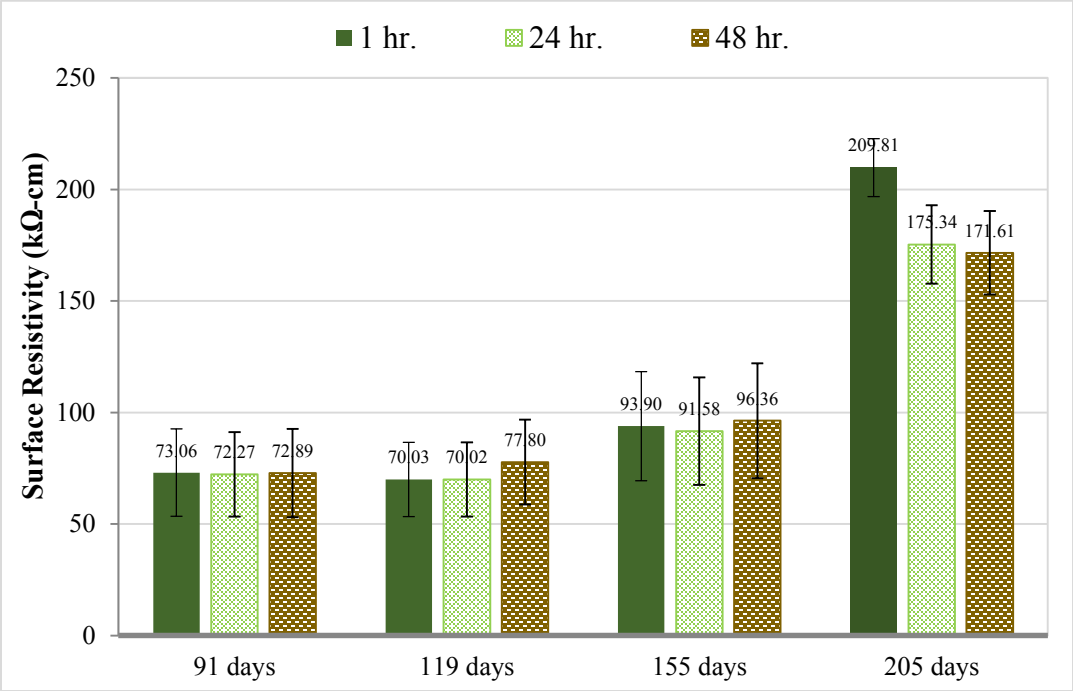

Figure 78. Differences through time in surface resistivity

Mix - 50TI30FA20S w/c 0.40.

The impact of having dry concrete and then saturating it by ponding represents the current on-site practice of saturating the local area for a few minutes at best (see Figure 25). However, in this research, this saturation method leads to higher resistivity values by at least 17% difference.

5 Discussion

This Chapter further discusses the results comparing outcomes among the phases. There are some limitations regarding this research, such as:

- For all the Surface resistivity measurements at different ages, samples were stored under the same laboratory conditions, RH>85%. Once the measurements started they were immersed in limewater or tap water according the case. The results are expected to be similar for other starting saturation, but this conclusion should be verified.
- In all cases, only one variable was analyzed at the time against surface electrical resistivity (i.e. saturation time vs. surface electrical resistivity). On site more than one variable can influence surface electrical measurements at the same time (i.e. temperature, saturation time, moisture degree, type of surface, etc.).

This section discusses three main topics; (a) the minimum duration to obtain reliable surface resistivity values on laboratory samples; (b) Geometry effect and type of solution for saturation; (c) misreading surface electrical resistivity results due to poor saturation based on results achieved in Chapter 4.

5.1 Minimum Duration Time to Achieve Reliable Surface Resistivity Values

A comparison between the samples with equal or similar water cement ratio (w/c) was established with different geometry and mixture properties from Phases One and Two. The surface resistivity was compared at different times 28, 56 and 91 days for standard cylinders Ø10x20cm and at 91, 119 and 155 days for circular slabs Ø30x12cm to identify the percentage difference in surface resistivity between samples partially saturated (after only hour) and fully saturated for 24 and 72 hours of fully immersion into limewater but stored before testing at RH >85%.

5.1.1 Differences on Resistivity values in Standard Cylinders Ø10x20cm

As can be seen in Figure 79 the resistivity for all the samples with water cement ratio close to 0.40 at 28 days is given. The mixture with major differences between first measurement (1 hour saturation) and measurements at 24 and 72 hours were for those with only Portland cement (100TI) with -7.86% and -9.60%, followed by the mixture 50TI-30FA-20S with differences of -7.36% and - 3.0% at 24 and 72 hours. For mixtures 50L50S and 50TI-20FA-30S the resistivity value obtained after 72 hours surpass the one obtained at the first measurement by +3.0% and +12.40% respectively.

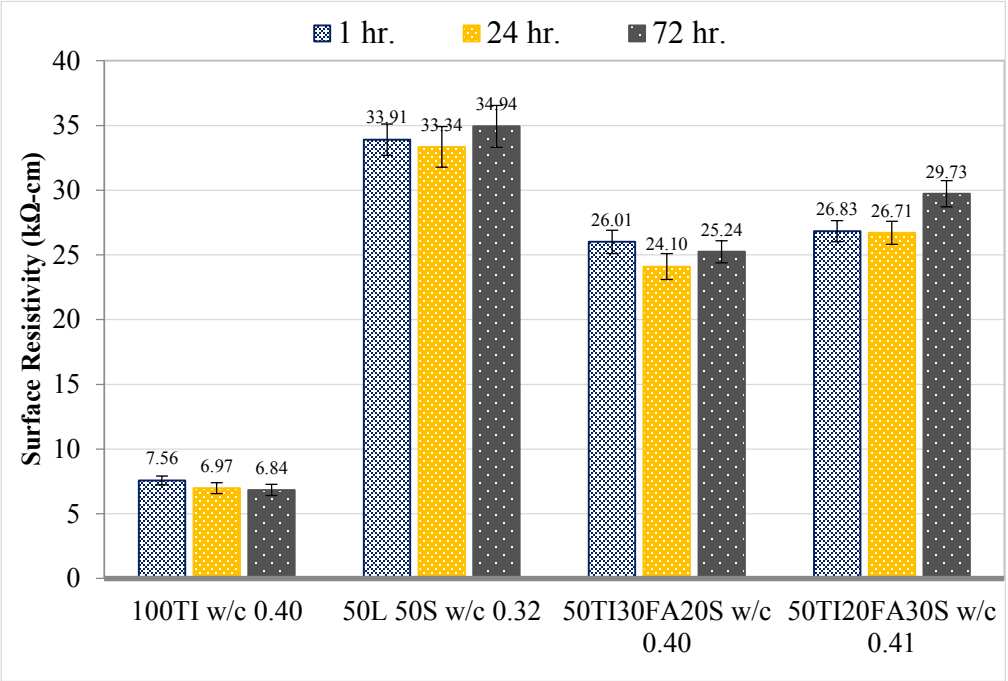

Figure 79. Resistivity Values on Mixes with w/c close to 0.40 (28 days).

However at 91 days the differences increased significantly for those samples with only Portland cement (100TI) between first measurement (1 hour saturation) and measurements at 24 and 72 hours were more significant, -29.97 % and - 31.50% respectively.

For the rest of mixtures, it can be seen in Table 25 a recompilation of the resistivity results obtained from Phase 1 over time of the 20 mixtures. The Table shows the percent differences between 24 hours and 1 hour, and 72 hours and 24 hours. Where the symbol (+) indicates the denominator (i.e. 1 hr.) has a higher value in comparison with the numerator (i.e. 24 hr.), in the other case the symbol is (-).

Table 25. Percent Differences through Saturation Time – Ø10x20cm samples.

Standard cylinder (Ø10x20cm)		Surface Resistivity (kΩ-cm) over time					
		28 days		56 days		91 days	
Mixtures	w/c	24 hr./1 hr.	72 hr./24hr.	24 hr./1 hr.	72 hr./24hr.	24 hr./1 hr.	72 hr./24hr.
100TI	0.40	+7.86%	+9.58%	-19.08%	-1.13%	-28.97%	-1.88%
	0.52	+9.03%	-0.98%	-15.72%	-0.76%	-28.50%	-1.08%
	0.52*	+9.27%	-0.23%	-9.13%	+1.11%	-18.04%	+1.89%
	0.60	+10.13%	-0.83%	-9.79%	+0.67%	-13.98%	+0.00%
50TI-50S	0.39	+7.28%	-0.94%	-22.97%	-2.70%	-28.90%	+1.06%
	0.52	+5.74%	-2.35%	-19.16%	-4.31%	-26.27%	+0.41%
	0.57	+2.02%	-3.87%	+5.36%	-1.71%	-0.25%	-0.72%
	0.63	+3.79%	-8.68%	+3.80%	-0.60%	-2.37%	+3.29%
50L-50S	0.32	+1.68%	-4.77%	+2.06%	-1.25%	-2.61%	+3.50%
	0.44	+3.62%	-3.14%	-16.01%	-2.50%	-2.66%	+0.09%
	0.48	+3.23%	-2.00%	-12.41%	-4.79%	-4.96%	+2.67%
	0.50	+4.48%	-3.21%	-13.04%	-1.61%	-1.39%	+3.17%
50TI-30FA-20S	0.36	+4.46%	-2.62%	+1.97%	+1.32%	+1.85%	+0.66%
	0.40	+7.36%	-4.73%	+2.37%	-0.36%	-0.30%	-1.71%
	0.53	+8.24%	-2.42%	+1.66%	-0.10%	+1.19%	+1.30%
	0.64	+2.46%	-11.35%	+5.83%	+2.31%	+1.33%	-0.33%
50TI-20FA-30S	0.37	+1.44%	-10.99%	+3.37%	-0.90%	+0.07%	+1.89%
	0.45	+0.00%	-12.38%	+3.71%	+0.88%	-0.19%	-0.43%
	0.53	+0.48%	-11.13%	+0.08%	-2.01%	-7.50%	-0.06%
	0.64	+3.13%	-8.45%	+0.40%	-2.53%	-4.98%	-1.39%

According to the data presented, the differences observed between the first measurements at 1 hour and those after 24 hours indicates that one hour is not enough time to achieve a constant and reliable resistivity values. This is particularly important as the samples were stored at RH >85% before testing representing a high initial moisture content. The differences were particularly noticeable for those mixtures with only Portland cement, especially for those with high w/c. In addition, it can be seen that the percentage difference

between 24 and 72 hours for the same mixtures is generally less than or equal to 1.0% at all ages.

For those blends with only two cementitious materials, 50TI-50S and 50L-50S a similar behavior as for those with only Portland cement was achieved especially for those with a w/c closer to 0.50 at 56 days and later. For those blends with three cementitious materials, Portland cement, fly Ash and slag, the percent differences are very small and in some cases not to seem important. However, to be conservative, 24 hours saturation results in stable surface resistivity measurements.

5.1.2 Differences on Resistivity values in Circular Slabs Ø30x12cm

Although there were differences in volume and geometry, circular slabs presented slight differences between the first and later measurements. Table 26 summarizes the data achieved at 91, 119 and 151 days and the percent differences between 24 hours and 1 hour, and 48 hours and 24 hours. Where the symbol (+) indicates the denominator (i.e. 1 hr.) has a higher value in comparison with the numerator (i.e. 24 hr.), in the other case the symbol is (-).

Table 26. Percent Differences through Saturation Time – Ø30x12cm samples.

Circular slab (Ø30x12cm)		Surface Resistivity (kΩ-cm) over time					
Mixtures	w/c	91 days		119 days		155 days	
		24 hr./1 hr.	48 hr./24hr.	24 hr./1 hr.	48 hr./24hr.	24 hr./1 hr.	48 hr./24hr.
100TI	0.40	-2.94%	+1.14%	+3.27%	+3.60%	+6.41%	-1.83%
	0.51	+0.56%	+1.81%	+6.12%	+1.91%	+8.30%	-2.91%
50TI-30FA-20S	0.40	+1.08%	-0.86%	+0.01%	-11.11%	+2.47%	-5.22%

From the data presented, 24 hours is deemed to be sufficient to obtain a reliable measurement according to the constant values obtained at different ages with different geometry samples for those with only Portland cement with low w/c stored at RH >85% during the time before the measurements. For other types of blends with more than one cementitious material, the saturation time effect is less remarkable.

For these reasons, 24 hours can be established as a minimum saturation time to obtain reliable values to cover a wide variety of blends with different supplementary cementitious materials. In addition, it is highly probable that, after 24 hours of sample saturation, additional hydration could occur, making comparative evaluations difficult.

5.2 The Geometry Effect on Surface Resistivity

From the two sets of geometries analyzed using the same probe spacing (38 cm), it is possible to determine that there is a clear influence of specimen geometry. After comparing both sets of samples (Ø10x20cm & Ø15x30cm) and (Ø10x20cm and Ø30x12cm). The sample with higher volume generally presents higher surface electrical resistivity values,

even after the geometry correction factor was applied. However, it was also found that, if the volume relation of the cylindrical samples is closer to 1.0 (i.e. Vol. Ø10x20cm/Vol. Ø15x30cm is closer to 1.0 than Vol. Ø10x20cm/Vol. Ø30x12cm) the surface resistivity difference is going to be minor if the storage condition and saturation degree were the same before testing regardless of the sample's age.

Based on data from Table 19 from Section 4.2.1, it can be seen in Figures 80 and 81 that the relation between the circular slabs and the standard cylinders can be represented by a linear trend. The "Line of Equality" represents the volume relation, values below the line indicate that Ø10x20cm sample has higher resistivity value; above the line is the Ø30x12cm sample has the higher value. In Figure 80, the trend lines can be seen for mixture 50TI30FA20S stored in tap water (TW) and limewater (LW). Due to the significantly lower resistivity values, the trendlines for the Portland mixtures can be seen in detail in Figure 81.

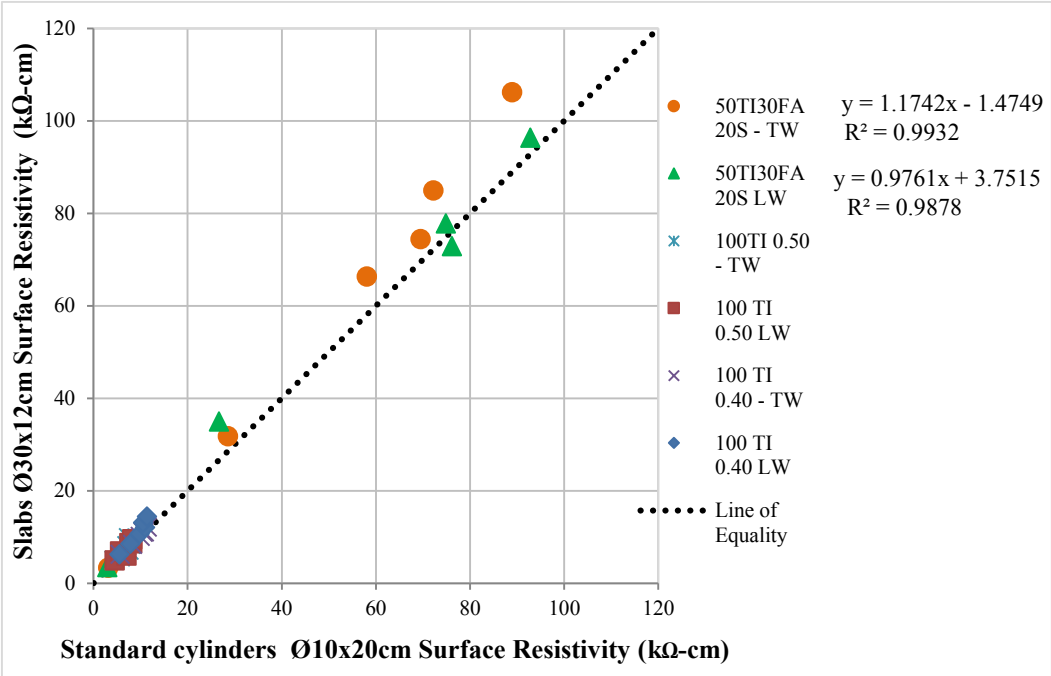

Figure 80. Geometry relation Phase Two – All mixtures

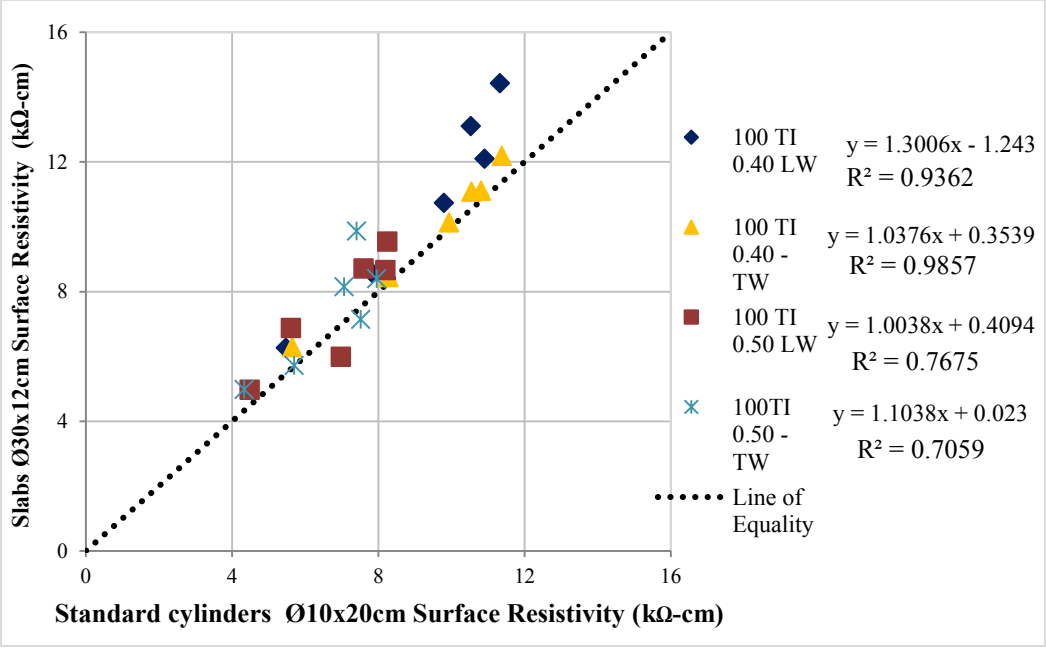

Figure 81. Geometry relation Phase Two – Portland mixtures

In this study it is possible that this difference is the product of two main reasons; (a) type of surface and (b) segregation.

The curvature of the surface is of greater influence in comparison to a planar surface since for planar surfaces the proximity between the contact probes with the aggregates varies, it can be shorter in comparison with curved surfaces (Figure 27). In this research, it is possible that some slight segregation occurred in the 12 cm depth of the slab. If this was the case, higher resistivity would be expected at the bottom as there would be less conductive paste present. In addition to the sample geometry, a relatively high-resistivity surface layer or covercrete can be generally formed by carbonation of the concrete. This is something that is more probable on the cement and mortar skin and are greatly influenced by curing and construction practices as mentioned in section 2.2.3. In this work, samples were not carbonated.

5.3 Misreading Surface Electrical Resistivity Results due to Poor Saturation and Temperature and Moisture Effect

The two types of practices commonly used on site projects clearly indicate that poor saturation can lead to misreading surface resistivity values. Therefore, any predictions cannot be validated for concrete early deterioration detection due to chloride penetration, corrosion, delamination or concrete degradation using these measurements. Misinterpretation surface resistivity results can generate false and extra work on future repairs or maintenances on the life cycle cost analysis on concrete elements.

These issues can be observed in the case of using the correlations established to identify rebar corrosion (Table 26) or chloride ion penetration (Table 27). For those concrete with only Portland cement where resistivity values an order of magnitude less than those with supplementary cementitious materials (SCMs) the risk of wrong judgement for those with only Portland cement is going to be higher. It can be seen that high water to cement ratio mixtures with supplementary materials present high resistivity compared to low Portland mixtures; these former mixtures would not be allowable in most instances.

Table 27. Electrical resistivity values for rebar corrosion rate and AASHTO, TP 95-11 (2011)

Electrical resistivity (kΩ.cm)	Corrosion risk level
> 20	Low rate
10 - 20	Moderate rate
5 - 10	High rate
< 5	Very high rate

Table 28. Correlation between electrical resistivity and chloride ion penetration.

Chloride Ion Permeability	Surface resistivity (kΩ-cm) of 10x20cm cylinder, probe spacing a=3.81 cm (1.5in)	Bulk resistivity (kΩ-cm)
High	<12	<6.3
Moderate	12 to 21	6.3 to 11
Low	21 to 37	11 to 20
Very Low	37 to 254	20 to 134
Negligible	>254	>134

Even after concretes are saturated after rainfall, resistivity values cannot get considered assertive for two reasons (a) Moisture degree and (b) Temperature variances. For the first, due to lack of full surface saturation as mentioned in Section 4.3.1 and according to Gowers and Millard (1999), an increase in the measured resistivity using the Wenner probe technique can be achieve after rainfall indicating the possibility of a double surface layer effect due to carbonation. Additionally, according to the findings of Larsen et al., (2007a) once moisture degree varies resistivity changes. As mentioned in Section 2.5.2 once the moisture degree decreased from 88% to 66% the resistivity value increased on average 6 times. For the second reason, Elkey and Sellevold (1995) reported that for ordinary Portland cement (OPC) concrete, resistivity changes 5% per °C at 21 °C under 30% saturation, whereas it changes 3% per °C under 70% saturation reason why further work is needed to more accurately account for temperature.

6 Conclusions

1. It was found for standard cylinders Ø10x20cm and Ø30x12cm slabs, particularly for those mixtures with only Portland cement with low w/c, that the minimum saturation time duration to achieve a reliable measured resistivity value is 24 hours. For other types of blends with different cementitious materials, 24 hours can be considered sufficient as after this time additional hydration could occur, making comparative evaluations difficult.

2. The use of supplementary cementitious materials, such as fly ash and granulated blast-furnace slag are highly recommended. Their use generates a more complex and refined pore network as it was confirmed during the test conducted in this research. For these mixtures, resistivity increased significantly over time.

3. For those mixtures containing both fly ash and slag (50TI30FA20S and 50TI20FA30S) compared to mixtures with 100TI at similar water cement ratio (w/c), the pore solution conductivity is on average 1.78 times less and 10 times higher for electrical resistivity. The pore solution is only one factor in determination of the surface resistivity.

4. The standardized laboratory method AASHTO TP 95 – 11 requires the storage of samples in limewater (diluted solution of calcium hydroxide) with volume ratio less or equal to 3:1 or 100% humidity, something that is difficult to achieve for on-site testing. In this research it was found that the use of tap water is feasible for saturation purposes. At early ages (7 and 28 days) there is not a clear major influence between limewater and tap water. However, at or after 56 days, the use of limewater leads to surface resistivity on average higher than that measured on those submerged continuously in tap water. A correction factor may be necessary at later ages. More work is needed to verify these findings.

5. The correction factor established by Spragg et al. (2013) helps to reduce the differences between sample geometries, but the large volumes still yielded higher surface resistivity. This can be due to the type of surface (curved or planar), the presence of segregation as well as surface roughness that can generate variations.

6. The correlations to normalize temperature based on standard cylinder geometry were not able to account for differences between laboratory and on-site resistivity measurements. More work is needed in this area.

7. Significant differences were obtained between the two tested saturation techniques and full laboratory saturation. Poor surface saturation as presented by using pressurized water and static ponding can lead to misinterpretation of resistivity of over 30% (average) even after rainfall lead to unreliable resistivity values.

8. The correlations established to identify rebar corrosion or chloride ion penetration as there is not a clear difference between the influence of water to cement ratio (w/c) or the use of supplementary cementitious materials (SCMs).

7 Recommendations

1. Further monitoring the cast samples used in Phase 2 can be completed to continue evaluate the resistivity performance over time, checking the increasing rate on the different mixtures. Also, it is possible to continue verifying if the differences in geometry and storage solutions remain or significant changes occur.

2. Although in this research all the measurements made in the laboratory were made under the same conditions, samples stored at RH>85% before testing and during testing time, samples were immersed into limewater or tap water solution at same temperature. Further effort can be made to compare the results obtained estimating the changes under different solution types and temperatures as well as stored under different moisture conditions before testing.

3. Furthermore, it is suggested to continue simulating the onsite saturation by water pressure or static ponding saturation and to further understand how much time is required for water to penetrate through concrete surface. Relative humidity sensors can be installed inside the circular slabs to support the findings achieved in this study. On each slab, a minimum number of 4 sensors can be installed that penetrate 10 cm inside from the circular slab edge. Each sensor can be spaced 1 cm from each other in the vertical axis, starting at 1 cm below the top surface.

4. In order to address the differences in surface resistivity due to geometry, the effect of type of surfaces (curved and planar) and correlations to normalize temperature, more different sets of samples can be tested. Ideally, increasing the number and variety of samples, including non-cylindrical geometries with different volumes can be cast using different mixtures and aggregate sizes. Then a comparison can be made with standard geometry samples (i.e. Ø10x20cm). Also verification can be made between the results achieved between the simulations developed by Morris et al. (1996). On the other hand, a simple cut of (1 to 2 cm) from the edge of standard cylinders (Ø10x20 and Ø15x30cm) through all vertical length of the cylinder can be done to evaluate and monitor differences between curved and plane surfaces and then establish a correction factor base on this findings.

5. Moreover, Gowers and Millard (1999) state that the sample thickness should be at least 4 times the probe spacing. Although the 10 cm diameter samples do not meet this criterion with 38 mm spacing, this combination is by far the most commonly used in practice. A review can be done in future to update this condition and establish possible influences.

6. To address the issue with the correlations to normalize the temperature effect, the samples can be tested in conjunction with the temperature and humidity sensors so it could be possible to update the correlations established by Liu et al., (2014) based only on standard cylinders (10x20cm). Additionally these samples can be stored

under different moisture degrees before testing and monitored over time under different temperatures.

References

1. Andrade, C., and Alonso, C., (1996) "Corrosion Rate Monitoring in the Laboratory and On-site", Construction & Building Materials, V.10. pp. 315 – 328.

2. ASP Construction (2003) "Health and Safety on Construction Sites Course" Student's Manual, 5th Edition, Revised Edition 2003.

3. AASHTO, TP 95-11 (2011) "Standard Method of Test for Surface Resistivity Indication of Concrete's Ability to Resist Chloride Ion Penetration." AASHTO Provisional Standards, 2011 Edition.

4. AASHTO T 277-05 (2007) "Standard Method of Test for Electrical Indication of Concrete's Ability to Resist Chloride Ion Penetration" AASHTO, 2007 Edition.

5. ASTM C1611 / C1611M – 14 (2014) "Standard Test Method for Slump Flow of Self-Consolidating Concrete". American Society of Testing and Materials (ASTM). Book of Standards Volume: 04.02

6. ASTM C39 / C39M - 14a (2014) "Standard Test Method for Compressive Strength of Cylindrical Concrete Specimens". American Society of Testing and Materials (ASTM). Book of Standards Volume: 04.02

7. ASTM Test C 666, (2008) "Mechanical Properties and Freezing and Thawing Resistance of Non-Air-Entrained, Air-Entrained, and Air-Entrained Superplasticized Concrete". American Society of Testing and Materials (ASTM).

8. ASTM C1202-12, (2012) "Standard Test Method for Electrical Indication of Concrete's Ability to Resist Chloride Ion Penetration", American Society of Testing and Materials (ASTM). EDT 2012.

9. Baker, R.F.M., (1985) "Illustration of Permeability and Porosity. Diffusion within and into Concrete", Paper presented at 13th Annual Convention of the Institute of Concrete Technology, University of Loughborough. Slough Institute of Concrete Technology. pp.21.

10. Barneyback, S., and S. Diamond (1981) "Expression and Analysis of Pore Fluids from Hardened Cement Pastes and Mortars". Cement and Concrete Research, Vol.11, No.2, pp. 279-285.

11. Bassuoni, M. T., Nehdi M. L., and Greenough T. R. (2006) "Enhancing the Reliability of Evaluating Chloride Ingress in Concrete Using the ASTM C1202 Rapid Chloride Penetrability Test", Journal of ASTM International, Vol. 3, No. 3, pp. 1-13.

12. Belviso, C.; Pascucci, S.; Cavalcante, F.; Palombo, F.; Pignatti, F.; Simoniello, T; and Fiore, Saverio (2011) "Multi-Technique Application for Waste Material Detection and Soil Remediation Strategies: The Red Mud Dust and Fly Ash Case Studies, Soil Contamination", ISBN: 978-953-307-647-8, InTech, DOI: 10.5772/24886. <http://www.intechopen.com/books/soil-contamination/multi-technique-application-for-waste-material-detection-and-soil-remediation-strategies-the-red-mud>, accessed 16 November 2014.

13. Bentz, D. A. (2007) "Virtual Rapid Chloride Permeability Test". Cement and Concrete Composites, Vol. 29, No.10, pp. 723 – 731.

14. Bockris, J.O. and Reddy, A.K (2002) "Modern Electrochemestry 1: Ionics secod edition, Plenum Press, New York, 2002. pp.769.

15. Bryant, W. J., Weyers, E. R., M. de la Garza, J. (2009) "In – Place Resistivity of Bridge Deck Concrete Mixtures," ACI Materials Journal, March – April, Vol. 106, no. 2, pp. 114 -122.

16. Castro, J., Spragg, R., and Weiss, J. (2012) "Water Absorption and Electrical Conductivity for Internally Cured Mortars with a W/C between 0.30 and 0.45" .Journal of Materials in Civil Engineering, Vol. 24, No. 2. pp. 223–231.

17. Chini A. R., Muszynski L. C., and Hicks J., (2003) "Determination of Acceptance Permeability Characteristics for Performance-Related Specifications for Portland Cement Concrete", Final report submitted to FDOT (MASc. Thesis), University of Florida, Department of Civil Engineering.

18. Chun-Tao Chen, Jiang-Jhy Chang, Wei-chung Yeih. (2014) "The effects of specimen parameters on the resistivity of concrete" Journal of Construction and Building Materials 71- Elsevier Ltd (September - 2014). Vol, 71, pp. 35-43.

19. DeSouza, Savio John, (1996) "Test Methods for the Evaluation of the Durability of Covercrete" M.A.Sc. Thesis University of Toronto, Department of Civil Engineering. pp. 88.

20. Di Bella, C., C. Villani, N. Phares, R. Hausheer, and J.Weiss (2012) "Chloride Transport and Service Life in Internally Cured Concrete". Presented at the Structures Congress 2012, Chicago.

21. Dullien, F. (1992) "Porous Media: Fluid Transport and Pore Structure". Academic Press, San Diego.

22. Elkey, W. and Sellevold, E.J. (1995) "Electrical Resistivity of Concrete Norwegian Public Roads Administration Publication, 1995. 33 pp.

23. Flower, DJM; Sanjayan JG. (2007) “Green House Gas Emissions due to Concrete Manufacture”. Department of Civil Engineering, Monash University, Clayton, VIC 3800, Australia. Int J LCA 12 (5). pp. 282–288.

24. Gowers, K.R. and Millard, S.G, (1999) “Measurement of Concrete Resistivity for Assessment of Corrosion Severity of Steel Using Wenner Technique” ACI Materials Journal, Technical paper, September - October 1999, Vol. 96, No. 5, pp. 536-541.

25. Heubeck, Christoph (2004) “Packing, Porosity, and Permeability lecture for the Earth History”. Institut für Geologische Wissenschaften Freie Universität Berlin. pp15.

26. Hooton, R. Doug. (1989) “What is needed in a Permeability Test for Evaluation of Concrete Quality”, Materials Research Society 1989, Vol.137, pp.141-149.

27. Hornbostel, K., Larsen, C.K., and Geiker, M.R. (2013) “Relationship between Concrete Resistivity and Corrosion Rate: A literature Review”, Cement and Concrete Composites, V.39. pp. 60-72.

28. Kessler, R.J.; Powers, R.G.; Paredes, M.A.; (2005) “Resistivity Measurements of Water Saturated Concrete as an Indicator of Permeability,” Corrosion 2005, April 3-7 2005. Paper 05621, pp. 1-10.

29. Kessler, R.J.; Powers, R.G.; Vivas, E.; Paredes, M.A.; and Virmani, P., (2008) "Surface Resistivity as an Indicator of Concrete Chloride Penetration Resistance," Concrete Bridge Conference, May 4-7, St. Louis, pp. 1 -17.

30. Kosmatka, Steven H.; Kerkhoff, Beatrix; Panarese, William C.; MacLeod, Norman F.; and McGrath Richard J., (2002) "Design and Control of Concrete Mixtures", EB101, 7th Editio, Cement Association of Canada, Otawa, Ontario. pp, 368.

31. Kreijger, P.C; (1984) "The Skin of Concrete – Composition and Properties", Matériux et Constructions. Vol.17, No. 100, pp. 275-283.

32. Larsen, C.K; Sellevold, E.J; Askeland, F; Østvik, J.M and Vennesland, Ø, (2007a) "Electrical Resistivity of Concrete. Part II: Influence of Moisture Content and Temperature". Norwegian Public Roads Administration, Technology Department Report No. 2482, pp. 16-24.

33. Larsen, C.K; Sellevold, E.J; Østvik, J-M.; and Vennesland Ø, (2007b) "Electrical Resistivity of Concrete. Part III: Long Term Field Measurements on Concrete Elements in the Tidal Zone". Norwegian Public Roads Administration, Technology Department Report No. 2482, pp. 25-38.

34. Lataste, J. F; Breysse, D and Frappa, M, (2003) " Electrical Resistivity Measurement applied to Cracking Assessment on Reinforced concrete Structures in Civil Engineering" NDT & E International, Vol. 36, No. 06, pp. 383-394.

35. Liu, Yanbo and Presuel-Moreno , (2014) " Normalization of Temperature Effect on Concrete Resistivity by Method Using Arrhenius Law" American Concrete Institute (ACI) Materials Journal. Title No. 11-M39. ACI Materials Journal/July-August 2014, pp. 433-442.

36. Lippiatt, B., and S. Ahmad, (2014) "Measuring the Life-Cycle Environmental and Economic Performance of Concrete: The BEES Approach". International Workshop on Sustainable Development and Concrete Technology, Beijing.

37. Lopez W. and Gonzalez J. A. (1993), "Influence of the Degree of Pore Saturation on the Resistivity of Concrete and the Corrosion Rate of Steel Reinforcement". Cement and Concrete Research, Vol. 23, No. 2, pp. 368-376.

38. McCarter W. J., Starrs G., Kandasami S., Jones R., and Chrisp T.M., (2009) " Electrode Configuration for Resistivity Measurements on Concrete", ACI Materials Journal, Vol.106, No. 3, pp. 258-264.

39. McCarter, W. J. (1996) "Monitoring the Influence of Water and Ionic Ingress on Cover-Zone Concrete Subjected to Repeated Absorption", Cement, Concrete and Aggregates, Vol. 18, No. 1, pp.55-63.

40. Millard S.G., Harrison J.A., Edwards A.J. (1989) “Measurement of the electrical resistivity of reinforced concrete structures for the assessment of corrosion risk”. Brit J NDT 1989; 31(11). pp. 617–621.

41. Millard S. G. and Gowers K. R., (1991) “The Influence of Surface Layers upon the Measurement of Concrete Resistivity, Durability of Concrete”, Second International Conference, ACI SP-126, Montreal, Canada, pp. 1197-1220.

42. Morris W., Moreno E. I., and Sagues A. A., (1996) “Practical Evaluation of Resistivity of Concrete in Test Cylinders Using A Wenner Array Probe, Cement and Concrete Research”, Vol. 26, No. 12, pp. 1779-1787.

43. Monfore, G. E. (1968), “ The Electrical Resistivity of Concrete, Journal of the PCA Research Development Laboratories”, Vol. 10, No. 2, pp. 35-48.

44. Montgomery, T., Jiang L., Sherman M. R., and Schlagel D. (2013) “Tackling Freezing-and-Thawing Deterioration of Historic Stadia. A 5-year rehabilitation of the Notre Dame Old Bowl Football Stadium”. Concrete International Magazine. Vol, 35, NO. 4 pp.38 – 44.

45. Neville, A.M. and Brooks, J.J. (1987), Concrete Technology, Longman, Harlow.

46. Nokken, M. R. and Hooton, R. D., (2006) “Electrical Conductivity as a Prequalification and Quality Control,” Concrete International, Vol. 28, No. 10, 2006, pp. 61-66.

47. Polder, R.B. and Larbi, J.A. (1995) “Investigation of Concrete Exposed to North Sea Water Submersion for 16 Years”. HERON 40, pp. 31-56.

48. Polder, R.B, Andrade, C., Elsener, C., Vennesland, Ø. Gulikers, J., Weidert, R., Raupach, M. (2000) “Test methods for onsite measurement of resistivity of concrete”. RILEM TC-154 -EMC: Electrochemical Techniques for Measuring Metallic Corrosion. Materials and Structures/Mat6riaux et Constructions, Vol. 33, December 2000, pp. 603-611.

49. Polder, R.B. (2001) "Test Methods For On Site Measurement of Resistivity of Concrete—A RILEM TC-154 Technical Recommendation". Construction and Building Materials Vol. 15. No. 2, pp. 125-131.

50. Polder, R.B. and de Rooij, M.R. (2005) “Durability of Marine Concrete Structures – Field Investigations and Modelling”. HERON 50, pp. 133-143

51. Powers, T.C., (1960). “Chemistry of Cement Proceedings”, 4th International Symposium, Washington DC, National Bureau of Standards, Monograph 43, US Deparment of Commerce, Washington DC Paper V-1 (192), pp. 577-613.

52. Powers, T.C., Copeland, L.E., Mann, H.M., (1959) “Capillary continuity or discontinuity in cement pastes”. Journal of the PCA Research and Development Laboratories. 1(2): p. 38-48.

53. Presuel-Moreno, Francisco; Suares, Andres; Liu, Yanbo, (2010) “Characterization of New and Old Concrete Structures Using Surface Resistivity Measurements,” Final Report. Florida Department of Transportation (Contract No. BD546, RPWO #08).

54. Presuel-Moreno, Francisco; Liu, Yanbo, (2012) “Temperature Effect on Electrical Resistivity Measurements on Mature Saturated Concrete” Nace International Conference & Expo Corrosion 2012, (NACE-2012-1732) pp. 5678-5696.

55. Rađenović, A.; Malina, J.; and Sofilić T. (2013) “Characterization of Ladle Furnace Slag from Carbon Steel Production as a Potential Adsorbent”, Advances in Materials Science and Engineering, Volume 2013 (2013), Article ID 198240. pp 6.

56. Proceq SA manual (2013) “Resipod Resistivity Mete”. Code 810 381 01E V.06 (2013) Proceq SA, Switzerland, <http://www.proceq.com/non-destructive-test-equipment/concrete-testing/moisture-corrosion-analysis/resipod.html >, accessed 21 January 2015.

57. Rupnow, Tyson D; and Icenogle, Patrick. (2011) "Evaluation of Surface Resistivity Measurements as an Alternative to the Rapid Chloride Permeability Test for Quality Assurance and Acceptance," Final Report (July 2011). Louisiana Department of Transportation and Development.

58. Savas B. Z., (1999), "Effect of Microstructure on Durability of Concrete" PhD Thesis, North Carolina State University, Department of Civil Engineering, Raleigh NC.

59. Slagment, (2010), AfriSam Products and Services, < http://www.afrisam.co.za/products-services/cement/slagment/ >. Accessed: 18 October 2014.

60. Shahroodi, Ahmad. (2010) "Development of Test Methods for Assessment of Concrete Durability for Use in Performance-Based Specifications" M.A.Sc. University of Toronto, Department of Civil Engineering, pp. 219.

61. Shi C., (2004) "Effect of Mixing Proportions of Concrete onits Electrical Conductivity and the Rapid Chloride Permeability Test (ASTM C1202 or ASSHTO T277) Results", Cement and Concrete Research, Vol. 34, No. 3, 2004, pp. 537-545.

62. Spragg, R. (2013) “The Rapid Assessment of Transport Properties of Cementitious Materials Using Electrical Methods”.M.S.C.E. Purdue University, West Lafayette, Indiana.

63. Spragg, R., Bu, Y., Snyder, K., Bentz, D., Weiss, J. (2013a) “Electrical Testing of Cement-Based Materials: Role of Testing Techniques, Sample Conditioning, and Accelerated Curing” Final Report. Joint Transportation Research Program, Indiana Department of Transportation and Purdue University. Report Number: FHWA/IN/JRTP-2013/28. DOI: 10.5703/1288284315230. pp. 1- 19.

64. Spragg, R., Villani, C., Snyder, K., Bentz, D., Bullard, J., and Weiss, J. (2013b) “Electrical Resistivity Measurements in Cementitious systems: Observations of Factors that influence the Measurements”. Transportation Research Record: Journal of the Transportation Research Board, Vol. 2342, Concrete Materials. pp. 90 – 98.

65. Snyder, K., Feng, X., Keen, B., and Mason, T. (2003) “Estimating the Electrical Conductivity of Cement Paste Pore Solution from OH, K, and Na Concentrations”. Cement and Concrete Research, Vol. 33, No. 6, pp. 793 – 798.

66. Swamy, R. N., (1996) “High Performance Durability through Design” International Workshop on High Performance Concrete, SP – 159, P. Zia, ed., American Concrete Institute, Farmington Hills, MI. pp.209 – 230.

67. Stanish K., Hooton R. D., and Thomas M. D. A.(1997), "Testing the Chloride Penetration Resistance of Concrete: A Literature Review", Department of Civil Engineering University of Toronto, Toronto, Ontario, Canada, FHWA Contract DTFH61-97-R 00022.

68. Strategic Highway Research Program (SHRP2), Condition Assessment, Technologies –Electrical Resistivity – NDToolbox, < http://www.ndtoolbox.org/content/bridge/er-description >, accessed 21 January 2015.

69. Taylor P., Tennis P., Obla K., Ram P., Van Dam T., and Dylla H. (2013), "Durability of Concrete", Second Edition, Transportation Research Circular E-C171. September 2013. Transportation Research Board Durability of the National Academies. pp. 1-78.

70. Wei, X., and Li, Z., (2006) "Early Hydration Process of Portland Cement Paste by Electrical Measurement". Journal of Materials in Civil Engineering, ASCE, V.18, No. 1. pp. 99-105.

71. Wenner, F. (1916) "A Method of Measuring Earth Resistivity". Bulletin of the National Bureau of Standards, Vol.12, pp.469-478.